

**Development of Bio-based and Biodegradable Film from
Carbon Dioxide Based Polymer and Poly(Lactic acid)**

by

Qirui Sun

**A Thesis
Presented to
The University of Guelph**

**In partial fulfillment of requirements
for the degree of
Master of Applied Science
in
Engineering**

Guelph, Ontario, Canada

©Qirui Sun, August, 2015

ABSTRACT

Development of Bio-based and Biodegradable Film from Carbon Dioxide Based Polymer and Poly(Lactic acid)

Qirui Sun
University of Guelph, 2015

Advisor: Dr.Amar Mohanty
Co-advisor: Dr.Manjusri Misra

In order to develop bioplastic alternative to conventional petro-based flexible packaging, this study focused on the fabrication and evaluation of a bio-based and biodegradable cast film. The material chosen for the matrix of film is a blend of poly(lactic acid) (PLA) and poly(propylene carbonate) (PPC). The effect of a chain extender at different loading levels on the mechanical, thermal and barrier properties of the films were investigated. With the chain extender, the compatibility and interfacial adhesion between the two polymer phases significantly improved. It is hypothesized that a PLA-chain extender-PPC copolymer is being formed during the reactive extrusion process, which was revealed by characterization studies. The elongation at break of the film with optimal amount of chain extender showed dramatic increase by more than 2000%. Differential Scanning Calorimetry (DSC) studies demonstrated that chain extender hindered the crystallization of the film which explained the decrease in both water and oxygen barrier.

Acknowledgments

I would like to express my sincere gratitude to my advisor Dr. Amar Kumar Mohanty for his patience, encouragement, motivation and immense knowledge that benefitted me throughout my MASc study and research. I wouldn't have accomplished all my tasks during my MASc program without his valuable guidance and continuous support. His mentorship has been always nurturing my belief in my ability to succeed. Sincere gratitude and appreciation also go to my co-advisor Dr. Manjusri Misra whose kindness, precious advice and firm support have been accompanying me all the time. I would like to also thank my committee member, Dr. Stefano Gregori for his assistance and insightful comments.

My sincere thanks go to Dr. Loong-Tak Lim for his timely suggestions and kind help. I also would like to give great thanks to all researchers of 'Bioproducts Discovery and Development Centre (BDDC, University of Guelph)' for their kindness, understanding, inestimable support and all the fun that we had during my time here. Their friendship means to me more than that I could describe.

I would like to express my deep gratitude and love to my parents whose patience, understanding and unending support have been the source of my power all the time. They kept me strong, focused and persistent. I am also deeply indebted to my fiancé Yuhan. Her understanding, unending support and encouragement are what kept me moving on along the way.

I greatly acknowledge the Ontario Ministry of Agriculture, Food and Rural Affairs (OMAFRA) – University of Guelph's Bioeconomy for Industrial Uses Research Theme (Project #200369) and Natural Sciences and Engineering Research Council (NSERC) Canada Discovery grant (Project #400322) for their financial support to carry out this research work.

Table of Contents

ABSTRACT.....	I
Acknowledgments.....	III
Table of Contents.....	IV
LIST OF TABLES.....	VI
LIST OF FIGURES.....	VII
LIST OF ABBREVIATIONS	X
LIST OF PUBLICATIONS.....	XII
Chapter 1 Introduction	1
1.1 Overview of Plastics	2
1.2 Bioplastics	4
1.3 Flexible Plastic Films for Packaging.....	7
1.4 Importance of Research on the Development of Bioplastics Films for Flexible Packaging Application	10
Chapter 2 Literature Review	13
2.1 Polypropylene Carbonate (PPC).....	13
2.2 Poly (Lactic acid) (PLA)	14
2.3 Polymer Blends	15
2.3.1 Physical Blending.....	16
2.4 Development of PPC-based Bioplastics	17
2.5 Incorporation of Chain Extender in the Biopolymer System	23
2.6 Film Processing.....	26
2.6.1 Film Casting Processing.....	26
2.6.2 Film Blowing Processing.....	30
2.7 Water Vapor and Oxygen Permeability	32
Chapter 3 Problem Statement and Hypothesis	35
3.1 Problem Statement.....	35
3.2 Hypothesis.....	35
3.3 Objectives.....	36
Chapter 4 Materials and Methods.....	37

4.1 Materials	37
4.1.1 Poly(propylene Carbonate)	37
4.1.2 Poly (lactic acid)	39
4.1.3 Joncryl ADR 4368-C	40
4.2 Methodology.....	42
4.2.1 Base Line Study	42
4.2.2 Primary Study.....	43
4.2.3 Tensile Properties Test.....	43
4.2.4 Differential Scanning Calorimetry (DSC)	44
4.2.5 Fourier Transform Infrared Spectroscopy (FTIR)	45
4.2.6 Scanning Electron Microscope (SEM)	45
4.2.7 Thermogravimetric Analysis (TGA)	45
4.2.8 Water Vapor Transmission Rate (WVTR) Measurements.....	46
4.2.9 Water Vapor Permeability Measurements using Dish Method.....	49
4.2.10 Oxygen Transmission Rate (OTR) Measurements.....	51
4.2.9 Statistical Analysis	54
Chapter 5 Results and Discussions.....	55
5.1 Tensile Properties Analysis	55
5.2 Fourier Transform Infrared Spectroscopy (FTIR)	68
5.3 Thermogravimetric Analysis (TGA)	71
5.4 Differential Scanning Calorimetry (DSC)	78
5.5 Fracture Surface Morphology Analysis (SEM).....	87
5.5 Water Vapor Permeability (WVP)	90
5.6 Water Vapor Permeability (WVP) From Dish Method	95
5.7 Oxygen Permeability (OP)	97
Chapter 6 Conclusion	102
Chapter 7 Reference	104

LIST OF TABLES

Table 2-1 List of typical chain extenders ^{32,51,58}	24
Table 4-1 Typical Properties of Poly(propylene Carbonate) (PPC)	38
Table 4-2 Typical Properties of Poly (lactic acid) (PLA)	40
Table 4-3 Characteristics of Joncryl ADR 4368-R.....	41
Table 5-1. Means, Standard deviation and statistical analysis of the tensile properties of PLA/PPC/Chain extender blend film.....	61
Table 5-2 Thermal properties obtained from TGA analysis of PLA/PPC/Chain extender blend films	72
Table 5-3 DSC parameters obtained from the DSC scan curves for PLA/PPC/Chain extender blend films	80
Table 5-4 Means, Standard Deviations and Tukey Pairwise Comparisons of WVP of PLA/PPC/Chain extender blend films with various concentration of Chain extender (Joncryl)	93
Table 5-5 WVP from Dish Method	96
Table 5-6 Means, Standard Deviations and Tukey Pairwise Comparisons of OP of PLA/PPC/Chain extender blend films with various concentration of Chain extender (Joncryl)	100

LIST OF FIGURES

Figure 1.1 Classification of Biopolymers	6
Figure 2.1 Cast film Processing	29
Figure 2.2 Film Blowing Process.....	31
Figure 4.1 Chemical structure of Poly(propylene carbonate) (PPC)	37
Figure 4.2 Chemical structure of Poly (lactic acid) (PLA)	39
Figure 4.3 Chemical structure of Joncryl ADR 4368-R	41
Figure 4.4 Illustration of water vapor transmission rate test principles	48
Figure 4.5 Schematic of Dish Method.....	50
Figure 4.6 Illustration of oxygen transmission rate test principles.....	53
Figure 5.1 Tensile Strength of PPC, PLA and PPC/PLA blends: (A) neat PPC, (B) neat PLA, (C) PPC/PLA (30/70), (D) PPC/PLA (50/50), (E) PPC/PLA (60/40).	56
Figure 5.2 Young's Modulus of PPC, PLA and PPC/PLA blends: (A) neat PPC, (B) neat PLA, (C) PPC/PLA (30/70), (D) PPC/PLA (50/50), (E) PPC/PLA (60/40).	57
Figure 5.3 Elongation at Break of PPC, PLA and PPC/PLA blends: (A) neat PPC, (B) neat PLA, (C) PPC/PLA (30/70), (D) PPC/PLA (50/50), (E) PPC/PLA (60/40).	58
Figure 5.4 Stress-strain curves of PPC, PLA and PPC/PLA blends	59
Figure 5.5 Stress-strain curves of PPC/PLA blend films with and without Joncryl	60

Figure 5.6 Tensile Strength of PPC/PLA blend films with and without Joncryl: (A) PLA/PPC (40/60) blend films, (B) PLA/PPC/Joncryl (40/60/0.2) blend films, (C) PLA/PPC/Joncryl (40/60/0.5) blend films, (D) PLA/PPC/Joncryl (40/60/1) blend films.....	65
Figure 5.7 Secant Modulus of PPC/PLA blend films with and without Joncryl: (A) PLA/PPC (40/60) blend films, (B) PLA/PPC/Joncryl (40/60/0.2) blend films, (C) PLA/PPC/Joncryl (40/60/0.5) blend films, (D) PLA/PPC/Joncryl (40/60/1) blend films.....	66
Figure 5.8 Elongatio at Break of PPC/PLA blend films with and without Joncryl: (A) PLA/PPC (40/60) blend films, (B) PLA/PPC/Joncryl (40/60/0.2) blend films, (C) PLA/PPC/Joncryl (40/60/0.5) blend films, u7(D) PLA/PPC/Joncryl (40/60/1) blend films.....	67
Figure 5.9 FTIR spectra of (A) PPC, (B) PLA, (C) PPC/PLA 60/40 blend film, (D) Joncryl and (E) PPC/PLA/Joncryl 60/40/0.5 blend film.	70
Figure 5.10 TGA curves of PLA film and PPC film.....	73
Figure 5.11 DTG curves of PLA film and PPC film.....	74
Figure 5.12 TGA curves of PPC/PLA 60/40 blend films with and without Joncryl	77
Figure 5.13 DTG curves of PPC/PLA 60/40 blend films with and without Joncryl	78
Figure 5.14 DSC first cooling curves (cooling rate of 5 °C/min) of PPC/PLA films and PPC/PLA films with 0.2%, 0.5% and 1% Joncryl.....	82
Figure 5.15 DSC second heating curves (heating rate of 10 °C/min) of PPC/PLA blend films and PPC/PLA blend films with 0.2%, 0.5% and 1% Joncryl from 20 °C to 50 °C	84
Figure 5.16 DSC second heating curves (heating rate of 10 °C/min) of PPC/PLA blend films and PPC/PLA blend films with 0.2%, 0.5% and 1% Joncryl from 120 °C and higher	86

Figure 5.17 SEM images of cyro-fracture surface of the PLA/PPC blend films with different concentration of Joncryl	89
Figure 5.18 WVP of PPC films, PLA films and PPC/PLA blend films with and without Joncryl.....	94
Figure 5.19 OP of PPC films, PLA films and PPC/PLA blend films with and without Joncryl.....	101

LIST OF ABBREVIATIONS

ASTM	American society for testing and materials
PLA	Poly (lactic acid)
PP	Polypropylene
PE	Polyethylene
LDPE	Low Density Polyethylene
HDPE	High Density Polyethylene
WVP	Water Vapor Permeability
OP	Oxygen Permeability
PCL	Polycaprolactone
PVC	Polyvinyl chloride
TGA	Thermogravimetric analysis/analyzer
DSC	Differential Scanning Calorimetry
Phr	Parts per hundred
PBAT	Poly (butylene adipate-co-terephthalate)
SEM	Scanning electron microscopy
PHBV	Poly (3-hydroxybutyrate-co-3-hydroxyvalerate)
PHA	Polyhydroxyalkanoate
WVTR	Water Vapor Transmission Rate
OTR	Oxygen Transmission Rate
FTIR	Fourier transform infrared spectroscopy
Joncryn	Joncryn ADR 4368-C
RPM	Rotation per minute

SCCM	Standard cubic centimeter per minute
BOPP	Biaxially Orientated Polypropylene
CPP	Cast Polypropylene
PET	Polyethylene terephthalate
PPC	Poly(propylene carbonate)
PS	Polystyrene

LIST OF PUBLICATIONS

International Journal Publication

Qirui Sun, Tizazu Mekonnen, Amar K. Mohanty, Manjusri Misra. “Novel biodegradable cast film from carbon dioxide based copolymer and poly (lactic acid).” Accepted by Journal of Polymers and the Environment (In Press August 2015).

Chapter 1 Introduction

The flexible plastic packaging industry has been dominated by petro-based plastics in recent years. Because of the poor degradability of petro-based plastics, huge consumption of these plastic packaging solutions has posed great problems in terms of waste disposal. Massive amounts of post-consumer plastic packaging are either placed in the landfill sites or processed through incineration, with only a small amount being recycled and reused. Landfilling is continuously producing hazards to the environment, while incineration emits large amounts of carbon dioxide, causing immeasurable damage to the environment. In addition, petroleum resources are depleting, which further comprises the sustainable development of the plastic packaging industry.

With the intention to establish the long-term sustainability of flexible plastic packaging industry, more sustainable alternatives to conventional petro-based plastic flexible packaging solutions need to be developed. Bioplastics are promising candidates because of their either bio-based or biodegradable nature, which can potentially help alleviate the disposal problem and heavy reliance on the fossil fuel.

In this study, two bioplastics were chosen as the matrix to develop a bio-based and biodegradable film, which are poly(lactic acid) (PLA) and poly(propylene carbonate) (PPC), respectively. Poly(propylene carbonate) (PPC) is a biodegradable polymer which can be synthesized using propylene oxide and carbon dioxide. It can contain more than 50wt% of sequestered CO₂. It exhibits excellent elongation at break, which can be utilized to modify plastics with low toughness. However, its strength and thermal stability are weaknesses that

require improvement. Poly(lactic acid) (PLA) is currently the most commercially available bioplastic globally, which is produced from corn. PLA possesses superior strength, but lacks elongation at break. It also presents reasonable barrier performances (oxygen and water vapor), which allows PLA to be applied in the flexible packaging field.

A preblend of PLA and PPC with optimal blending ratio was prepared as the matrix for developing the film. A chain extender was incorporated into the film system to enhance the compatibility between the two bioplastics, aiming for improved overall performance (thermal, mechanical and barrier). By combining the advantages of PPC and PLA along with proper compatibilization from introducing the chain extender, a bio-based and biodegradable flexible plastic film with high performance could be achieved. This study explored the fabrication of this film and characterized various performances of the developed films.

1.1 Overview of Plastics

One of the most profound aspects in our human daily lives is the material. Materials give us the foundation to make tools, build structures, design products, etc. The advancement of materials has continuously provided humanity with more and better choices and improving the quality of our lives. The advent of plastics was a significant breakthrough in the history of materials advancement¹. Given the advantages of light weight, superior mechanical properties, and cost competitiveness, plastics displaced metals and wood in many applications and took up a huge share of the material market. The development of plastics has made them increasingly attractive.

Currently, plastics are widely used throughout the world in different fields for various applications, such as automotive parts, electronic devices, construction, and packaging. These plastics are polymeric materials that consist of a large number of polymer chains. They are

synthesized via condensations or polymerizations of organic monomers.² Most of the plastics are derived from petroleum sources and majority of the plastics cannot be composted.

The global consumption of petroleum-based plastics in 2012 was reported to be more than 288 million tons with an annual increase of 5%³. Such dependence demonstrates how much effects the fluctuation of oil price would have on the cost of petroleum-based plastics. In addition, the depleting source of the oil also is emphasizing the unsustainable nature of the modern plastic industry.

Over time, using petroleum-based plastics produces problems from an ecological and environmental point of view. Production of petroleum-based plastics involves carbon dioxide emission which contributes to global warming⁴. In addition, because of their inherently poor biodegradability and compostability, most petroleum-based plastics are very resistant to being degraded over a long time period. The disposal of plastics has become a severe problem. Up until recently, landfilling and incineration have been the two major means of disposing the waste plastics and have been causing massive damage to the environment this whole time⁵⁻⁷. Landfill sites have been continuously expanding due to the large consumption of plastics for the last decade. Massive quantities of plastic debris remain in landfill sites, producing harmful chemicals and gases to the environment. Incineration is emitting enormous amount of carbon dioxide to the atmosphere, which poses great threats to the environment in terms of escalating the global warming.

As such, in order to provide alternative materials to these petroleum-based plastics, great interest has been drawn towards developing functional bio-based or biodegradable plastics. One class of these plastics can be made from renewable sources like agriculture feedstock. The

application of these bioplastics can be greatly helpful with reducing the large consumption of petroleum^{4,8,9}. Another class of bioplastics is either biodegradable or compostable, allowing them to be disposed without leaving hazards to the environment. The implementation of these bio-based or biodegradable plastics is the future trend of the plastic industry¹⁰⁻¹².

1.2 Bioplastics

Due to concerns regarding the current reliance of the plastic industry on petroleum and the environmental problems raised by the mass consumption of conventional plastics, bioplastics are of great current interest to academic researchers as well as industry managers¹³.

Bioplastics are produced using biopolymers or their blends and composites. In regards to the definition of biopolymer, there has been some misunderstanding about it. A biopolymer is not necessarily both bio-based and biodegradable¹⁴. Some biopolymers are bio-based but not biodegradable, whereas some biopolymers are biodegradable but not bio-based. Based on the source of the raw material and the biodegradability, biopolymers can be classified into three categories, which include petro-based biodegradable polymers, renewable source based polymers, and polymers from mixed sources (renewable and non-renewable)^{14,15}. The categorizations of different biopolymers are depicted in Figure 1.1.

As for the petro-based biodegradable polymers, they are synthesized using raw materials derived from petroleum resources¹⁶. This class of polymers takes up the major share of the market as their superior properties and broad application fields. Examples of polymers in this class are poly(butylene adipate-co-terephthalate) (PBAT) and polycaprolactone (PCL).

Renewable source based polymers are polymers that are synthesized using completely renewable resources, such as, agricultural feedstock or by-products of biotechnological processes⁸. As advancements in technology, the production of this class of biopolymers already starts to grow rapidly. Some popular members in this class are poly(lactic acid) (PLA), bio-based polypropylene (PP) and bio-based polyethylene (PE).

Those polymers from mixed sources are synthesized using a combination of both petro-based and bio-based monomers⁸. Some examples are poly(trimethylene terephthalate) (PTT) and bio-based thermosets.

The main objective of bioplastic development is conservation of fossil resources and air quality³. Since many bioplastics are derived from renewable sources, the use of these bioplastics can help to diminish the heavy dependence on the petroleum raw materials that are consumed by manufacturing the conventional plastics. In the case of bio-based bioplastics, the production contributes less carbon dioxide emission to the environment than that of the petroleum-based plastics, resulting in reducing the carbon footprint during the manufacturing. In other words, by using bioplastics, fossil-based raw materials are preserved and carbon dioxide emissions are reduced, resulting in the mitigation of global warming¹⁷. Moreover, the biodegradability and compostability of some bioplastics can greatly help in reducing the garbage volume and the impact from the over-landfilled areas.

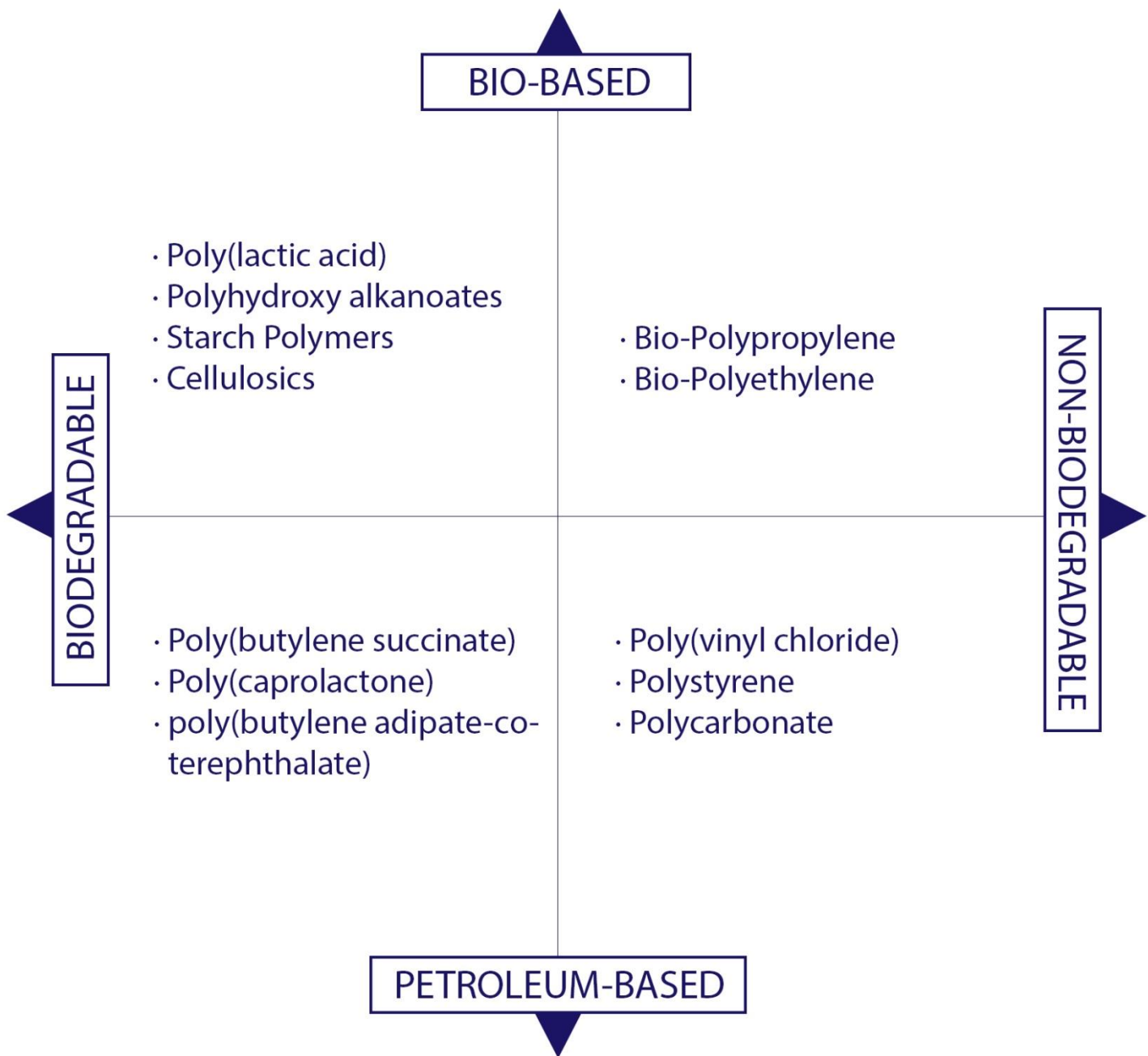


Figure 1.1 Classification of Biopolymers

(Modified after reference - Endres, H.-J.; Siebert-Raths, A. Engineering Biopolymers. Eng. Biopolym. 2011.)

1.3 Flexible Plastic Films for Packaging

The flexible packaging industry has had two major breakthroughs in its history. In the 1920s, the introduction of cellophane became a better alternative to traditional packaging materials. A significant fraction of the packaging material for various products was shifted from metals and glass to cellophane since cellophane provided much more convenient and lighter weight flexible packages¹⁸. Flexible packages also require less material, resulting in reducing cost. Additionally, flexible packages are beneficial in terms of providing economic savings in storage space and transportation. All of these advantages made the flexible packaging industry grow dramatically fast. In the early 1950s, another revolution took place due to the commercialization of plastic films. Better properties and lower cost made plastic films a superior flexible packaging material as compared to cellophane. Ever since then, the flexible packaging industry has been dominated by plastic films¹.

There are two common forms of the flexible packages, which are wraps and bags. Wraps are plastic films which have not been made into package shapes. With this method, the product is simply wound up in the plastic film and stored. In regards to bags, plastic films are formed in shapes either before or at the same time as when the product is being packaged. The most commonly applied technique for the shaping of these plastic films is the heat-sealing of the edges.

Two plastic resins which are majorly being used to produce flexible plastic films for packaging are chosen to be listed and discussed below.

Low-Density Polyethylene (LDPE) and Linear Low-Density Polyethylene (LLDPE)

Low-density polyethylene and linear low-density polyethylene are widely used for the flexible packaging films in various applications. LDPE has a long molecular chain branching structure that is produced by a high pressure and high temperature copolymerization process. LLDPE is produced through a high temperature but low pressure copolymerization process in the presence of few monomer, such as butane, hexane or octane¹⁹. It has a linear structure consisting of polyethylene backbones that possess branches of short chains or monomer units²⁰. LDPE and LLDPE are flexible materials with excellent mechanical properties and good processability. Due to LLDPE's branching structure, its crystallization is hindered, resulting in lower crystallinity than LDPE. As such, LLDPE presents higher tensile strength, puncture resistance and impact strength than LDPE. On the other hand, LDPE is superior to LLDPE in terms of processability as the extrusion of LLDPE requires higher screw speed and pressure²¹. In addition, LDPE can be sealed at lower temperature with a wide temperature range, exhibiting better heat-sealing properties than LLDPE. LDPE and LLDPE have very good water vapor barrier properties while being poor barriers to gases like oxygen and carbon dioxide¹. They can also maintain their excellent flexibility at very low temperatures thanks to their sub-zero glass transition temperatures. However when being exposed to heat, they cannot retain their good performance. Furthermore, blending LDPE and LLPDE is a promising approach to obtain flexible packaging material with superior performance²². Because of their excellent processability, they are suitable for either film casting processing or film blowing processing. In current industry, they are mostly produced with film blowing processing techniques.

Polypropylene (PP)

Polypropylene is synthesized via polymerization of propylene monomers. Most of the currently used PP has an isotactic structure²³. The density of the PP is only 0.88-0.91g/mol, which is the

lowest density among the commodity plastics. The stiffness of PP is better than that of LDPE, which gives it the advantage to be applied in the high-speed packaging applications where demand stiffer materials¹. The clarity of PP is another advantage and can also be further enhanced by incorporation of polymer that consists of ethylene monomers to decrease the crystallinity. Unorientated PP films present insufficient strength (30 MPa), particularly under low temperature condition. To deal with its lack of strength, PP produced from biaxial extension film process like film blowing process exhibits much better strength than that of the unorientated film^{1,24}. It also has superior water vapor barrier properties. However, the heat-sealing property of PP film is not favorable. Typically, coating or coextruded with sealants is needed to help PP film seal well.

Ethylene vinyl alcohol (EVOH), poly(ethylene terephthalate) (PET) and polyvinyl chloride (PVC) are also widely used as flexible packaging materials. They either possess favorable barrier properties in terms of oxygen or water or show superior mechanical properties. Currently, the majority of the flexible packaging market is taken by these conventional petro-based plastics. Since flexible packaging is a substantial component of modern society and a mostly short-lived product, the consumption of packaging materials is huge and shows a continuously uptrend. This enormous consumption of petro-based plastics raises great environment concern in terms of the disposal of these materials. Landfilling has been commonly used for the disposal of flexible packaging materials, which are continuously accumulating large quantities of waste plastic debris in the environment as contaminants and toxicities to nature.

Reuse and recycling are critical actions that are being undertaken to reduce the impact from the landfilling problem. However, post-consumer packaging material is challenging to reuse and recycle as there is often a variety of plastics in each composition. For example, packages with

multi-layered structures and packages with an aluminum foil center layer, which are designed to achieve favorable barrier properties, are extremely difficult to be recycled in terms of separating the individual layers respectively. The separation, identification and recycling of each individual layer requires more steps and energy than that for recycling traditional plastics. In addition, many flexible packages are contaminated by food products, which become another obstacle for reuse and recycling of flexible packaging materials.

As such, it is imperative to develop an alternative way to make the flexible packaging solutions more sustainable and eco-friendly. Bioplastics are considered to be promising candidates as packaging materials to help the sustainable growth of the flexible packaging industry.

1.4 Importance of Research on the Development of Bioplastics Films for Flexible Packaging Application

As mentioned previously, the flexible packaging industry needs to provide more sustainable and eco-friendly solutions in order to attain long-term sustainability of its growth. Therefore, the development of bioplastics for packaging applications is of great interest to researchers, industrial managers and government. In Europe, the entire flexible packaging market, which includes both the manufacturer and consumer, is moving towards “greener” solutions, such as reusable and recyclable packaging, bio-based packaging and biodegradable or compostable packaging. This trend has been promoted by EU directives as well. Several world-wide initiatives have been launched with a mutual focus on developing bioplastics to replace conventional petro-based flexible packaging materials²⁵. Europe is currently leading the movement in advancing bioplastics packaging across the globe. It can be seen that the future trend is to turn the flexible packaging market from petro-based material dominant to bioplastics

dominant. Moreover, the bioplastic industry has started to grow in an increasing rate recent years, which can be seen by the rising annual production and demand of the plastics over the world^{26,27}, which will continue to promote the development of the bioplastic packaging.

However, even though the bioplastic packaging industry is growing rapidly and has all sorts of factors promoting it, it still falls far behind conventional plastic packaging industry.

Insufficient performance of bioplastics as compared to the conventional plastics is one important issue that limits the growth of the bioplastic packaging industry. Despite the biodegradability or bio-based nature of bioplastics, they also possess their own drawbacks when being applied as flexible packaging materials.

Mechanical and thermal performance are two critical factors that determine materials' viability of being processed and manufactured in a large scale and applied in different packaging solution fields. Many bioplastics are deficient in some aspects of these two performances when compared to the conventional petro-based plastics. For instance, in this study, PPC presents large elongation but low strength, whereas, PLA owns high strength with almost no elongation. PPC is also lack of thermal stability and shows very low glass transition temperature.

In addition, the barrier performance of the material is another pronounced factor for flexible packaging in terms of maintaining the shelf-life of the packaged products. Most of bioplastics can be efficient in one barrier property either for oxygen or water barrier but deficient in the other one. For example, the oxygen barrier property of PLA surpasses that of PP and PE, whereas, the water barrier property of PP and PE are much better than that of PLA.

As a result of aforementioned economic trend of flexible packaging industry and insufficient performance of bioplastics, the development of bioplastic film is increasingly important in

terms of achieving bioplastic flexible packaging with optimum performance that can be comparable to the conventional plastics and be able to meet various requirements of flexible packaging industry.

Chapter 2 Literature Review

2.1 Polypropylene Carbonate (PPC)

Polypropylene carbonate (PPC) is a bio-based amorphous, thermoplastic polymer, which can be synthesized from CO₂ and PO using a supported catalyst.¹² More than 50% of CO₂ by weight can be converted into PPC, showing the cost competitiveness and environmental friendly advantages of PPC. In addition, PPC is a biodegradable polymer; its degradation and decomposition can easily occur in the soil, in some solvents and under weathering conditions. These factors demonstrate its potential to be a substitute for petroleum-based plastics and resolve the major landfill issue caused by the low degradability of petroleum-based plastics¹³.

Moreover, PPC can also provide some favorable properties as a thermoplastic polymer when applied in industrial products. One of the favorable properties is its good melt flow characteristics. The ester units in PPC's structure provide chain flexibility, resulting in the feasible melting process-ability of PPC. However, the poor thermal stability of PPC limits the maximum process temperature to some degree, as PPC may begin to decompose during the process¹⁴. Currently, many studies have been conducted to improve the thermal stability of PPC, and to further enhance the process-ability of PPC when applying into large scale applications.

Another favorable property of PPC is the large elongation at break, which gives opportunities to add fillers into PPC or blend PPC with other polymers to enhance its poor stiffness (tensile strength and Young's modulus) to a useful range to be eligible for many industrial uses, while maintaining the acceptable toughness.¹³ Many PPC-based biodegradable blends and composites have been proposed for applications as industrial products, such as films and automotive parts.

According to the aforementioned considerations, the conversion of CO₂ to PPC is a feasible way to utilize waste CO₂ instead of emitting it into the atmosphere and reduce the environmental burden. This polymeric material PPC can also store CO₂ during the life of the products and provide means for longer CO₂ sequestration. The non-toxicity and good biodegradability of PPC also provides a choice of an environmentally friendly material, rather than conventional plastics.

2.2 Poly (Lactic acid) (PLA)

Poly (Lactic acid) (PLA) is an aliphatic polyester thermoplastic derived from renewable sources, which are primarily sugar and starch. PLA is compostable and non-toxic. It possesses excellent strength and modulus, but poor ductility and HDT. Because of these advantages, PLA has been considered to be the most promising and practical biopolymer. The earlier application of PLA was limited to only medical products, such as stitches and implanted devices²⁸. With the advancing of PLA technology, its uses are expanding in packaging to a number of new industrial products.

The synthesis of PLA can be accomplished by the polymerization of lactic acids. The raw material used to produce lactic acid is mainly derived from sugar, corn and starch, which is inexpensive and easy to obtain. The basic synthesis of lactic acid involves a biotechnical process, which starts with the fermentation of dextrose. After the fermentation, low Mw PLA is produced via a condensing reaction process. Lactic acid enantiomers are obtained through the conversion of low molecular weight PLA, which is followed by purifications. At last, the high Mw PLA is produced through a ring-opening polymerization process^{28,29}. The monomer of PLA, lactic acid, can exist in both D- and L- enantiomers. The ratio of these two enantiomers in the

PLA can provide materials with variable properties³⁰. This advantage allows PLA to be designed and produced specifically to match different requirements.

The superior properties of PLA are the main reason that makes it such an attractive biopolymer. It presents good biodegradability and biocompatibility. Unoriented PLA provides considerably good strength and modulus. Orientated PLA shows even better performance than many conventional plastics, such as PS²⁸. Its tensile and flexural strength and modulus surpass high density polyethylene and propylene, whereas its impact strength and strain at break are much lower than those of HDPE and PP. It has a relatively low heat deflection temperature, which also limits its application in high temperature environment³⁰⁻³². PLA also possesses reasonable barrier properties in regards to oxygen and water vapor, which is comparable to some of the conventional plastics, like PET, PS and etc. Since PLA lacks toughness, numerous studies have been focused on enhancing its toughness. In addition, through proper modification, the barrier performance of PLA can be good enough to fulfill the requirements for many packaging applications^{3,4,33}.

2.3 Polymer Blends

Polymer blends are usually referred to “polyblends” and sometimes as “alloys” to get an idea from metallurgy³⁴. Polymer blends are defined as any combination of two or more polymers resulting from physical blending. Nowadays, polymer blends are attracting more global interest in academic research as well as industries. Their current and potential technological significance is remarkable, which can be proved by their ubiquitous presence in consumer products³⁵. In comparison with copolymerization, polymer blends are able to provide a means of combining useful properties of different polymers and substances through physical process steps instead of

chemical approaches. Moreover, the pursuit of further understanding of the physical properties and mechanical performances of polymer blends has developed new principles and revealed new opportunities for research and addressing practical issues.

There are two major factors of the polymer blends that have been studied most in recent research³⁶. One of them is the immiscibility. Due to the thermodynamic issues, the polymer blend system is generally not miscible, and the degree of compatibility varies in a wide range. Since the compatibility and miscibility of polymer blends has critical significance to morphology and properties, numerous studies have been conducted to modify and improve the immiscibility of the blends.

Along with the immiscibility, the interaction of melt flow with the interfacial behavior and the viscosities of the blend system is another major factor. This factor can also be identified as the morphology of the blends. The morphology highly depends on the blend concentration^{36,37}. When at low concentration of either component, the dispersed phases form nearly spherical drops, whereas at high loading cylinders, fibers, and sheets form. It is said that at both ends of the concentration scale, the blend is dispersed, and in the middle, it is co-continuous. Overall, the polymer blends can provide an incredibly wide range of various morphological states from coarse to fine, which are being intensively studied and investigated. Since the tension transfer inside the polymer blends is greatly affected by the states of morphology, it is of great importance to modify and control the morphology of polymer blends.

2.3.1 Physical Blending

The physical blending is referred to the simple compounding of polymeric materials through melt-processing without any chemical reactions taking place³⁵. The outcome of physical

blending is called a polymer blend. Physical blending is reported as a convenient route to create new materials with improved properties. Additionally, this process also has its advantages in terms of cost competitiveness and time-saving. Since physical blending can be accomplished with conventional machinery in a short time period without expensive investment, it is much preferred by industries.

The goal of physical blending is defined as to improve or tailor the properties of polymeric materials to certain desired applications; in most cases, to maximize the performance of the materials. To be more specific, physical blending is able to accomplish diverse objectives in light of obtaining desired materials, such as cost reduction, general improvement of mechanical properties, impact resistance, decrease of sensitivity to water, increase of barrier properties, improved biocompatibility, etc. Many successful cases of employing physical blending as a materials modification approach can be seen in current research and industry.

2.4 Development of PPC-based Bioplastics

As a biodegradable and bio-based polymeric material, PPC is considered to be a good candidate to complement and replace some of the petroleum-based plastics in various applications.

Additionally, its large elongation at break is useful for many applications. Numerous studies have highlighted the benefits of producing PPC in terms of helping to mitigate the CO₂ emission while reducing the current reliance on the conventional fossil-based plastics³⁸.

However, the property profile of neat PPC cannot fulfill many requirements, as it is neither typical for engineering plastics nor rubbers.

PPC presents an amorphous structure and a relatively low glass transition temperature which is within the range of human body temperature. Additionally, the inherent low stiffness and poor

thermal stability also limit PPC's industrial application to a large extent³⁹⁻⁴¹. Many studies have been conducted focusing on improving the properties of PPC and exploring new applications of PPC.

PPC/Inorganic Nano-filler Composites

ZnO nano-filler has been employed to improve the stiffness of PPC. It was reported that PPC and ZnO nano-filler were prepared through melt compounding in a rotary mixer at 180 °C.

Good dispersion of the nano-size filler in the PPC matrix was observed, indicating good binding between the PPC matrix and particles, which was suggested to partially contribute to the improvement of the stiffness of PPC⁴². The tensile strength and the elastic modulus were improved to 32 MPa and 1700 MPa with 10% wt filler in the composites compared to the neat PPC. Moreover, the increase of these two properties remained constant with more content of filler in the composites. However, the elongation at break was reduced with the addition of filler and showed a constant decreasing trend with an increasing level of filler content⁴³. In addition, it was observed that the smaller the filler particle, the better the dispersion of the filler in the PPC matrix, consequently resulting in further improved stiffness. Along with the mechanical properties, both the oxygen and water barrier properties of the composites were greatly enhanced compared to neat PPC⁴⁴. Based on the aforementioned improvements and advantages, PPC and ZnO nano-filler composite is considered to be an excellent candidate to be applied in the packaging field. More noticeably, good antibacterial properties were also obtained, which further solids the feasibility of implementing this composites for packaging application. However, all the process and test results are only at the laboratory scale. Future study on the large-scale production and implementation of this material needs to be conducted.

PPC/Corn Starch Composites

Blending PPC with natural corn starch has been implemented and studied by several research groups. In the research, PPC and the corn starch were blended through melt compounding at 150 °C⁴². During the process, no obvious degradations of PPC in molecular weight were observed, which indicates the feasibility of processing these blends. It was reported that the tensile strength of the composites was improved with no more than 40% starch content. When the starch content went above 40%, the tensile strength slowly decreased. However, as soon as the starch content exceeds 60%, the tensile strength decreases dramatically, even below the value of neat PPC. This is probably caused by a good compatibility between PPC and the OH groups in corn starch⁴⁵. On the contrary, the elongation at break shows a decreasing trend with the addition of the starch from 1.5% to 35%, resulting in brittle samples. The thermal properties of the composites (glass transition temperature and thermal decomposition onset temperature) have little dependence on the composition of the composites; however the overall thermal properties of PPC still improved in the composites^{42,45}. The PPC- starch composites are totally bio-based and biodegradable, which gives favorable environmental friendly properties. In addition, the improved mechanical and thermal properties of the composites give this material great potential to be applied in automotive parts. However, further studies on preventing the decrease of the ductility are still requested.

PPC/PHB Blends

Poly (3-hydroxybutyrate) (PHB) is biodegradable thermoplastic polyester. Its superior biodegradability and bio-compatibility makes it a favorable material under the circumstances of global warming. Additionally, PHB also has very similar properties to polypropylene, which is

a commonly used petroleum-based plastic. But, the brittleness and high price of PHB limits its commercial application⁴⁷. Since PPC is a ductile material with high elongation at break, it was proposed that blending PPC with PHB could be an applicable routine to produce polymer blends with improved and optimized properties.

The blend of PHB and PPC was prepared through solution blending with the chloroform as the solvent at room temperature. After that, the blends were cast into film samples⁴⁷. Two independent glass transition temperatures in the blends were observed, indicating the immiscibility between PPC and PHB. Additionally, no changes were detected in the two independent glass transition temperatures. The crystallization behavior of PHB did not show any significant changes as PPC was added into the system. The SEM observation of the blends showed a clear phase separation between the PPC and PHB phases. All of the above observations demonstrated that there was no miscibility between the two polymers. However, the elongation at break of PHB was significantly enhanced with little decrease in the tensile strength, which is considered to a favorable characteristic of the blends. Although, the blend of PPC and PHB presented no miscibility, the properties of the blends were improved compared to the two original^{47,48}. Thus, it is worthwhile to generate more future studies to modify and improve the miscibility of the PPC/PHB blends so that a new green material with favorable properties can be provided.

PPC/PHA Blends

Polyhydroxyalkanoate (PHA) is a bio-based and biodegradable polymer, which has great potential application in a wide range, including the packaging and biomedical fields. The issue with PHA is its fragile mechanical behavior, which results in extremely brittle materials⁴⁸. With

the intention of utilizing the ductility of PPC to modify the brittleness of PHA, the blend of PPC and PHA was prepared through extrusion blending at 170 °C. Then, the blends were transformed into tensile samples by injection molding at 170 °C, and films were also prepared by extrusion⁴⁹. After the characterization, it was reported that the fragile mechanical behavior of PHA was modified by PPC, as improved elongation at break was observed. The impact strength of the blends also significantly increased compared to the neat PHA, which is a significant improvement in terms of being utilized in packaging applications. Moreover, the barrier properties of PPC for both oxygen and water were enhanced due to the high crystalline content of PHA. This study demonstrated that blending PHA and PPC could be a practical and feasible way to extend their application field as bioplastics, especially in the packaging field. Achieving phase compatibilization would be the next objective of this study. Also, the feasibility of large scale production of the blends requires further investigation.

PPC/PLA Blends

Poly (Lactic acid) (PLA) is a brittle polymer with high stiffness, which can be derived from fully renewable feedstocks⁴⁸. In one study, a blend of PPC and PLA was prepared through extrusion blending at only 110-120 °C⁵⁰. Two independent glass transition temperatures assigned to PLA and PPC respectively were observed. It was reported that the T_g of PPC phase increased from 22 to 34 °C with increasing PLA component in the blends, whereas the T_g of PLA phase decreased slightly by 3 °C as increasing the addition of PPC in the blends. The changes of the T_g of both polymers indicated the partial miscibility between PLA and PPC. The Young's modulus changed linearly with the increasing PLA content in the blends from 100 to 3200 MPa for pure PPC; meanwhile, the yield strength was enhanced from 4 to 60 MPa. It was

proposed that a substantial interfacial adhesion existed between the PLA and PPC phases, resulting in the linear behavior of the Young's modulus and yield strength. Two rubbery plateaus were observed on the stress-strain curves when the PLA content changed from 30% to 60%. It was suggested that a reversal of the continuous phase from PLA to PPC occurs at approximate 30% PPC content, giving the explanation for the various mechanical behaviors. It was also mentioned that the thermal stability of PPC was improved in the blends compared to neat PPC.

However, another study on the PLA/PPC blends gave different experimental data and conclusions from the aforementioned study. In this study, the blend of PPC and PLA was also prepared through extrusion blending, but at a temperature of 170 °C⁴⁸. There were no changes observed in the T_g of the two polymer phases. Moreover, it was reported that a good dispersion of the components in the matrix was detected, illustrating a good compatibility. The Young's modulus ranged from 600 to about 3800 MPa, and the yield strength linearly changed from 4 to 80 MPa.

One possible reason for the different experimental data can be the various sources of the polymers which these two studies used. However, the inconsistent results and conclusions from these two studies still demonstrate the lack of thorough understanding of the PLA/PPC blend system. Thus, there is a strong need for further study to analyze and investigate the PLA/PPC blend system in order to obtain optimal blends for future applications as a bio-based and biodegradable material.

2.5 Incorporation of Chain Extender in the Biopolymer System

Despite the advantages of biopolymers, their inherent deficiency in mechanical properties, melt flow, melt strength and thermal stability limit their processing window and large scale applications. Great efforts have been dedicated to the modification of biopolymers in terms of tailoring their properties to meet different requirements for various applications, such as packaging and automotive applications. PLA is currently the most commonly used and commercially available biopolymer. With the intention of enhancing its melt strength and thermal stability and to maintain its high molecular weight during the melt extrusion and molding process, chain extenders are of great interest in being applied in the PLA system.

Chain extenders are normally low molecular weight multifunctional compounds. They consist of different multiple functional groups in the molecule chains. Poly-functionality and thermal stability are generally merits of these chain extenders. Several chain extenders were reported in the literature, and are listed in Table 2-1 here.

Table 2-1 List of typical chain extenders^{32,51,58}

Classifications	Chain extenders
Diisocyanate compound	Hexamethylene diisocyanate (HDI)
Dianhydride compound	Pyromellitic dianhydride (PMDA)
Bisoxazolines compound	1,3-Phenylene bis(2-oxazoline-2) (PBO)
Multi-functional epoxy compound	Joncryl ^R ADR 4368F; Joncryl ^R ADR 4368C
Diimide compound	Polycarbodiimide (PCDI)
Tris(nonyl-phenyl) compound	Tris(nonyl-phenyl) phosphate (TNPP)

It is suggested that the addition of chain extenders help reconnect the polymer chains that break down during the processing, resulting in improved molecular weight in the polymers⁵¹. This is caused by the reaction between the chain ends of the polymer and the functional groups of chain extenders. Since the reduction of the molecular weight of polymers (degradation), especially for some biopolymers, always occurs during the processing i.e. melt extrusion, injection molding, the presence of chain extenders can maintain the high molecular weight of processed polymers or even increase the molecular weight, which always leads to more stability and better properties^{52,53}. In addition, the reactions between polymers and chain extenders usually happen fast enough to be done during the extrusion of polymers without the need of extra residence time, which is preferable when processing polymers⁵⁴. Because of the multiple functional groups in chain extenders, it is proven that polymer chains can form long chain branch structures and crosslinking structures during processing with chain extenders. The formation of long chain branch structures further controls the

degradation of polymers while enhancing the melt strength of polymers as well as the mechanical properties of polymers, such as tensile strength and elongation⁵⁵. As for the occurrence of crosslinking, strength and thermal stability gain further improvement as a result of decreased polymer chain mobility. It was also noted that the incorporation of chain extenders can be used as a reactive compatibilizer in polymer blends^{55,56}. However, with increased molecular weight induced by chain extenders, the viscosity of melt polymers increased, causing a dramatic reduction of the melt flow index (MFI) of the polymers^{56,57}. Hence, the processing window can be limited since many of the processes cannot be accomplished with the polymers having a very low melt flow rate, i.e. injection molding.

In many cases, chain extenders are used in poly (ethylene terephthalate) (PET) products. PET is widely used in bottles and films for packaging applications as it provides outstanding mechanical performance, barrier performance and chemical resistance⁵⁹. However, degradation always takes place during the processing of PET. The application of chain extenders has proven to be successful in preserving the high molecular weight of PET through reconnecting the chain fragments during the melt processing^{52,54,56}. Better recyclability and mechanical performance are also achieved with the application of chain extenders^{60,61}.

In recent years, as the development of biopolymers has increased, PLA has been of great interest for tailoring into applicable products. Because the degradation of PLA during the melt extrusion is one of the issues that prevent PLA from being widely manufactured, avoiding degradation and maintaining the high molecular weight as well as the mechanical properties are subjects to be extensively studied^{62,63,64}. Many researchers found it might be promising to apply chain extenders in the PLA system^{55,62,65}. One study shows that the thermal stability as well as the molecular weight of the PLA was enhanced through the melt extrusion with chain extenders.

Three types of chain extenders were studied: TNPP, PCDI and Joncryl ADR4368-R⁶³. The occurrence of chain extension was suggested to be the mechanism for improvement. In TNPP and PCDI, formations of long linear chains were found. As for Joncryl, long chain branched structures and cross-linking contributed to the chain extension. In another study, a multifunctional chain extender (CESA) was applied in the PLA/PBAT blend system⁵³. The melt strength and elongation at break of the blend were reported to be largely improved due to the incorporation of chain extender. The thermal stability was enhanced as well. It was also mentioned that the improved compatibility between the PLA and PBAT could be one of the main reasons that led to those improvements. Hence, the chain extender also revealed its function as a compatibilizer.

To conclude based on many studies done by other researchers, the application of chain extenders in the biopolymer system can be a promising way to enhance the processibility and performance of the polymers. This gives a greater chance for biopolymers to be used in large scale applications in various fields.

2.6 Film Processing

Packaging application has been taking up a huge share of the plastic industry. Plastic films are seen everywhere in the daily life as being used for packaging material. Millions of tons of plastic films are being manufactured every day. The two most commonly applied techniques for plastic film processing are film casting processing and film blowing.

2.6.1 Film Casting Processing

Film casting processing is a conventional way to produce thermoplastic films. Many of the thermoplastic films that are being used in different packaging applications are manufactured using this technique⁶⁶. The basic components and principles of the process is portrayed in Figure 1. This processing typically involves a single-screw extruder in the first stage, which melts and extrudes the polymer pellets fed from the feeder. Right after the extrusion, molten polymer is casted into film through a flat die which is attached to the end of the extruder barrel^{34,67}. After the film is stretched in the air by the roll, it is then solidified and quenched on a chill roll while retaining the film's shape. Typically, air knives are applied when the film reaches the chill roll to gain better formation and cooling of the cast films^{25,34}. The schematic of film casting processing is shown in Figure 2.1. In most cases, after this casting process, films are subjected to further processing, such as thermoforming, stretching to develop biaxial orientation or coating on other products to obtain the final product⁶⁸⁻⁷⁰. There are several important factors in this film casting process that have been reported:

- 1) Draw ratio
- 2) Air gap length
- 3) Roll temperature

Draw ratio is defined as the ratio of velocity of the chill roll to the velocity of the film coming out from the flat die. Draw ratio is critical in determining the thickness and physical structure of the forming film. In addition, it is also important to understand the draw ratio and manipulate it since changing processing material requires relative adjustment to the draw ratio^{67,71,72}.

Increasing the draw ratio has always been a means to enhance the productivity. However, lack of proper understanding of the role of draw ratio in the film casting processing will always lead to undesirable consequences, such as the formation of neck-in and edge bead of the film or film

breakage⁷³⁻⁷⁵. The air gap length is defined as the length between the flat die exit and the point where the film touch the first take-up chill roll. This air gap length determines the how long the film is kept in the air, affecting the cooling and strain rate experience, crystallization and physical appearance of the films⁷⁶⁻⁷⁸. In terms of avoiding trapping air and eliminating the film defects, shorter air gap length is recommended for most of the material. It was found in one study that longer air gap length arose more formation of neck-in of the film⁷⁹. The increase of neck-in appearance may lead to formation of thicker films^{45,46}. Roll temperature also has an effect on the film forming when the film is cooled and solidified on the chill roll. The effect is varied depending on the properties of the material⁸⁰. Some studies reported that in regards to the film casting process of PLA, the condensation and slippage of the film need to be avoided by a relatively high roll temperature (25-50 °C)²⁸.

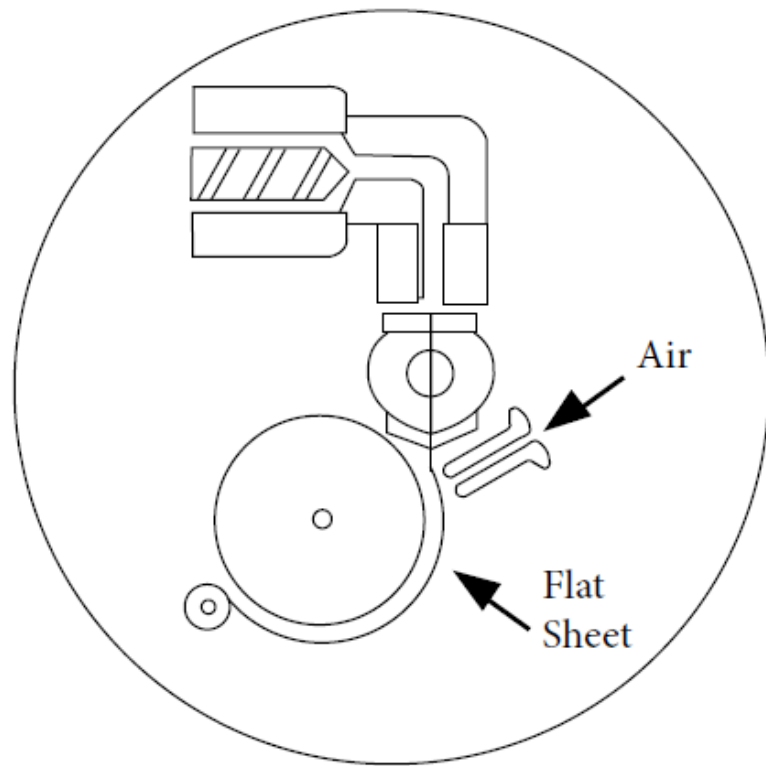
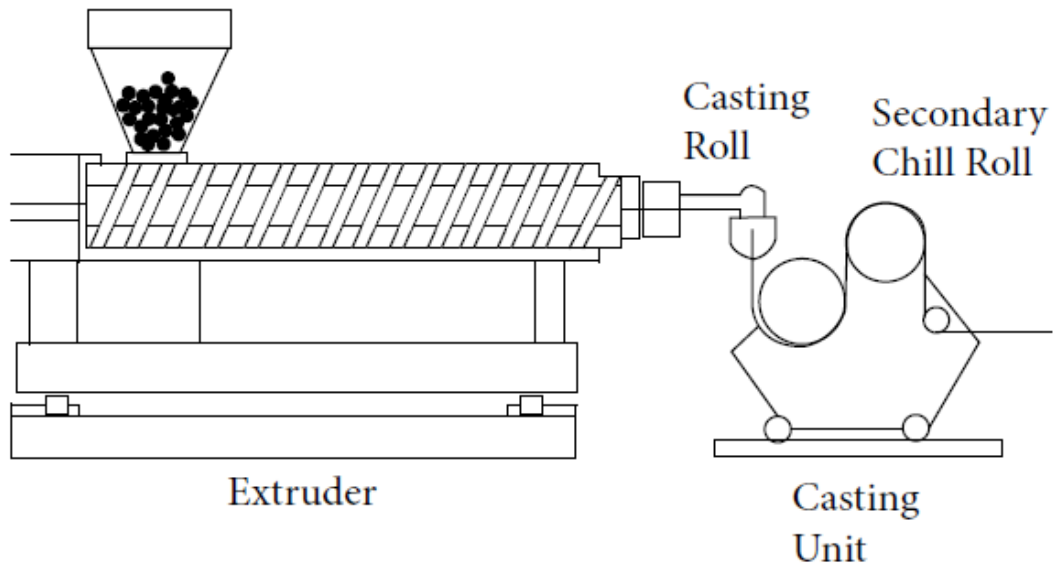


Figure 2.1 Cast film Processing

2.6.2 Film Blowing Processing

Film blowing processing is an industrial technique to manufacture plastic films. The majority of plastic films are produced with this film blowing process. The cross-section of the typical elements of the process is depicted in Figure 2.2. It involves an extruder, an annular die, a tube (also called bubble) formed by the polymer, air suppliers and several rolls (nip rolls and guide rolls)⁸¹. The polymer pellets are firstly fed in the hopper and melt extruded through the extruder. The molten polymer then exits from the annular die and forms a bubble with the assistant of the supplied cooling air. Compressed air is supplied in the center of the bubble. The cooling air supply surrounds the middle to the upper part of the bubble. The polymer formed bubble then solidifies and is collected by the guide rolls and nip rolls into flat sheet or film. The place that is above the die at which the solidification occurs is called the freeze line⁸¹. The cooling air can be used to control where the freeze line occurs. Above the freeze line, the deformation of the polymer formed bubble is negligible. Three important factors during this film blowing process are the thickness reduction (TR), draw ratio (DR) and blow-up ratio (BUR). The thickness ratio (TR) is defined as the ratio of the space between the annular die and the bubble to the thickness of the film at the freeze line, which is normally around 20-200. The draw ratio (DR) is defined as the ratio of the velocity of the polymer at the freeze line to the velocity of the polymer at die, which is reported typically within the range of 10-40. As for the blow-up ratio (BUR), it is the ratio of the diameter of the polymer formed bubble at the freeze line to the diameter of the inner die, which typically falls in the range of 1-5⁸². The blowing and drawing process of the polymer film during the film blowing process can shape the film into a biaxial orientation non-uniformly. Films with biaxial orientation exhibit much better properties compared to those films with only one axial orientation in terms of mechanical properties, barrier properties, etc^{83,84}. Hence,

achieving films with biaxial orientation is the primary attractive characteristic of this film blowing processing.

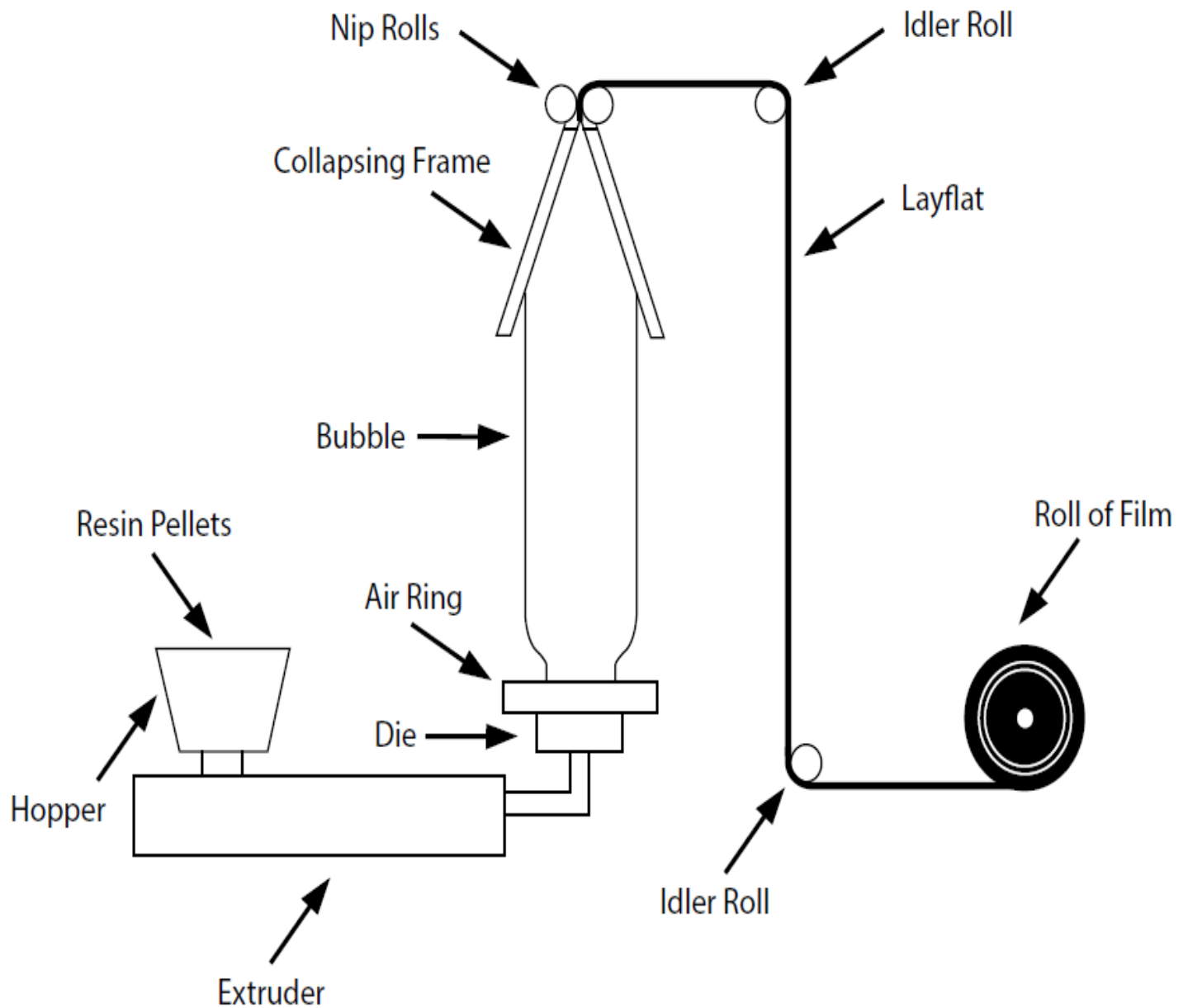


Figure 2.2 Film Blowing Process

2.7 Water Vapor and Oxygen Permeability

The permeation of water vapor and gas through the polymer film mainly consists of three processes, which are listed below:

1. Sorption of the permeant molecules into the polymer film (adsorption and absorption)
2. The diffusion of permeant molecules inside the polymer matrix throughout the film.
3. The desorption of the permeant molecules from the other side of the film surface.

Thus, the permeability of the certain permeants is affected by the solubility of the permeant in and the diffusion coefficient of the permeant in regards to the polymer film, which can be expressed with the equation:

$$P = DS$$

where P stands for permeability, D represents diffusion coefficient and S is the solubility coefficient, respectively.

The solubility coefficient is related to the variance between solubility parameters of polymer and the permeant, molar volume of the permeant, temperature and major characteristic of polymer. The solubility coefficient of different permeants as to different films can vary in a large range.

The diffusion coefficient can be affected by the activation energy of the permeant in the polymer matrix, the fraction free volume of the polymer structure, the crystallinity of the polymer, polarity of the molecular chains of the polymer, pressure difference of the permeants between the two sides of the film and temperature.

Therefore, the permeation of the water vapor and gases is a complicated process, which can be affected by too many variables, resulting in the unpredictability of the permeability of water vapor and gases. There has been great interest recent years in attempting to diminish the permeability of water vapor and oxygen as lower permeability means less mass transfer between the packaged products and outside environment. Frequent mass transfer of oxygen and water between the packaged products and outside environment can greatly compromise or deteriorate the quality of the products in many ways, leading to shorter shelf-life.

The term “barrier property” is always used in the packaging field, which represents the ability of the material to prevent certain permeants from permeating through, such as water vapor or gas. The barrier property is just an expression without actual value whereas permeability coefficients of the permeants can be used to quantify the barrier property. Higher permeability indicates poorer barrier property in terms of certain permeant; and better barrier property comes with lower permeability. Hence, water vapor and gases permeability coefficients of various polymer films have been extensively studied. Biopolymers are currently of increasing interest in the plastic industry. In order to develop possible candidate for packaging industry with biopolymers, numerous studies have been conducted on the permeability of biopolymers, such as PLA and PPC.

Auras and his group studied the oxygen and water vapor permeability of poly (lactic acid) (PLA) under different temperature and relative humidity³¹. The results showed that higher temperature led to higher oxygen permeability whereas lower water permeability was detected with increasing temperature. The relative humidity did not have significant impact on both oxygen and water permeability. It was also reported that the oxygen permeability of PLA was lower than that of PS but higher than that of PET; and the water permeability of PLA was higher than both

PET and PS but in a comparable range. Their study indicated that PLA has the competitive performance as the conventional plastics in terms of oxygen and water barrier.

Another study conducted by Weber and coworkers have compared the biopolymers and conventional polymers in terms of their water vapor transmission rate (WVTR) and oxygen transmission rate as a low to high range. The OTR of PLA was reported to be lower than PS and PE but higher than PHA, PVDC and EVOH. The WVTR of PLA was claimed to be lower than EVOH but higher than PS PE and PHA²⁹. Studies also showed that the higher degree of crystallinity the PLA led to the lower permeability of both oxygen and water vapor⁸⁵.

There has also been some research focusing on studying the barrier performance of PPC. However, the results with regards to the oxygen and water vapor permeability of PPC from different research are not considerable consistent; and sometimes are contradicting. One study completed by Seo and his coworkers showed that the oxygen permeability of PPC is 25.3288 cc*mil/100in²-day-atm (calculated by myself in regards to their reported OTR)⁴⁴. Another study found the oxygen permeability of PPC to be 7.117 cc*mil/100in²-day-atm. It can be noted that the oxygen permeability coefficients from these two studies have large difference⁸⁶. There is also one study that claimed the oxygen permeability of PPC to be 0.00304 cc*mil/100in²-day-atm, which is even much lower than that of EVOH (0.0254 cc*mil/100in²-day-atm)⁴⁹. The reason for all these inconsistent results for the permeability of PPC could be the difference of the PPC they used as there is no specific grade designated for each PPC. And the properties of PPC from different manufactures can be significantly different because of the variance in the choice of catalysts and copolymerization processes⁸⁷. The various test equipment and test conditions seem not to be the reason for the inconsistency of the results as the calculation of permeability already takes those variables into consideration.

Chapter 3 Problem Statement and Hypothesis

3.1 Problem Statement

As the biggest contributor to the global warming, carbon dioxide (CO₂) emissions have largely been focused on. The major concern is to address the massive emission of CO₂. Direct utilization of CO₂ in making industrial products is a novel way to sequester CO₂. Poly(propylene carbonate) (PPC), which is a biodegradable polymer, can be synthesized by the copolymerization of CO₂ and propylene carbonate. This polymer is a possible alternative for synthetic polymers; however, it has its own drawbacks. It has low thermal stability, which makes it difficult to process. Its poor stiffness also limits its applications. Poly(lactic acid) (PLA), also as a promising biopolymer, has been extensively studied due to its favorable properties. Blending PPC with PLA can be an effective way to minimize the drawbacks of both parent polymers. The blend of PLA and PPC is a biodegradable system with possibility to be applied for packaging applications. However, in order to obtain more favorable mechanical, thermal and barrier performances, the appropriate blending ratio for PPC and PLA in the blends and proper compatibilization of the blends still need to be investigated.

3.2 Hypothesis

1. A biopolymer blend can be produced from physical blending PLA with PPC in an optimal blending ratio that is able to demonstrate enhanced mechanical, thermal and barrier performances as compared to the individual parent polymers.
2. The incorporation of the chain extender, in this case Joncryl ADR 4368-C, can achieve in improving the compatibility between PLA and PPC in the PLA/PPC blend, resulting in

enhanced mechanical, thermal and barrier performance. The compatibilized blend aims to be utilized for the packaging applications.

3.3 Objectives

The overall objective of this project is to develop a new class of bio-based and biodegradable green polymer film by combination of CO₂-based polymer PPC with PLA. The main challenges can be to achieve the balanced mechanical properties, especially toughness and strength and reasonable barrier properties of the final product as well as favorable thermal properties in comparison with the respective properties of the petroleum-based composites currently used in the industry. The developed bio-based polymer film is targeted to substitute for a class of petroleum-based composites currently used in flexible packaging applications.

Specific objectives are:

1. Determine the optimal blending ratio between the PLA and PPC to achieve blends with balanced mechanical performance in terms of ductility and strength as well as enhanced thermal performance in regards to PPC.
2. Prepare PLA/PPC blends with different concentration of Joncryl. Then, blends with different formulation are processed into cast films with the optimized film casting processing parameters.
3. Determine the mechanical, thermal and barrier performances of the produced films.
Explore the effect of the incorporation of chain extender on the PLA/PPC blend films.

Chapter 4 Materials and Methods

4.1 Materials

4.1.1 Poly(propylene Carbonate)

One of the biopolymers used in this study was poly(propylene carbonate) (PPC). The chemical structure of PPC is portrayed in Figure 4.1. This PPC resin was obtained from Henan Tianguan Enterprise Group Co. Ltd. (China). It was synthesized by the copolymerization of carbon dioxide and propylene oxide in the presence of catalyst. It has a density of 1.20-1.28 g/mol. PPC does not present any melting temperature sine the polymer has a totally amorphous structure. Some of the properties of PPC are presented in Table 4-1.

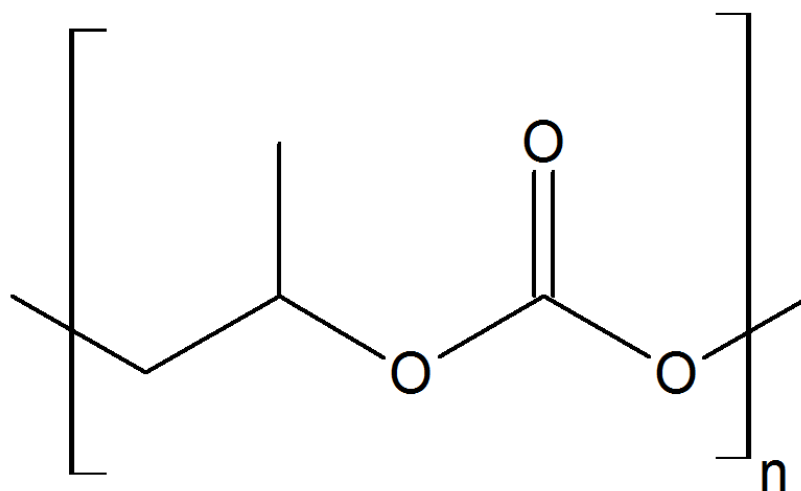


Figure 4.1 Chemical structure of Poly(propylene carbonate) (PPC)

Table 4-1 Typical Properties of Poly(propylene Carbonate) (PPC)

Density (25°C) (g/ml)	1.20-1.28
Number-Average Molecular Weight (g/mol)	200,000-500,000
Notch Izod Impact Strength (J/m)	>25
Glass Transition Temperature (°C)	25-39
5% Weight Loss Temperature (°C)	> 250
Ash content (%)	Less than 3
Hardness (Shore)	20-50
Melt Flow Index (g/10min)	0.5-1
PC (propylene carbonate) content (%)	Less than 1
Tensile Strength (MPa)	10-20
Elongation at Break (%)	>300
Polydispersity	4-6

*Data was obtained from the Henan Tianguan Enterprise Group Co. Ltd.

4.1.2 Poly (lactic acid)

The other biopolymer used in this study was poly (lactic acid) (PLA). The chemical structure of PLA is depicted in Figure 4.2. This PLA resin was purchased from NatureWorks LLC (United States). The grade of PLA used was 3001D. It has a density of 1.24 g/mol and a melting temperature around 170-180°C .Some of the typical properties of PLA are presented in Table 4.2.

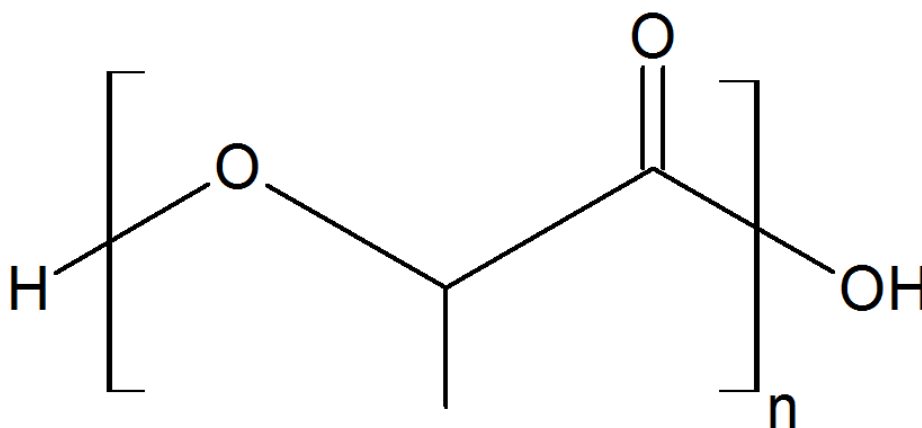


Figure 4.2 Chemical structure of Poly (lactic acid) (PLA)

Table 4-2 Typical Properties of Poly (lactic acid) (PLA)

Density (25°C) (g/ml)	1.24
Clarity	Transparent
Flexural Strength (MPa)	108
Heat Deflection Temperature (°C)	55
Flexural Modulus (MPa)	3600
Melt Flow Index (g/10min) (210°C, 2.16kg)	22
Tensile Strength (MPa)	62
Elongation at Break (%)	3.5
Notch Izod Impact Strength (J/m)	16

4.1.3 Joncryn ADR 4368-C

The Chain extender used in this study was the Joncryn ADR 4368-C supplied by BASF. In this study, this chain extender is represented by the term “Joncryn”. Joncryn has a very high functionality and has been reported as an extremely effective chain extender. It can facilitate the formation of long chain branched and cross-linking structures to achieve the chain extension. Figure 4.3 portrays the typical structure of the Joncryn multifunctional chain extenders, which are styrene-acrylic oligomers. In the structure, R1-R6 represents alkyl groups, such as H, CH₃ or higher alkyl groups. X, Y and Z are in the range of 1-20. The characteristics of Joncryn are depicted in Table 4-3.⁸⁸

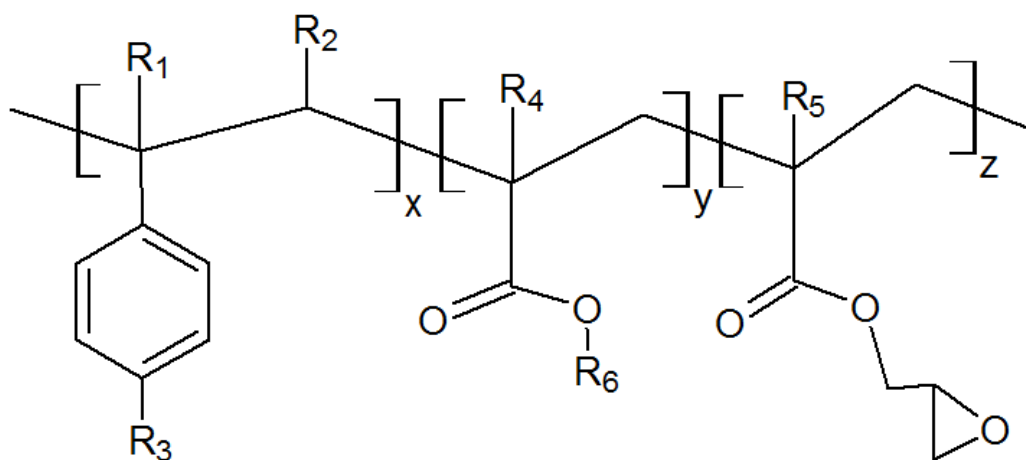


Figure 4.3 Chemical structure of Joncryl ADR 4368-R
(Redrawn after the data sheet from BASF)

Table 4-3 Characteristics of Joncryl ADR 4368-R

Functionality (<i>f</i>)	9
Appearance	Solid flake
Density (25°C) (g/ml)	1.08
Glass Transition Temperature (°C)	54
Epoxy equivalent weight (g/mol)	285
Molecular weight (Mw) (g/mol)	6800

*Data was obtained from the BASF.

4.2 Methodology

4.2.1 Base Line Study

Injection Molding Blend Samples Preparation

In order to determine the optimal blending composition between PPC and PLA blends, melt blending and injection molding of PLA and PPC at different weight percent (wt%) PLA/PPC ratios were conducted. For this, (neat PPC, 40%PLA/60%PPC, 50/%PLA/50%PPC, 70%PLA/30%PPC and neat PLA) were prepared and their mechanical properties were evaluated. Prior to blending, the neat polymers were dried in an oven at 80 °C for 15 h to avoid hydrolysis during processing. After drying, the neat polymers and blend samples with different compositions of PLA/PPC were processed in a DSM Xplore micro-extruder (Netherlands) equipped with a co- rotating twin screw. The melt processing parameters: Extruder temperature, residence time and screw speed were set at 175 °C, 2 min and 100 RPM, respectively based on preliminary trial optimization of parameters. After extrusion, the melted materials were injection molded with a DSM Xplore micro-injection molding equipment at 175 °C to form tensile and flexural bars in accordance with ASTM D638.

Mechanical Properties Characterization

Tensile strength, modulus and percent elongation at break of the neat PLA, PPC and their blend injection molded samples were measured using an Instron Universal Testing Machine (Instron3382, 10 kN load cell) with a strain rate of 5 mm/min according to ASTM D638 method.

For all the reported results, at least five specimens for every formulation were measured and the averages of the values were reported.

Based on the mechanical performance, PLA/PPC 40/60 blend exhibited the best performance compared to the other formulations. (shown in see results and discussion section).

4.2.2 Primary Study

In regard to the conclusion from the base line study, PLA/PPC 40/60 blend was selected as a base blend for conducting further films study. To produce films, PLA, PPC and Joncryl pellets were dried prior to blending process. Then PLA and PPC were blended in 40/60 ratio with the addition of 0.0, 0.2phr, 0.5phr and 1.0phr Joncryl using a Leistritz twin screw extruder (Germany). The processing parameters on the extruder were kept constant at a temperature, residence time and screw speed of 175°C, 2min, 100 rpm, respectively. The extruded blend strands were then pelletized immediately after the extrusion. Film casting process was performed using a cast film extruder, Microtruder RCP-0625, Randcastle, New Jersey, USA. The processing parameters for film making were set to a temperature at 180°C and screw speed of 23.2 rpm, based on preliminary experimentation trials. The outcome film has a thickness in the range of 0.09-0.12mm.

4.2.3 Tensile Properties Test

For the PLA/PPC blend films with 0, 0.2phr, 0.5phr and 1phr of Joncryl, the ASTM D882 method was followed to perform the tensile testing. The method employed in this study is different from previous base line study as the ASTM D882 is specifically designed for film testing. Specimens were cut into strips from the extruded films. The dimension of the specimen

strips were 0.09-0.11mm in thickness, 9.90-10.00 mm in width and 150 mm in length. The initial distance between the two grips was set to be 100mm according to ASTM D882. The cross-head speed of the test was set to be 25mm/min. According to ASTM D882, the film sample which fails due to a tear failure will give anomalous data and cannot be compared with the data from normal failure. As for tear failure, ASTM D882 defined it as a failure that is initiated by the fracture at the edge of the sample and is completed by the progress of the fracture across the sample⁸⁹. In such a case, ten samples were tested for each formulation to account for the potential of the tear failure during the test. Five results for each formulation with normal failure were recorded and the average value was reported.

4.2.4 Differential Scanning Calorimetry (DSC)

A thermal analysis (TA) instrument Q200 was used to perform the DSC analysis in nitrogen atmosphere. For every specimen, the sample mass was accurately measured between 5-10 mg. An aluminum pan was used to hold the specimens and was loaded into the instrument. After loading the specimen, the instrument started to scan and heat up. The specimens were scanned from room temperature to 200°C with a heating rate of 10°C/min. When the temperature reached 200°C, the specimen was cooled down from 200°C to -40°C with a cooling rate of 5°C/min. Then, a second heating scan was performed on the specimens from -40 °C to 200°C with the heating rate of 10°C/min. The first cooling cycle was used to analyze the melt crystallization behavior of the specimens and the second heating cycle was used to investigate the glass transition temperature (T_g), and melting temperatures of the specimens. The results were analyzed using TA instrument Universal Analysis software.

4.2.5 Fourier Transform Infrared Spectroscopy (FTIR)

The infrared (IR) spectra of PLA, PPC, Joncryl and the blend plastic films were analyzed using FTIR (Thermo Scientific Nicolet, 6700 ATR-FTIR) at room temperature. Finely milled dried samples of PLA, PPC, Joncryl, and dried blend film specimens with and without Joncryl were used for the analysis. 100 scans were conducted with 4 cm⁻¹ resolution for the FTIR. The measurements between 4500 and 400 cm⁻¹ were recorded. For the background, the same conditions were applied.

4.2.6 Scanning Electron Microscope (SEM)

The morphologies of PLA/PPC 40/60 blend films with and without Joncryl were examined using a HITACHI S-570 (Tokyo, Japan) scanning electron microscope (SEM) under an acceleration voltage of 8-10 kV. Before examining the films, a layer of gold and palladium particles with a thickness of 20 nm was coated on the surface of the films to enhance the electron conductivity of the sample while reducing the chances of heat accumulation on the surface of the sample, which will possibly lead to deformation of the film surface.

4.2.7 Thermogravimetric Analysis (TGA)

TGA was performed on the specimens by using a TA Instrument Q500 with a flow rate of 60 ml/min nitrogen atmosphere. The specimens were heated up from 26 °C (room temperature) to 450 °C at a rate of 20 °C/min. The temperature at which the maximum degradation rate occurred was detected with derivative thermogram (DTG).

4.2.8 Water Vapor Transmission Rate (WVTR) Measurements

The water vapor transmission rate values of the blend films were obtained from a Permatran-W[®] Model 3/33 (USA, MOCON). All the test films were placed between two aluminum foil masks with the test area of 5 cm² and the two foil masks were sealed together with vacuum grease. Before testing, calibrations of the equipment were performed using calibration films from MOCON. Also, after every 3 to 4 experiments, the calibration process was repeated using a reference film supplied by MOCON to ensure the validity of the results. After masking the film sample with aluminum foils, the sample was placed in a test cell and was clamped between two chambers. As such, the chamber which is filled with test gas (water vapor) is the outer chamber. The other side is the inner chamber which is filled with carrier gas (nitrogen). There are two test cells on the equipment; therefore, each time two samples are being tested at the same time. The test was performed according to ASTM F 1249 standard. Referring to the standard, the test condition was set to a temperature of 37.82 ± 0.1 °C and a relative humidity of 100%. In order to generate 100% relative humidity, a sponge filled with HPLC water was attached to the inside wall of the outer chamber. Temperature was controlled by the equipment. Nitrogen flow rate was set to 100 SCCM (standard cubic centimeter per minute) for cell A, B, Z and 50 SCCM for R. Cell Z is the zero cell and Cell R is the reference cell. A reference film is placed in the cell R. The Illustration of water vapor transmission rate test principles is demonstrated in Figure 4.4. The test principle is basically that the water vapor molecules generated by the wet sponge permeate through the film from the outer chamber to the inner chamber. After permeation, the water vapor molecules is taken by the dried nitrogen in the inner chamber and carried to the sensor of the equipment. The sensor is able to quantify how much water vapor is being taken to the sensor by the nitrogen. The test period was set to be 45

minutes every cycle for each cell. As such, every 45 minutes, the computer gives a data point calculated by the sensor about how much water vapor in quantity diffuses through the sample and reaches the sensor. The sensor automatically takes the test area of the sample and the time into calculation, giving data with unit of $\text{g/m}^2\text{-day}$. The data will be recorded by the computer continuously. Since testing barrier properties of films is a delicate work (no matter water vapor or oxygen), the entire system which the test is performed in has to be free of water vapor molecules from outside sources. In light of this, prior to starting every test, a two-hour conditioning process, which only uses dried nitrogen to flush the entire system to clear out any existing water vapor molecules, was performed for each test cell. Another process called rezero is performed throughout the whole test. This process happens every 45 minutes when the test is switched to the other cell after finishing the test in previous cell. This process is to make sure no water vapor exists in the next cell before testing by flushing with nitrogen. After the recorded data value reached a steady state, this value was reported and the test was stopped. For every test, it normally took 8-12 hours to reach a steady state. At least four experiments were repeated for each film formulation. The average value and standard deviation were reported.

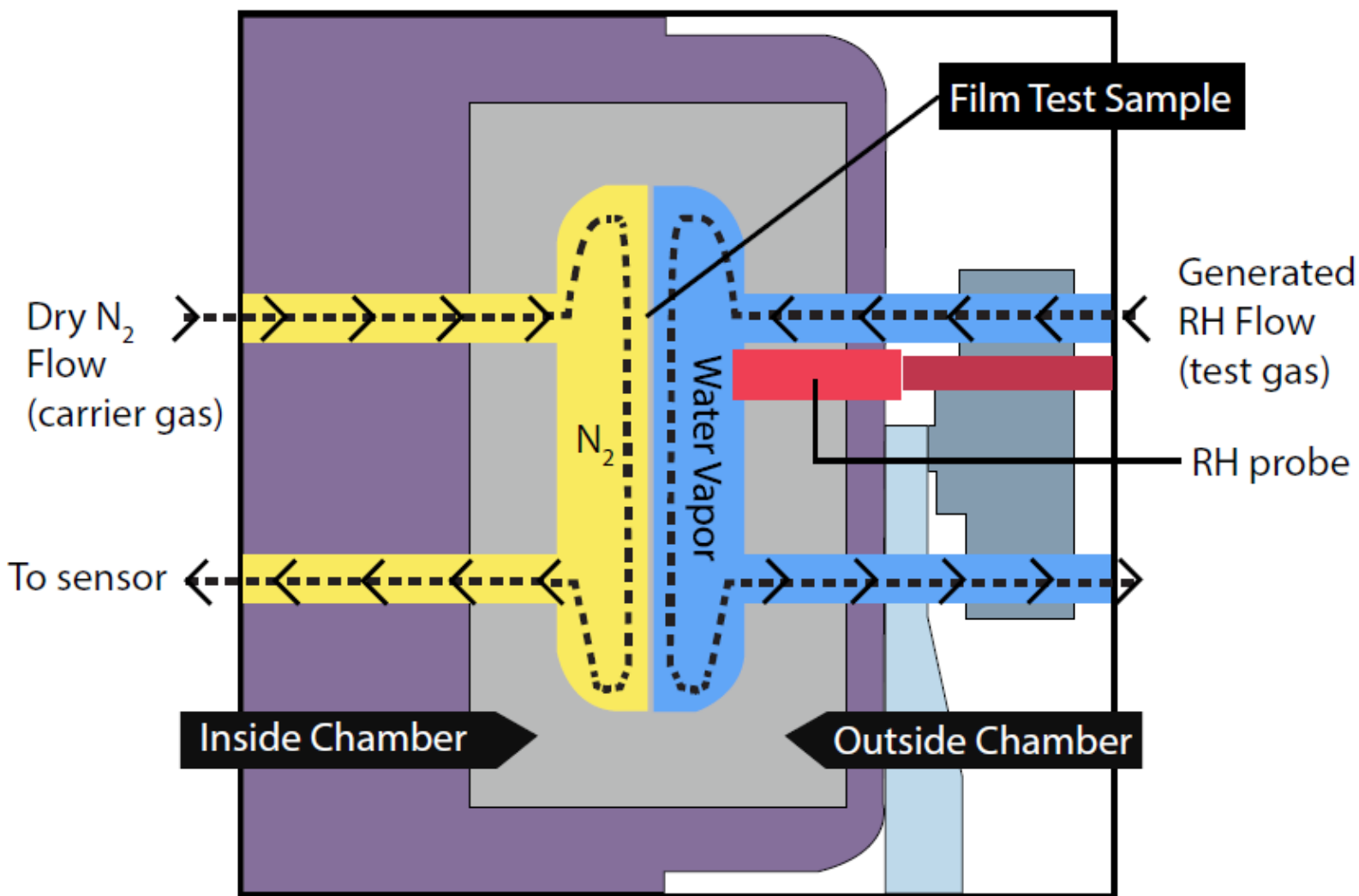


Figure 4.4 Illustration of water vapor transmission rate test principles

(Redrawn after Permatran-W® Model 3/33 operation manual from MOCON Inc.)

4.2.9 Water Vapor Permeability Measurements using Dish Method

As aforementioned, the testing of barrier properties is a delicate test that requires strictly controlled test conditions to obtain accurate and valid results. Therefore, another measurement of water barrier properties of my film samples was conducted using a different method named dish method to confirm the water vapor permeability results acquired from the previous method. This test is performed according to ASTM E96 standard. The basic principle of this test is to cover a dish, which is impermeable to the water vapor, with the film specimen; and the dish is filled with desiccants. Then, the film covered dish is placed into environment with controlled temperature and relative humidity. At last, the water vapor transmission rate can be obtained by measuring the weight gain of the dish every hour. Because the weight gain only depends on the how much moisture permeates through the film specimen and is absorbed by the desiccants. The steps of performing this test are portrayed in Figure 4.5. In this study, steel cups were used as the dish with a test area of 19.625 cm^2 and the silica gel was used as the desiccants. Prior to starting the test, the silica gel was dried in the oven at 105°C for 24 hours.

Step 1

Dry desiccant (silica gel) in the oven at 105 °C for 24 hours;
Prepare film samples with a diameter greater than 6cm.

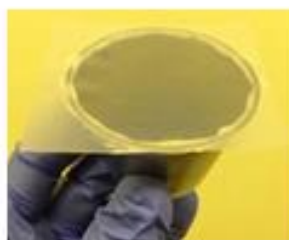
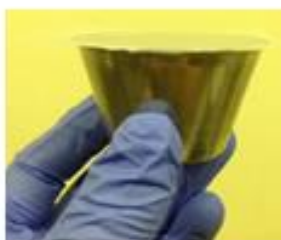
Step 2

Dried silica gel

Prepared film sample

Steel cup

Epoxy glue as sealant



Step 3

Measure the initial weight of the specimens

Step 4

Placed the specimens into the environment chamber with a 100% RH and 37.8 °C



Step 5

Measure the weight of the specimens every hour until the weight gain/hour becomes stable

Figure 4.5 Schematic of Dish Method

4.2.10 Oxygen Transmission Rate (OTR) Measurements

The oxygen transmission rate values of the blend films were obtained on an OX-TRAN® Model 2/21 (USA, MOCON). The equipment was connected with oxygen and nitrogen/hydrogen cylinders. The installation of samples is the same procedure as the water transmission rate test. As such, the chamber which is filled with test gas (oxygen) is the outer chamber. The other side is the inner chamber which is filled with carrier gas (nitrogen and hydrogen). There are two test cells on the equipment; therefore, each time two samples are being tested at the same time. The test was performed according to ASTM D 3985 standard. Referring to the standard, the test condition was set to be a temperature at 23 ± 0.1 °C and a relative humidity of 0%. Temperature was controlled by the equipment. Oxygen flow rate was set to 20 SCCM (standard cubic centimeter per minute). Nitrogen/Hydrogen flow rate was set to 10 SCCM. The Illustration of oxygen transmission rate test principles was depicted in Figure 4.6. The test principle is basically that the 100% concentration of oxygen flows into the outer chamber and permeates through the specimen to the inner chamber. After the permeation, the oxygen molecules will be taken by the nitrogen/hydrogen mixed gas in the inner chamber and carried to the sensor of the equipment. The sensor is able to quantify how much oxygen is being taken to the sensor by the carrier gas. The test period was set to be 45 minutes every cycle for each cell. As such, every 45 minutes, the computer gives a data point calculated by the sensor about how much water in quantity (cc) diffuses through the sample and reaches the sensor. The sensor automatically takes the test area of sample and the time into calculation, giving a data with unit of $\text{cc}/\text{m}^2\text{-day}$. The data will be recorded by the computer continuously. The entire system which the test is performed in has to be free of water vapor molecules from outside sources. In light of this, prior to starting every test, a two-hour conditioning process, which only

uses the carrier gas to flush the entire system to clear out any existing oxygen, was performed for each test cell. The rezero process is the same as the water vapor transmission test to ensure no oxygen exists in the next cell before testing. As the sensor for this oxygen transmission rate is super sensitive, the test will be stopped automatically when there is large amount of oxygen reaching the sensor, which is called over-range. Masking the film with aluminum foils to minimize the test area is a precaution to prevent this over-range situation from occurring. Another precaution is the application of individual zero process, which is to test the specimen without oxygen flow (test gas) prior to starting actual test. The actual test begins only until the sensor gives an OTR value extremely close to zero. However, even these precaution processes, some poor oxygen barrier material still cannot be tested on this machine, which in our cases is the neat PPC film. Several trials have been done to reproduce the PPC film and measure its oxygen transmission rate. Although the optimization of the film casting process of neat PPC film has been done multiple times and the PPC film is obtained with homogenous appearance, the oxygen transmission rate test on PPC film still kept reaching over-range state and provided no results. As for the end of the test, after the recorded data value reached a steady state, this value was reported and the test was stopped. For every test, it typically took 12-30 hours for the individual zero process and 10-12 hours for the actual to reach a steady state. At least three experiments were repeated for each film formulation. The average value and standard deviation were reported.

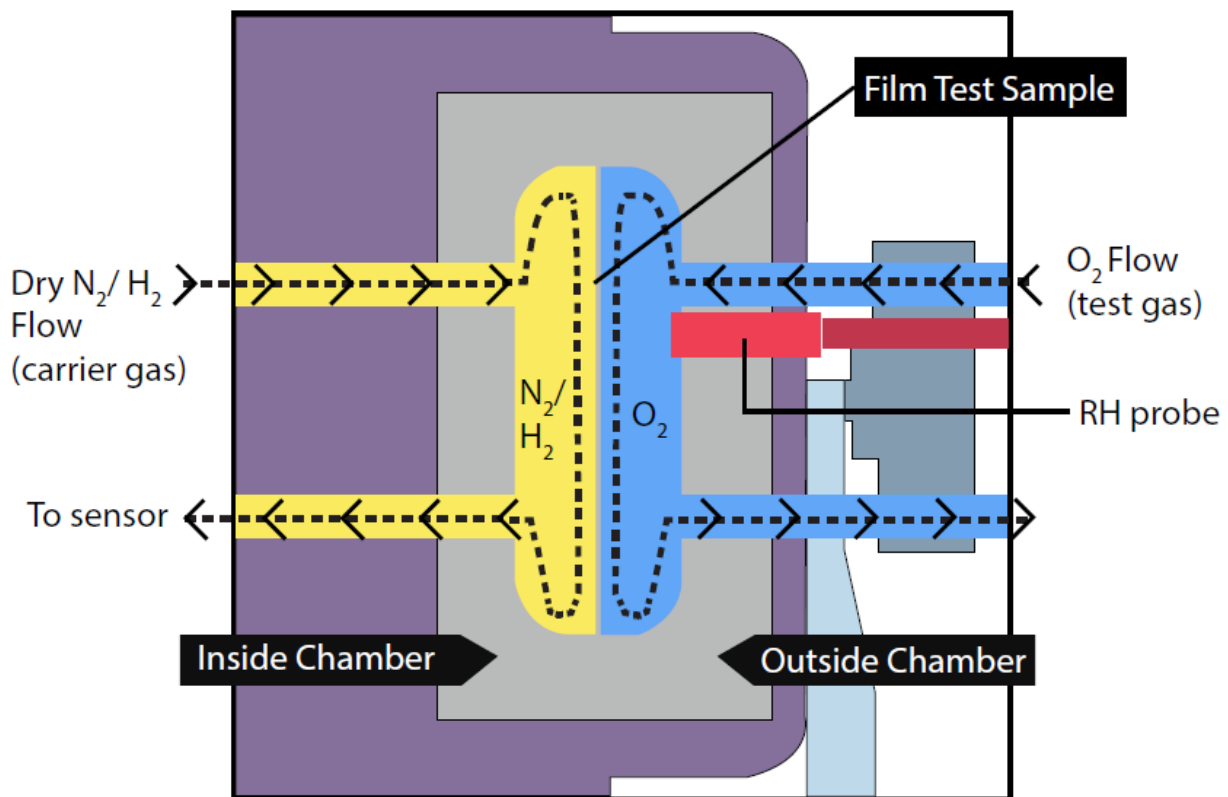


Figure 4.6 Illustration of oxygen transmission rate test principles
 (Redrawn after OX-TRAN® Model 2/21 operation manual from MOCON Inc.)

4.2.9 Statistical Analysis

The experiment was conducted with a completely random design with 4 factors which are treating the PLA/PPC blend with 0, 0.2, 0.5, 1phr concentration of Joncryl. All the mechanical properties for each formulation were assessed with at least 5 replicates. As for the oxygen permeability, at least 3 replicates for each formulation were prepared and investigated, while in the case of water vapor permeability, testing was performed on at least 4 replicates. The results from these experiments were statistically analyzed using the ANOVA one-way variance analysis procedure on the Minitab Ver. 16 (Minitab Inc., State College, PA). A significance of 0.05 for all the analysis was used. The means and standard deviations were analyzed and compared with the Tukey Pairwise comparison test.

Chapter 5 Results and Discussions

5.1 Tensile Properties Analysis

Mechanical property testing of PLA/PPC blends was performed to determine the optimum blend composition for further processing and development of the blend based films. As such, blends with 70PLA/30PPC, 50PLA/50PPC and 40PLA/60PPC were prepared and tested. As shown in Figure 5.1 and 5.3, it was observed that neat PLA showed high tensile yield strength with very low elongation at break. Samples failed without necking at a strain of around 5%. On the other hand, studies have reported that neat PPC exhibited much higher elongation at break with apparent long necking before break⁵⁰, indicating that the inherent brittleness of PLA could be modified by blending with PPC. As for the binary PPC/PLA blends, it was noted that the elongation at break of the blend shows significant increase while the tensile strength at yield decreased with increasing PPC content in the blend. The maximum value of elongation at break, 216%, was obtained from the blend of 40PLA/60PPC, with tensile strength around 50 MPa. It was also observed that the Young's modulus value of the blend was lower than that of neat PLA but much higher than that of neat PPC. (Figure 5.2) The Young's modulus value was gradually reduced with increased loading of PPC and varies significantly with different formulations compared to tensile strength and elongation at break. The 40PLA/60PPC blend showed a significant increment in the elongation at break with slight decrease from 52MPa to 48MPa in tensile yield strength, compared to the blend composed of 50PLA/50PPC. Also, as the concentration of PPC in the blend increased, a further loss in tensile modulus was observed.

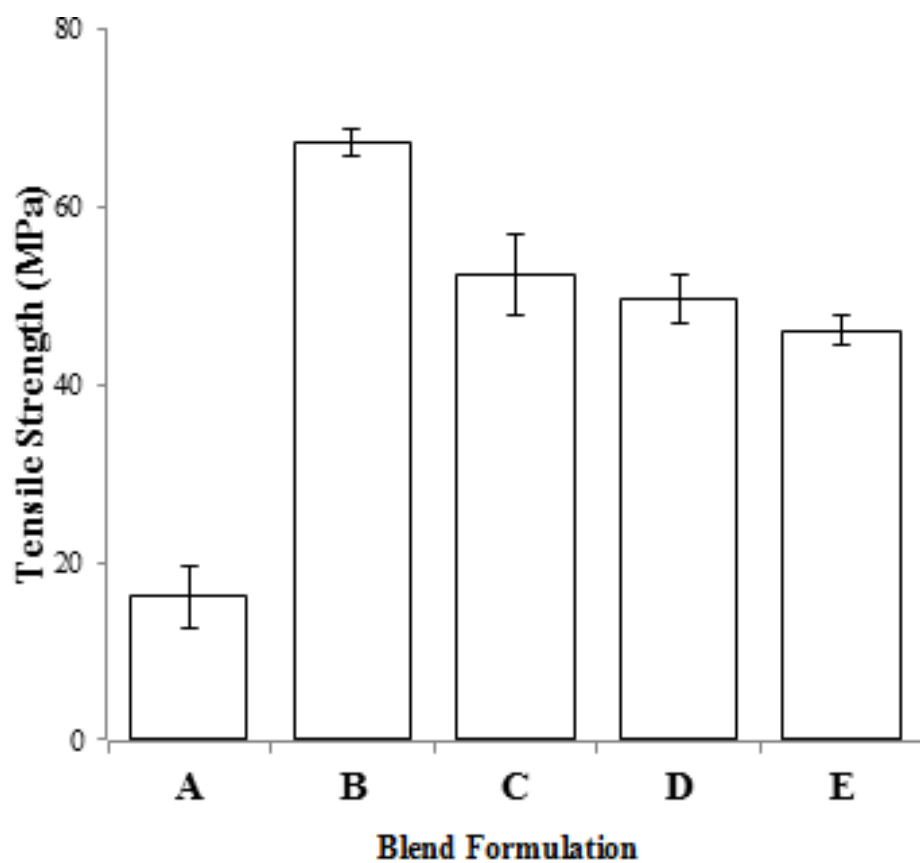


Figure 5.1 Tensile Strength of PPC, PLA and PPC/PLA blends: (A) neat PPC, (B) neat PLA, (C) PPC/PLA (30/70), (D) PPC/PLA (50/50), (E) PPC/PLA (60/40).

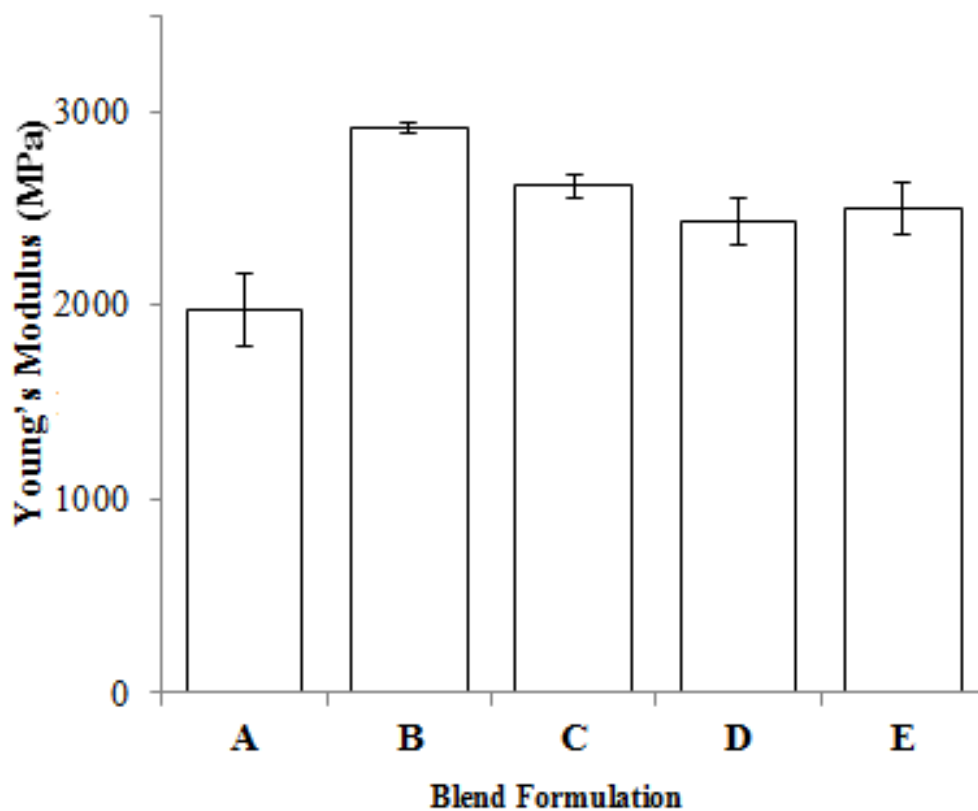


Figure 5.2 Young's Modulus of PPC, PLA and PPC/PLA blends: (A) neat PPC, (B) neat PLA, (C) PPC/PLA (30/70), (D) PPC/PLA (50/50), (E) PPC/PLA (60/40).

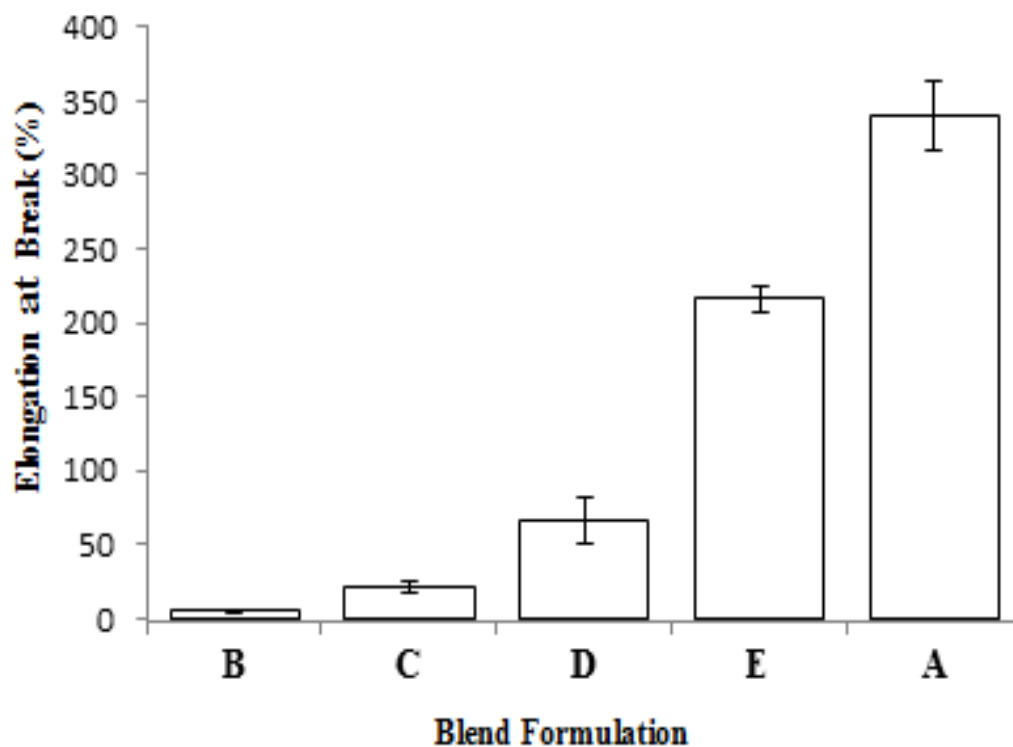


Figure 5.3 Elongation at Break of PPC, PLA and PPC/PLA blends: (A) neat PPC, (B) neat PLA, (C) PPC/PLA (30/70), (D) PPC/PLA (50/50), (E) PPC/PLA (60/40).

Figure 5.4 shows the typical stress-strain curves of PLA/PPC blends with different formulations. From the stress-strain curve, it can be noted that PLA/PPC with 40/60 formulation presents balanced stiffness while gives a large rise to the toughness, making it an optimal formulation for PLA/PPC blend in terms of increasing ductility without losing much strength. Additionally, a narrower processing temperature window is expected with higher content of PPC in the blend, because of relatively poor thermal stability of PPC. As such, the mechanical property testing of the blend exhibited that 40PLA/60PPC blend could be considered as the optimal composition for film development taking the tensile strength, Young's modulus and elongation into account.

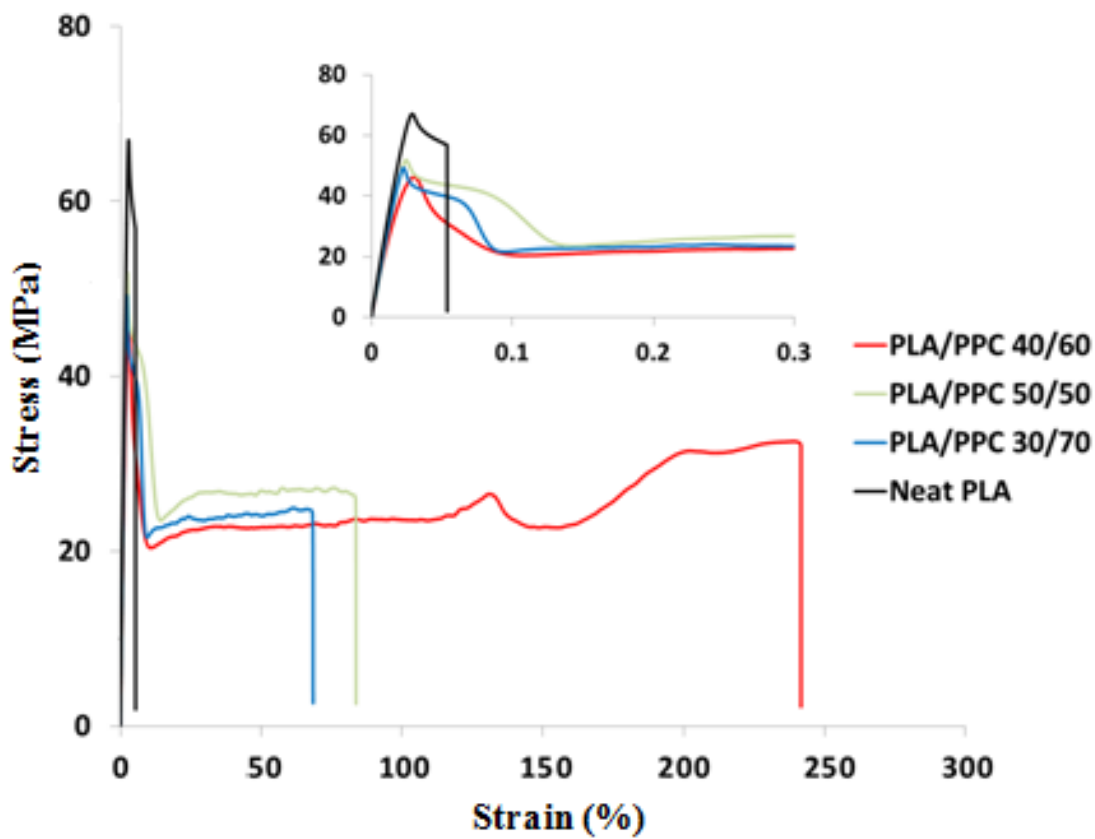


Figure 5.4 Stress-strain curves of PPC, PLA and PPC/PLA blends

Figure 5.8 illustrates typical stress-strain curves of 40PLA/60PPC blend films with different level of Joncryl: 0, 0.2, 0.5 and 1phr. For all films, three main regions were discernible: elastic deformation, yielding, and stress hardening. It is noted that for the PPC/PLA blend without Joncryl, the elastic deformation region ended quickly as strain increased, but this region was extended significantly with the inclusion of Joncryl into the blend. This extension revealed large increment in the strength of the films, giving promise to reversible deformation of the films under certain load. The curve showed significant yielding region followed by intense stress hardening for all films. With more Joncryl in the blend, the area of stress hardening region is

becoming larger, indicating increased elongation at break. However, when Joncryl reached 1phr in the blend, the stress hardening region ended at much lower strain percentage than that of blend with 5phr Joncryl.

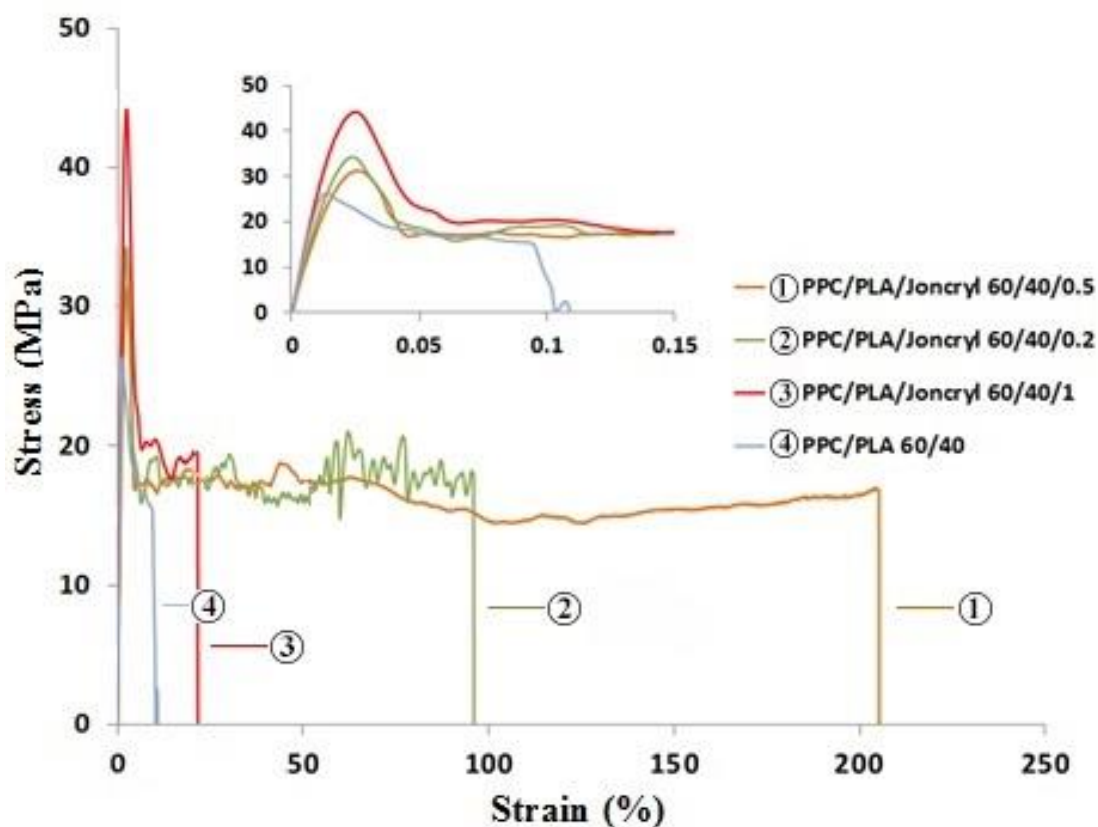


Figure 5.5 Stress-strain curves of PPC/PLA blend films with and without Joncryl

As presented in Table 5-1, mechanical properties in terms of tensile properties of PLA/PPC/Joncryl with increasing concentration of Joncryl. The means and standard deviations of all the properties are reported in the table. A statistical analysis was performed on all the reported data by using Tukey's method in with a one-way ANOVA variance analysis. A significance of 0.05 was used in all the tests. The statistical results are represented with

alphabetical letters for each value of mean in the table. Within a same column (presenting the same property), each different letter signifies a statistical range of value that it falls into and is statistically different from other values from dissimilar ranges represented by other letters. For each column, the highest value for that particular property is represented by the letter “A”. As the value decreases, the representation letter changes from “A” to “B” to “C” and so on.

Table 5-1. Means, Standard deviation and statistical analysis of the tensile properties of PLA/PPC/Chain extender blend film

Joncryl concentration(phr) in the PLA/PPC blend films	Tensile Strength At Yield (MPa)	Standard Deviation	Secant Modulus at 1% strain (MPa)	Standard Deviation	Elongation at break (%)	Standard Deviation
0phr	25.80 (B)	1.58	1567.3 (B)	169.4	12.80 (C)	2.59
0.2phr	33.64 (A)	2.97	1917.6 (A)	94.7	132.60 (B)	28.1
0.5phr	35.38 (A)	3.32	1832.4 (A)	91.3	262.20 (A)	57.3
1phr	36.08 (A)	3.40	1921.6 (A)	163.6	21.00 (C)	8.94

As shown in Figure 5.5, 5.6 and 5.7 and Table 5-1, increasing Joncryl content from 0.2 to 1phr in the PPC/PLA blend films resulted in higher tensile strength and Young’s modulus values as

compared with PPC/PLA blend films without Joncryl. Also, the elongation at break of the films was largely enhanced with the loading of Joncryl. Specifically, at 0.2phr Joncryl content, the films showed a 140% increment in tensile yield strength and 122% in secant modulus while the elongation at break was enhanced by 1035%. The films with 0.5phr Joncryl exhibited a 137% increment in both tensile strength and 116% in secant modulus, along with a huge increase by 2040 % in the elongation at break as compared to the film without Joncryl. Interestingly, as for the films with 1phr Joncryl, the tensile strength and secant modulus showed a 140% and 123% increase as compared with the pure blend, but the elongation at break did not display any significantly difference according to the statistical analysis. The lower elongation at break of film with 1% Joncryl as compared with 0.2 and 0.5phr Joncryl samples could be related to the occurrences of more cross-linkings between the polymer chains when loading more Joncryl was added into to the blend system⁹⁰⁻⁹². Moreover, it was suggested that the incorporation of Joncryl does not only extend the polymer chains but also was able to resulting in forming a long chain branched structure⁹³. With higher concentration of higher Joncryl content in the blend, there is a higher probability of a more frequent cross-linking by joining chain ends with functional groups. With the presence of more cross-linking and long chain branching structures, the mobility of the polymer chain in the blend system is expected to decrease significantly. Thus, during the strain hardening period, it would be difficult for the polymer chains to move and rearrange, resulting in low elongation at break. Similar observation was reported in the study conducted by Khonakdar et al⁹⁴. In their case, with more inclusion of chain extender in HDPE, increased cross-linking between the polymer chains imposed more restriction on the elongation behavior of the polymer, resulting significant decrease in elongation at break. Another possible reason for the drastic decrease in the elongation for film with 1phr Joncryl might be that the decrease in

the amount of molecular chain ends leads to the occurrence of stress concentrations as frequent chain extension largely reduces the number of chain ends⁹⁵. These stress concentrations can be responsible for the reduction in the ductility of the film with 1phr Joncryl. Similar observation has been seen by other researchers when the PLA is the minor component in the blend, chain extended PLA dispersed phase acted as stress concentrators in the presence of Joncryl. The elongation at break was drastically decreased in their case as well⁶⁴. The improvement in tensile strength and secant modulus of the films could mainly be due to the formation of higher molecular weight, longer chain structure and less cross-linking. However, there is only minimum increase in the strength and modulus from 26 to 33 after adding 0.2phr Joncryl into the PLA/PPC blend film. Moreover, no significant difference in the strength and modulus is observed when increasing the concentration of Joncryl to 0.5phr and 1phr according to the statistical analysis. This is attributed to the small amount of Joncryl in the blend system, which may not be sufficient to enhance the strength and modulus in a large extent. This has also been observed in other studies^{31,96}. As for the elongation at break at lower concentration of Joncryl concentration, the increased elongation at break the improvement might be caused by two main factors. One of them can be the formation of PLA-Joncryl-PPC copolymer. Since PPC and PLA have similar chemical structure and they all have functional end groups, the Joncryl has the potential to react with both PLA and PPC, forming a copolymer. The formation of PLA-Joncryl-PPC copolymer can greatly reduce the interfacial tension while increasing the interfacial adhesion, resulting in much better compatibility. The compatibilization function of Joncryl has been confirmed with several studies. It was reported in one study that the incorporation of Joncryl could increase the compatibility of the blend system through the formation of intensive ester linkages between the PLA/PBAT polymer chains⁵⁵. Another study

also proposed the formation of copolymer PLA-Joncryl-PBAT with the compatibilization of Joncryl⁶⁴. In such case, the compatibility of PLA/PPC blend system in the films could be improved by the addition of Joncryl due to the formation of copolymer between the PLA/PPC polymer chains and Joncryl chains, providing improvement in interfacial adhesion between the two polymer phases. The ductility of the matrix (PPC) with improved compatibility with PLA promises the observed high elongation at break of the films. As a result, PLA/PPC/Joncryl films with highly improved mechanical properties were obtained and the optimal concentration of Joncryl for this blend film is 0.5phr.

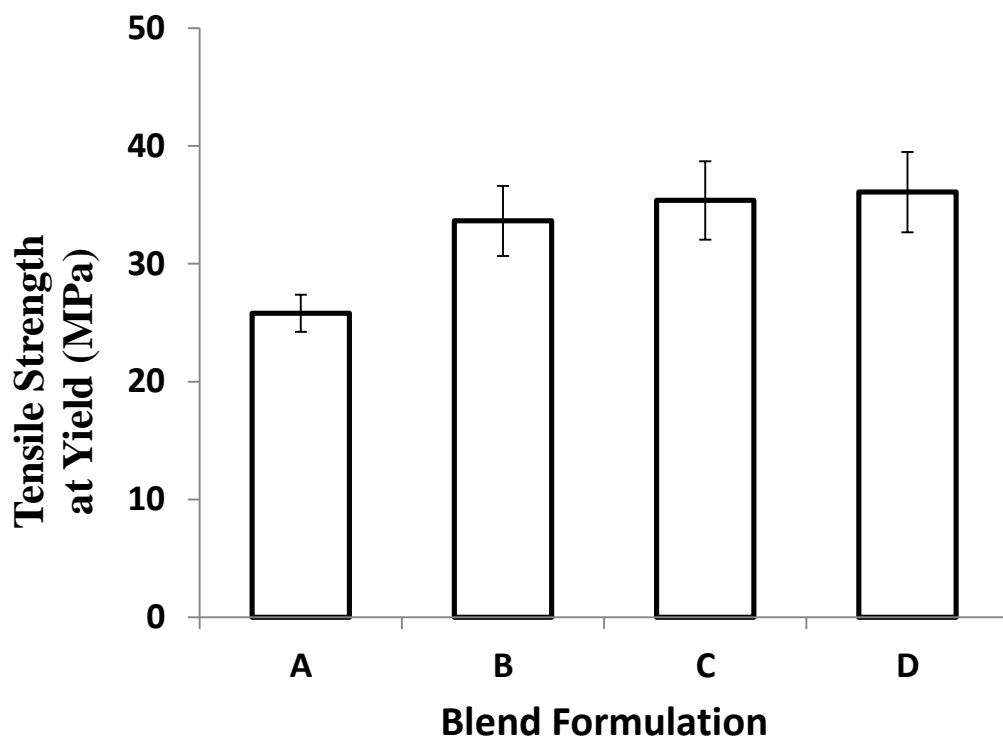


Figure 5.6 Tensile Strength of PPC/PLA blend films with and without Joncryl: (A) PLA/PPC (40/60) blend films, (B) PLA/PPC/Joncryl (40/60/0.2) blend films, (C) PLA/PPC/Joncryl (40/60/0.5) blend films, (D) PLA/PPC/Joncryl (40/60/1) blend films.

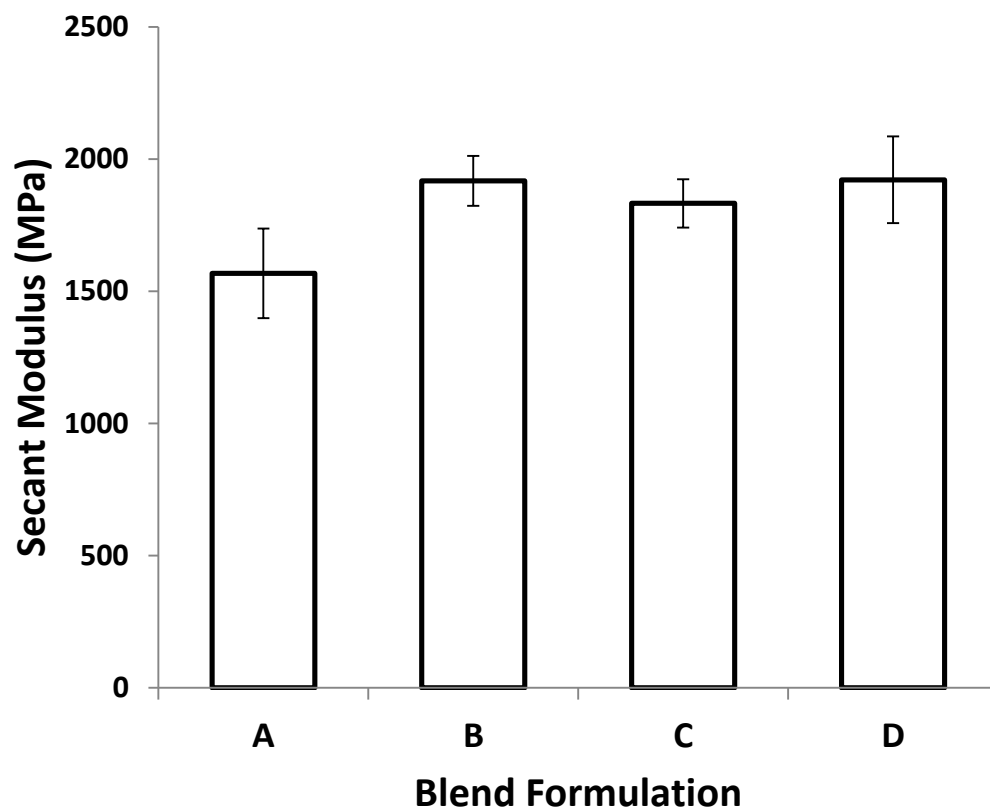


Figure 5.7 Secant Modulus of PPC/PLA blend films with and without Joncryl: (A) PLA/PPC (40/60) blend films, (B) PLA/PPC/Joncryl (40/60/0.2) blend films, (C) PLA/PPC/Joncryl (40/60/0.5) blend films, (D) PLA/PPC/Joncryl (40/60/1) blend films.

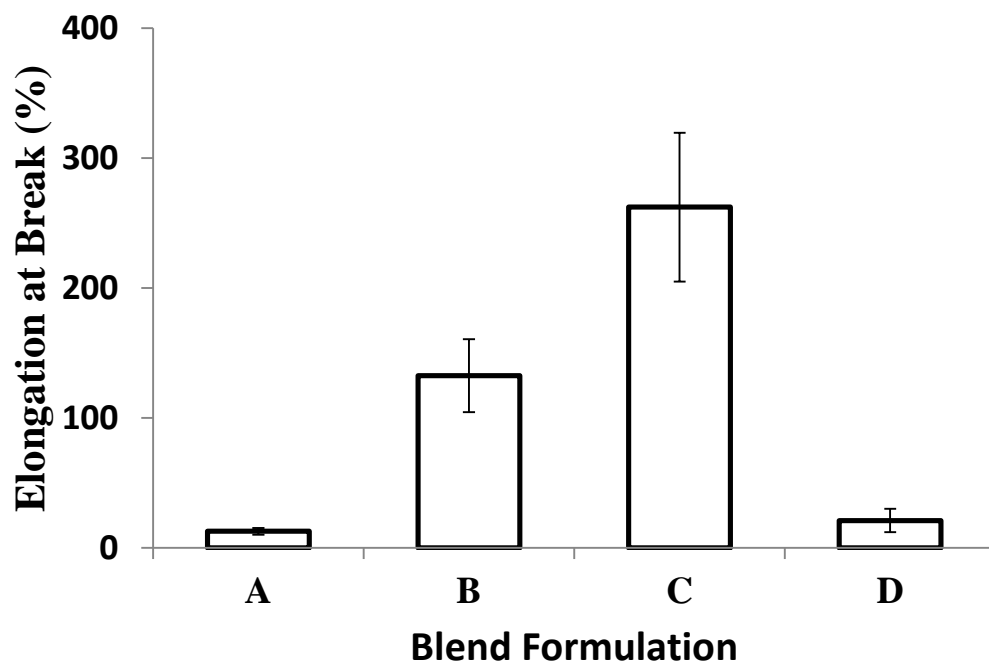


Figure 5.8 Elongatio at Break of PPC/PLA blend films with and without Joncryl: (A) PLA/PPC (40/60) blend films, (B) PLA/PPC/Joncryl (40/60/0.2) blend films, (C) PLA/PPC/Joncryl (40/60/0.5) blend films, (D) PLA/PPC/Joncryl (40/60/1) blend films.

5.2 Fourier Transform Infrared Spectroscopy (FTIR)

It is important to understand the interactions between the components of a polymer blend. If there are no recognizable changes in the IR spectra of the polymer blend in terms of the interactions between components, the polymers in the blend are considered to be completely immiscible. However, if there are some distinguished interactions (obvious changes in the specific bond stretching region) that can be observed from changes in IR spectra, the polymers in the blend can be considered to be compatible⁹⁷. Therefore, the employment of FTIR is important to identify the interactions occurring in polymer blend systems, and also to investigate the dispersion behavior of the component polymers in the blend. It is imperative to note here that the compatibility and miscibility play a significant role on the mechanical properties, thermal properties and barrier properties of the polymer blend. In light of this, FTIR spectra of PPC, PLA, Joncryl, and PPC/PLA 60/40 blend film with and without Joncryl were collected. Since no apparent differences were observed between the IR spectra for PPC/PLA blend films with different concentration of Joncryl, a typical PPC/PLA blend film with 0.5% Joncryl was selected as representative sample in this research work for FTIR analysis.

Figure 5.9 shows the FTIR spectra of neat polymers and their blend films. In the 1700-1800 cm⁻¹ region, the spectra of both PLA and PPC showed a strong carbonyl stretching. The peak of the carbonyl group in PPC was observed to shift towards higher wavenumbers with the addition of PLA in the blend, which gave a strong evidence that there was appreciable chemical interaction occurring between the two polymers⁴¹. An extensive investigation on poly (vinyl phenol)/PCL blends exhibited similar carbonyl absorption peak shift⁹⁸. Another study suggested that the formation of a strong chemical interaction between the parent polymers could increase the stretching absorbance frequency of carbonyl C=O group while initiating a shift to higher

frequency⁵⁰. In light of this observation, it could be concluded that strong chemical interaction related to carbonyl groups took part in the PPC - PLA blend system. Another possibility is that a chemical reaction occurring between PPC and PLA that could result in co-polymer chains through ester-ester interchange reactions. As for the PPC/PLA blend film and the typical blend film with 0.5% Joncryl in the 1800-1700 cm⁻¹ region, the stretching peak of Joncryl-compatible film (e) exhibited slight shift towards lower wavenumber compared with the neat blend (c). This could be ascribed to the reaction between the functional groups of Joncryl and carboxyl groups of PLA/PPC blend. This is also another indication of strong interaction occurring between the blend material and Joncryl functional groups.

Absorbance peak at 1223 cm⁻¹ could be correlated with the –C-O-C- groups in the PPC⁹⁹. With the addition of PLA, it could be observed that the –C-O-C- stretching vibration peak shifted to lower wavenumbers for the PPC/PLA blend. This is another indication of chemical interaction taking place at the –C-O-C- bond or around the –C-O-C bond through the blending of the two polymers.

The vibration peak appeared around 1180 cm⁻¹, 915 cm⁻¹, 860 cm⁻¹, 760 cm⁻¹ and 710 cm⁻¹ in the Joncryl spectra is attributed to the stretching peak of CH₂–O–CH epoxy groups^{55,99–101}. After blending Joncryl with the PLA/PPC blend, the stretching peak of epoxy groups in Joncryl almost disappeared, indicating that the epoxy groups were consumed as a result of the chemical reactions with the two polymers in the blend system. Epoxy functional groups, being very reactive at high temperatures, can trigger the formation of a carbonyl-hydroxyl covalent bond within the polyesters¹⁰². The aforementioned shift of carboxyl functional groups in both PLA and PPC is also possible in line with the reaction of the epoxy functional groups of Joncryl with the carboxyl groups of the polymers.

Based on the FTIR spectra of the neat polymer and their blends, the disappearances and shifting of several specific stretching absorption peaks, it can be deduced that several appreciable interactions between the molecular chains of PPC/PLA blend and Joncryl took place during the melt processing. This shows that Joncryl played a significant role in the interactions of the blend composition and increasing the compatibility of the blend, which also agrees with our result from morphology (SEM) studies.

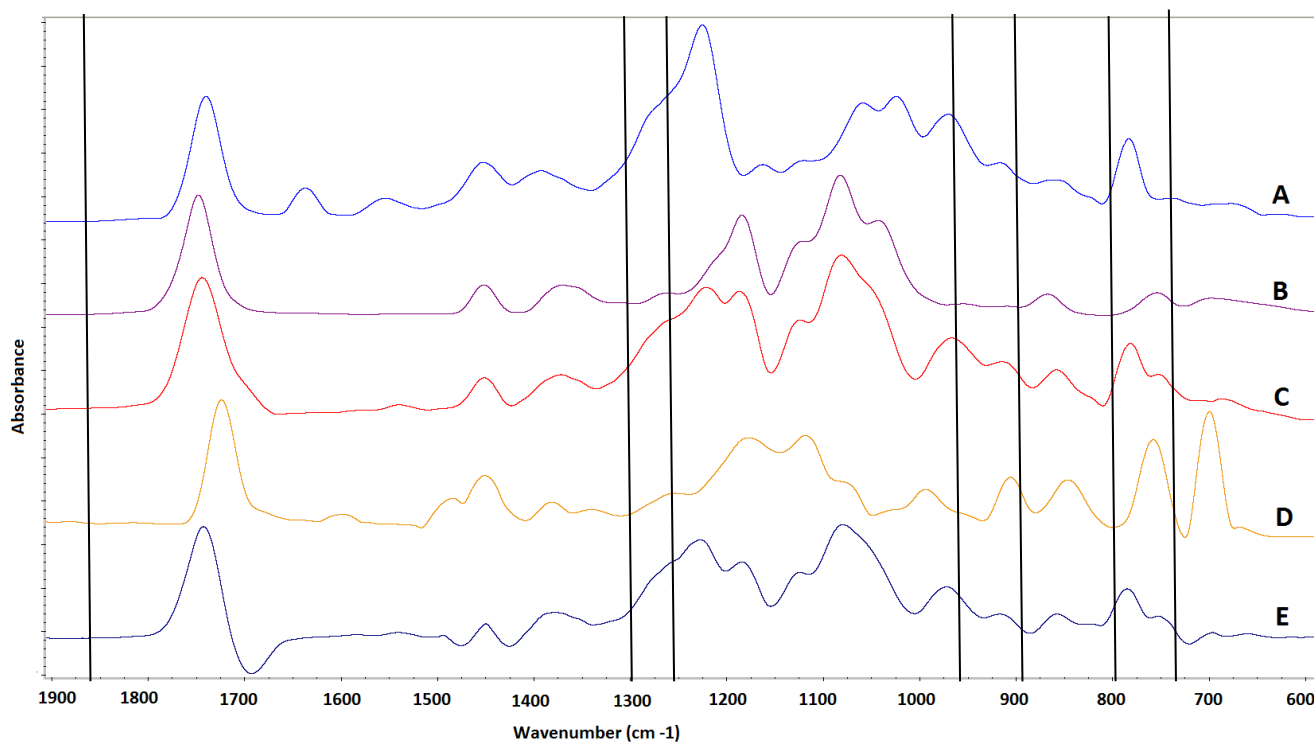


Figure 5.9 FTIR spectra of (A) PPC, (B) PLA, (C) PPC/PLA 60/40 blend film, (D) Joncryl and (E) PPC/PLA/Joncryl 60/40/0.5 blend film.

5.3 Thermogravimetric Analysis (TGA)

TGA analysis was first performed in the presence of nitrogen on neat PPC film and neat PLA film to investigate the thermal degradation behavior of the neat polymer films. TGA and DTG curves showed the thermal degradation behavior of neat polymer films as a function of temperature and are presented in Figure 5.10 and 5.11. From the TGA test, four parameters were measured: the degradation temperature at which 5% weight loss occurs ($T_{5\%}$), the onset degradation temperature (T_{onset}), the degradation temperature at which the maximum degradation rate (first DTG peak) occurs (T_{Max}), and the degradation temperature at which the second DTG peak occurs (T_{sec}). These are listed in Table 5-2.

Table 5-2 Thermal properties obtained from TGA analysis of PLA/PPC/Chain extender blend films

	T _{5%} (°C)	T _{Onset} (°C)	T _{Max} (°C)	T _{Sec} (°C)
Material				
Neat PPC	224	267	302	342
Neat PLA	325	324	367	N/A
PLA/PPC 40/60	260	282	307	344
PLA/PPC/Joncryl 40/60/0.2phr	261	280	307	343
PLA/PPC/Joncryl 40/60/0.5phr	259	281	306	344
PLA/PPC/Joncryl 40/60/1phr	260	280	307	345

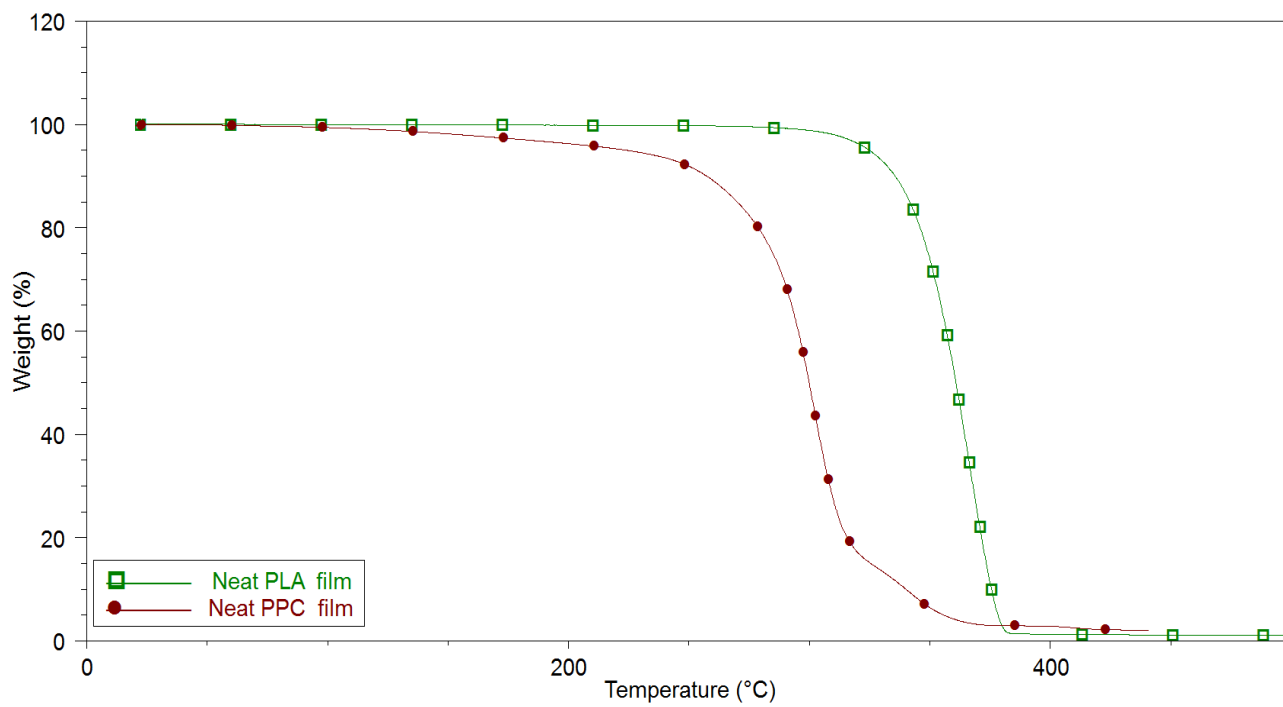


Figure 5.10 TGA curves of PLA film and PPC film

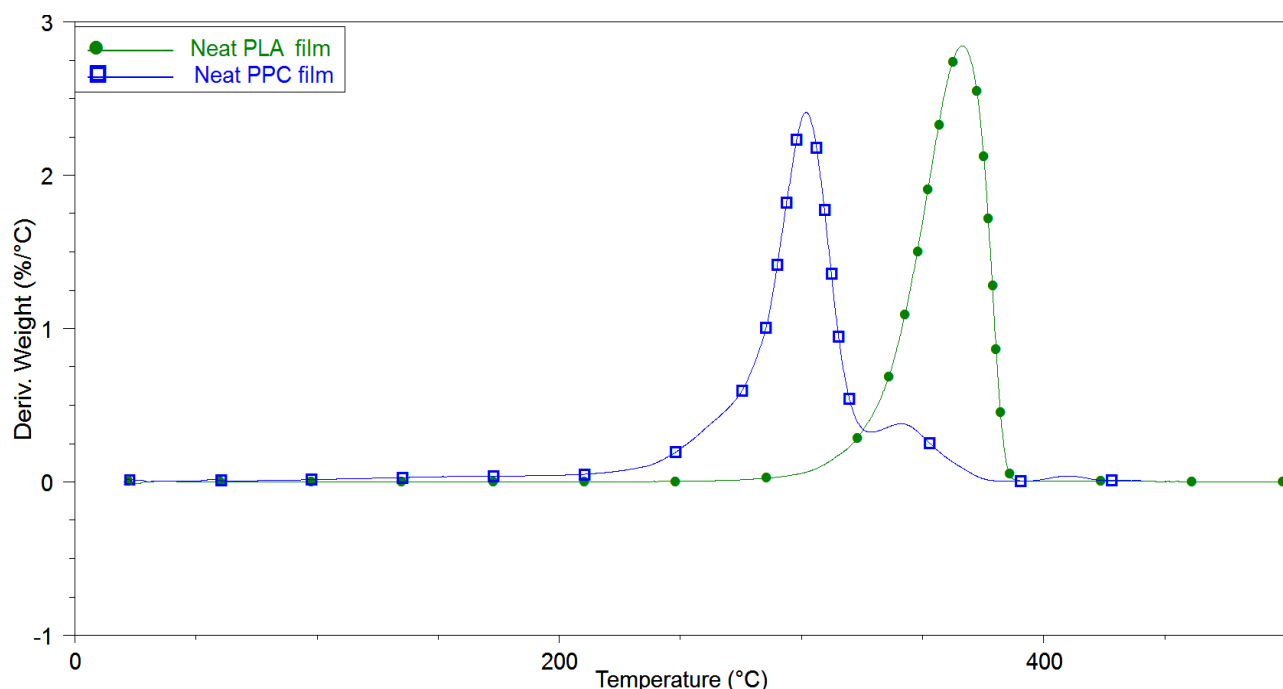


Figure 5.11 DTG curves of PLA film and PPC film

In the Figure 5.11, neat PLA film shows much better thermal stability than the neat PPC film.

The $T_{5\%}$ of PLA film is 100°C higher than that of PPC film; and the onset degradation temperature of PLA film is also 57 °C higher than that of PPC film (Table 5-2). The poor thermal stability of PPC has always been a great concern, as it greatly limits the application and processing window of PPC^{103–105}. It was reported that PPC can easily be decomposed between 150-180°C^{46,87}. However, in our case, the onset degradation temperature and the $T_{5\%}$ for neat PPC film is 267 and 224°C, which is much higher than what has been reported. This could be attributed to the ultrahigh molecular weight of the PPC used in this study as it was reported that the PPC with high molecular weight can be more thermally stable below 200°C than the PPC with low molecular weight^{41,60,106}. In the Figure 5.12, it can be noted that there is only one peak in the DTG curve of PLA at 367°C whereas two peaks are observed for the DTG curve of PPC

at 302 and 342°C. The maximum degradation occurs at 367°C for neat PLA, which is again 60°C higher than that for PPC. As for the thermal degradation of PPC, there are two steps with different mechanisms involved in the process. One of them is reported as an unzipping reaction induced by backbone biting between the functional groups. The other one is suggested to be the random main chain scission reaction^{107,108}. The main by-product produced from the unzipping process is cyclic propylene carbonate while the by-product from the random chain scission is carbon dioxide^{109,110}. Studies showed that the unzipping process occurs first in the thermal degradation of PPC with low molecular weight, followed by the random chain scission reaction. On the contrary, for the thermal degradation of PPC with high molecular weight, the random chain scission takes place before the unzipping process. This is because that there are fewer reactive end groups in the high molecular weight PPC than in the low molecular weight PPC as the reactive end groups facilitate the unzipping process during the thermal degradation¹¹⁰⁻¹¹². Hence, in our study, the ultrahigh molecular weight PPC most likely mainly underwent the random chain scission process first during the TGA test. Although there are few reactive groups in this PPC, the unzipping process could still take place afterwards since the product from the random chain scission process provided reactive end groups. As such, the first DTG peak could be correlated to the random chain scission process of the thermal degradation of PPC; and the second DTG peak could be assigned to the unzipping process^{41,106}. The overall evaluation of thermal performance of neat PLA and PPC films gives the suggestion that PLA may be able to help improve the thermal stability of the blend when blended with PPC. Furthermore, with respect to the presence of the unzipping process during the thermal degradation of PPC, the incorporation of Joncryl has the potential to enhance the thermal stability of PPC by reducing

the occurrence of unzipping process since the multiple functional groups from Joncryl can react with the reactive end groups of PPC^{51,52}.

TGA analysis was also performed on the neat PLA/PPC blend films, in addition to films with the incorporation of 0.2phr, 0.5phr, 1phr Joncryl to investigate the effect of Joncryl on the thermal stability of the films. Figures 5.12 and 5.13 show the thermal degradation behavior of blend films as a function of temperature and the main parameters obtained from the TGA are presented in the Table 5-2. It is observed that blending PPC with PLA has enhanced the thermal stability in comparison with the neat PPC. Both the T_{onset} and $T_{5\%}$ of the blend is higher than that of neat PPC, especially the $T_{5\%}$. Similar observation is also seen by other researchers^{40,113}. However, the DTV curves show that the maximum degradation temperature for the PLA/PPC blend has no significant difference from that of the neat PPC, indicating the degradation of PPC still dominates the degradation. As for the blend with different concentration of Joncryl, no significant variation between the four blends was observed, illustrating that the addition of Joncryl did not affect the onset thermal degradation behavior of the PPC/PLA blends. Although all the TGA curves seem overlapped in Figure 5.13, indicating no apparent differences between the thermal degradation behaviors of different film formulations, the DTG curves reveal that the addition of Joncryl had an effect on the thermal degradation rate of the blend. It is observed that with increasing the Joncryl content in the blend system from 0phr to 1phr, thermal degradation rate of the blend has been reduced gradually. Hence, the incorporation of Joncryl enhanced the thermal stability of the PLA/PPC blend by slowing the degradation rate. This can be attributed to the reconnections of the molecule chains induced by Joncryl. Both PLA and PPC were reported to have random chain scission mechanism during their degradations^{63,114}. The multiple functional groups on the molecular chains of Joncryl can react with those PLA and PPC chain

ends which are generated during the random chain scission and reconnect them onto one oligomer of Joncryl, preventing further degradation from proceeding^{55,95}.

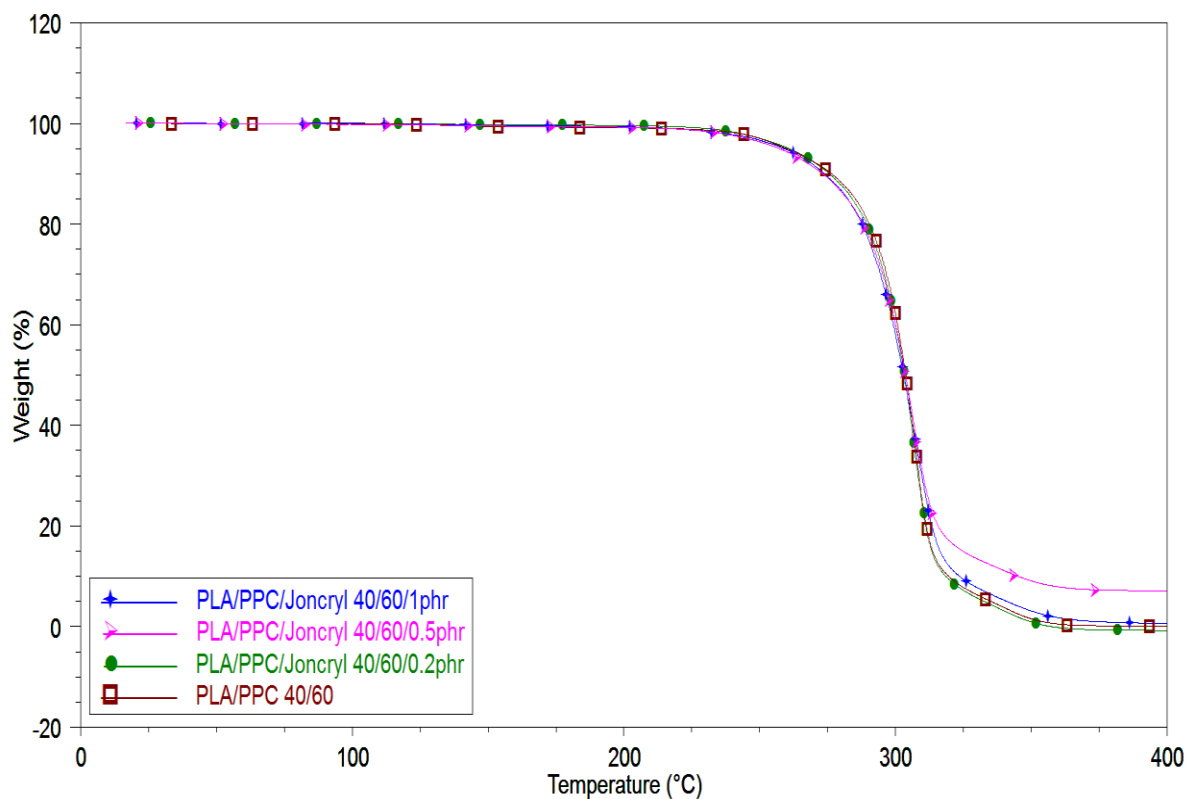


Figure 5.12 TGA curves of PPC/PLA 60/40 blend films with and without Joncryl

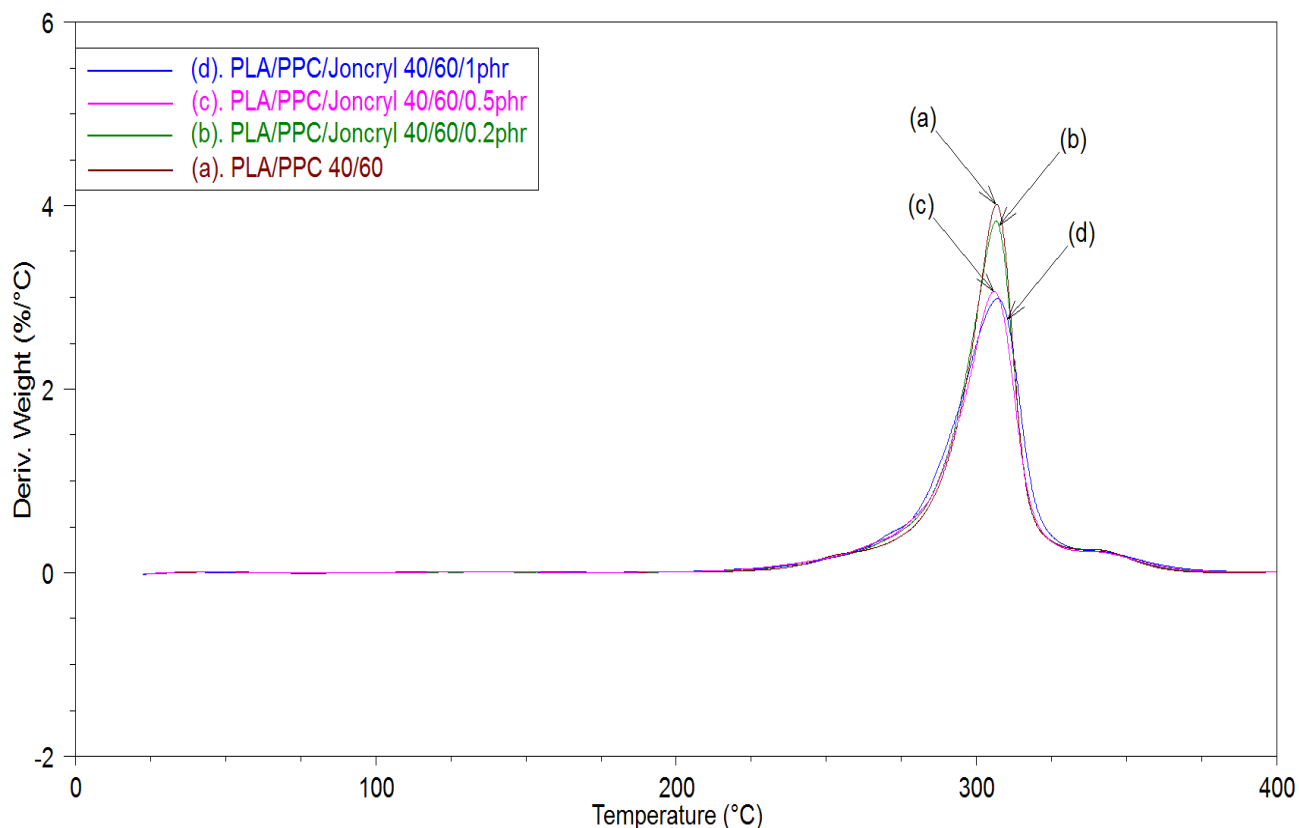


Figure 5.13 DTG curves of PPC/PLA 60/40 blend films with and without Joncryl

5.4 Differential Scanning Calorimetry (DSC)

Non-isothermal differential scanning calorimetry (DSC) analysis was conducted on the film specimens to investigate the thermal properties of the PLA/PPC films with and without Joncryl. The non-isothermal DSC first cooling curves and second heating curves of PLA/PPC and PLA/PPC/Joncryl films are shown in Figure 5.14, 5.15 and Figure 5.16, respectively. With the aim to investigate the crystallization behavior of the PLA/PPC and PLA/PPC/Joncryl films and the effect of the Joncryl on the crystallization of the films, it is important to compare the degree of crystallinity of these film samples^{115,116}. As such, the degree of crystallinity ($X_{c,PLA}$) of the

PLA components for all the film samples was calculated, as PLA is the only crystal phase present in the films. The $X_{c,PLA}$ was obtained by using the following equation

$$X_{c,PLA} = \frac{(\Delta H_{m,PLA} - \Delta H_{cc,PLA})}{\Delta H_{m,PLA}^0 \times W_fPLA} \times 100$$

Where the $\Delta H_{m,PLA}$ is the heat of melting of the PLA crystal in different films obtained from the melting peak on the second DSC heating scan. The $\Delta H_{cc,PLA}$ is the heat of cold crystallization of the PLA components in different films. As on the second DSC heating scan for all the film samples, no cold crystallization was observed, $\Delta H_{cc,PLA}$ was zero in this study. The $\Delta H_{m,PLA}^0$ is the theoretical heat of melting of a 100% crystalline PLA, which is reported as 93 J/g^{117,118}. The W_fPLA is the weight fraction of PLA component in the formulation of all the films. All the DSC parameters obtained from the cooling and heating scan for PLA/PPC and PLA/PPC/Joncryl films were listed in Table 5-3.

Table 5-3 DSC parameters obtained from the DSC scan curves for PLA/PPC/Chain extender blend films

Joncryn content (phr) in PLA/PPC (40/60) BLEND	Melt crystallization temperature(°C)	ΔH_{mc} (J/g)	Tg(°C)	First melting temperature (°C)	Melting temperature(°C)	ΔH_{m1} (J/g)
1	106.98	12.51	34.94	157.11	165.5	2.08
0.5	108.44	13.43	37.47	158.33	166.49	2.27
0.2	109.45	14.26	34.85	159.63	167.97	3.12
0	110.96	15.59	38.79	161	169	5.01
Neat PLA	N/A	N/A	60.1	N/A	168.7	N/A

Joncryn content (phr) in PLA/PPC (40/60) BLEND	ΔH_{m2} (J/g)	ΔH_c (J/g)	Xc (%)
1	6.34	N/A	23
0.5	7.93	N/A	27
0.2	8.73	N/A	32
0	10.98	N/A	43
Neat PLA	31.63	25.14	7.0

The first DSC cooling scan (Figure 5.14) revealed that a uniform single exothermic peak was observed for all the films with different Joncryn concentration. These exothermic peaks were attributed to the melt crystallization of PLA component, as PPC presents a solely amorphous

structure. It was also observed that the melt crystallization temperature of the films shifted to lower values from 110°C to 106°C almost uniformly, with an increase of Joncryl concentration. This can be ascribed to the adverse effect from the addition of Joncryl on the crystallization of the films. It was suggested that the melt crystallization temperature is an indirect signal that indicates the crystallization rate and crystallinity, and a lower crystallization temperature always represents a lower crystallization rate as well as lower crystallinity^{33,65,95,119}. As such, loading Joncryl into the blend system resulted in decreasing the crystallization rate and crystallinity⁶⁰. This is again proved by the reduction of heat of melt crystallization of the PLA component in the film (ΔH_{mc}) along with increasing Joncryl content as summarized in Table 5-3. The decreased crystallization temperature, rate and crystallinity can be caused by the formation of long molecular chains and branched structures in the polymer blend. Study showed that the addition of Joncryl could connect short chain polymer ends with its multiple-functional groups to form longer chains and also could branch multiple molecule chains to form branched structure^{33, 120}. In light of this, the presence of long chains and branched structures may reduce the mobility of the chains structure resulting in hindering the chain packing during the crystallization of PLA component in the blend^{65,93}.

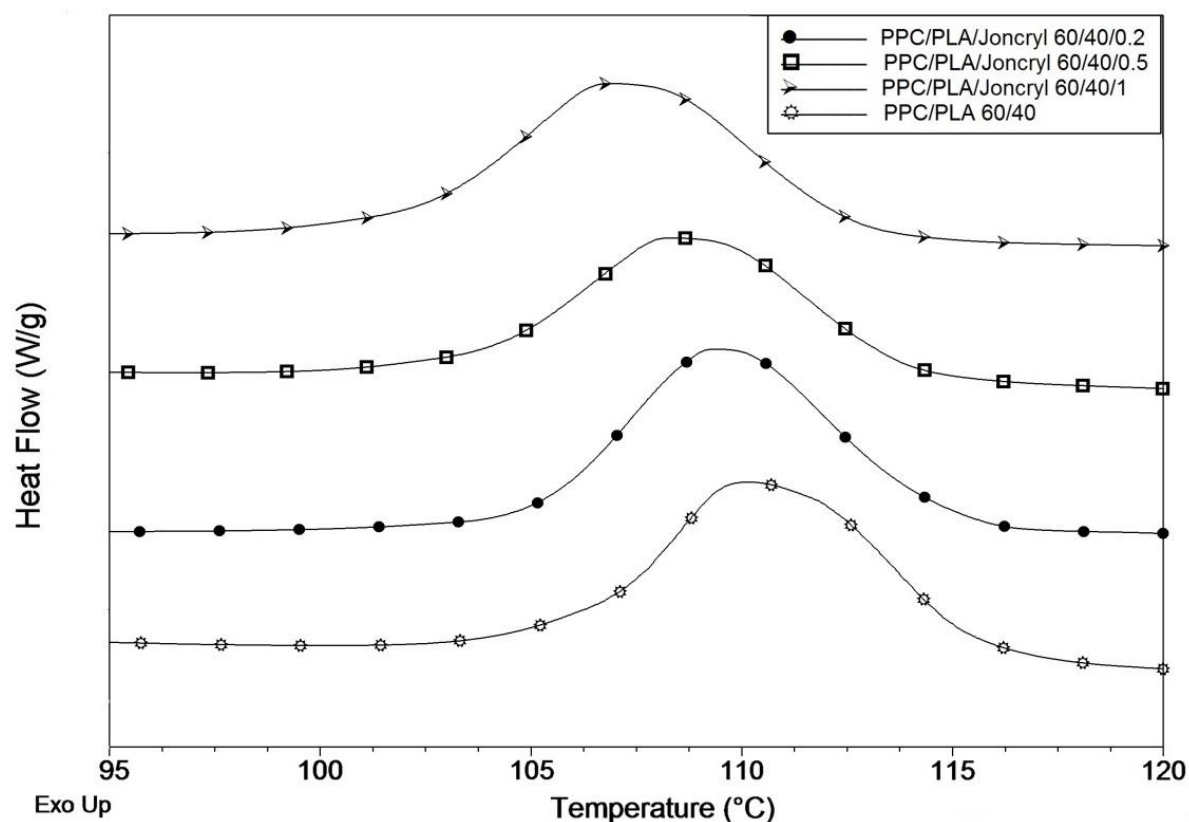


Figure 5.14 DSC first cooling curves (cooling rate of 5°C/min) of PPC/PLA films and PPC/PLA films with 0.2%, 0.5% and 1% Joncryl

The non-isothermal DSC second heating curves of the PPC/PLA blend film and films with 0.2%, 0.5% and 1% Joncryl were also presented in Figure 5.15 and 5.16. From the DSC curves between 20 to 50°C (Figure 5.15), it was noted that there was only one single glass transition temperature in all the blend films. Other researchers have reported that PPC has a T_g value of around 30-40°C while PLA has a T_g value of around 55-60°C, which was also observed from DSC analysis of neat PLA and PPC in the previous study^{50,87,121}. The difference between T_g values of PLA and PPC is normally only around 10-15°C. It was mentioned in one study¹²¹ that when blending PLA with PPC, the two individual glass transition temperatures corresponding to

the two parent polymers had a tendency to move towards each other, approaching the intermediate value. This finding was also confirmed by another study conducted by Ma et al.⁵⁰. In their study, when the amount of PLA and PPC component in the PLA/PPC blend were adjusted close to each other, the difference between their two individual T_g values decreased further and further. Especially for PPC, the T_g increased greatly from 22 to 43 °C as the PPC content in the blend increased. The occurrence of appreciable T_g value convergence was considered as a strong evidence that there is partial miscibility between the two parent polymers^{47,71,117}. Based on the discovery from these two studies, it can be suggested that the T_g convergence took place in our PLA/PPC/Joncryl blend films as well, especially with a blend formulation of 40% PLA and 60% PPC. Hence, because of the nature of neighboring T_g values of PLA and PPC and the T_g convergence in the blend, the observation of single T_g in this paper is probably due to the close proximity of T_g values of the PLA and PPC in the blend, which resulted in the overlapping of the T_g values. It can also be seen that the T_g of the blend slightly shifted to lower values from 38.79 to 35°C with the addition of Joncryl in the blend system. This can be attributed to the reduced crystallinity of the PLA component in the blend induced by the incorporation of Joncryl as lower crystallinity leaves more amorphous fraction volume to the molecule chains. As such, higher chain mobility decreased the glass transition temperature. As the content of Joncryl in the blend increased, there was no significant variation in the T_g of the PLA/PPC/Joncryl blend films. The reason for this could be that increasing the amount of Joncryl developed more long chain branching structures and even cross-linking structures in the blend, which also limited the mobility of the molecule chains^{122,123}. The increase of the chain mobility due to lower crystallinity could be counterbalanced by the depressing influence on the

chain mobility caused by long chain branching structure and cross-linking structures among the molecule chains.

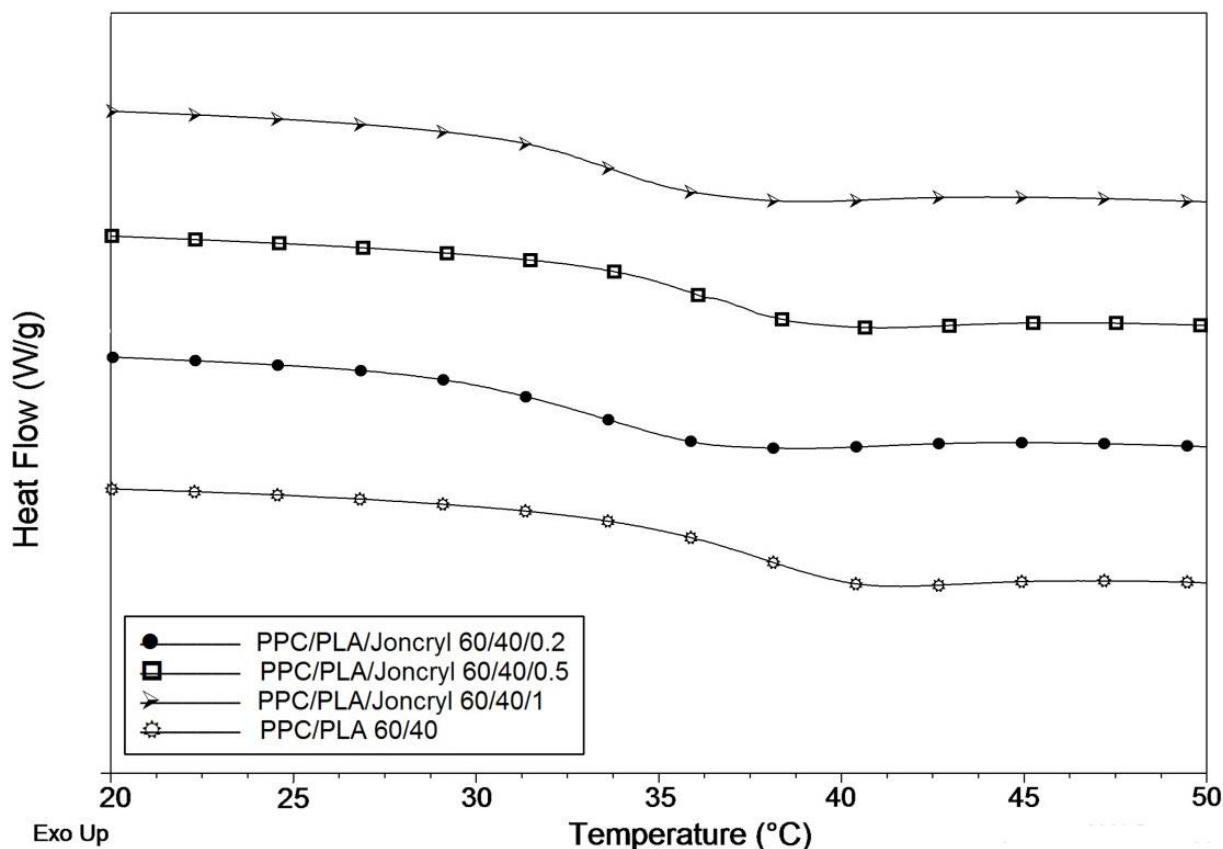


Figure 5.15 DSC second heating curves (heating rate of 10 °C/min) of PPC/PLA blend films and PPC/PLA blend films with 0.2%, 0.5% and 1% Joncryl from 20 °C to 50 °C

It was observed in Table 5-3 that PLA/PPC blend exhibited much higher crystallinity than neat PLA. This could be caused by the acceleration influence of PPC on the crystallization rate of PLA in the blend system. It was also observed in another study that PPC induced faster growth rate of the PLA spherulites, leading to accelerated crystallization rate of PLA⁴⁰.

As shown in the Figure 5.16, all blend films displayed two melting temperature peaks between 160°C and 170 °C. The first melting peak was considered to be caused by the melt re-crystallization of the polymers, specifically the PLA polymer. The re-crystallization occurred during the second heating cycle while the existing crystals with less perfect PLA crystalline structure gained enough time to melt and produce more PLA crystals. This endothermic process was correlated to the first melting peak on the curves¹²⁴. After the re-crystallization, the higher and more perfect PLA crystals which consisted of both the original crystals and crystals produced from re-crystallization were melted during the second melting peak. It was suggested that less structurally perfect crystals have a similar structure to high perfect ones, but the lamellar thickness of the less perfect ones is smaller^{64,125}. Also, it could be observed that both melting peaks shifted to lower values with increased loading of Joncryl into the polymer blend system. For the first melting peak, a decrease in the melting temperature revealed that the nucleation of less structurally perfect PLA crystals occurred during the first cooling cycle. Additionally, these less perfect crystals were even less perfect than before due to the interruption effect on chain packing from the addition of Joncryl^{64,122}. As for the second melting peak, the temperature was reduced due to the decreasing number of perfect PLA crystals and the decrease in perfection of the PLA crystals structure. Since Joncryl have an effect on interrupting the molecular chain packing, the crystallization of perfect PLA crystals was hindered. Therefore, with the addition of Joncryl, the overall crystallization behavior of PLA was interrupted and hindered resulting in a decrease of melting temperature of the polymer blends as shown in Figure 5.16. In addition, according to the calculated crystallinity of the four blend films, the crystallinity stayed in a downward trend consistently as the concentration of Joncryl increased, which is further evidence that Joncryl has an adverse impact on the crystallization of

PLA in the blend. Different from other chain extenders, Joncryl tends to form long chain branched structure with polymers instead of forming long chain linear structure. Moreover, with higher amount of Joncryl, the formation of cross-linking is also found^{59–61}. The presence of these two structures highly restrains the mobility of the molecular chains, which makes the packing of chains a slow and difficult procedure. As such, the crystallization of PLA is hindered in our PLA/PPC blend. This has also been observed by many researchers when applying Joncryl into the polymer system^{56,125}.

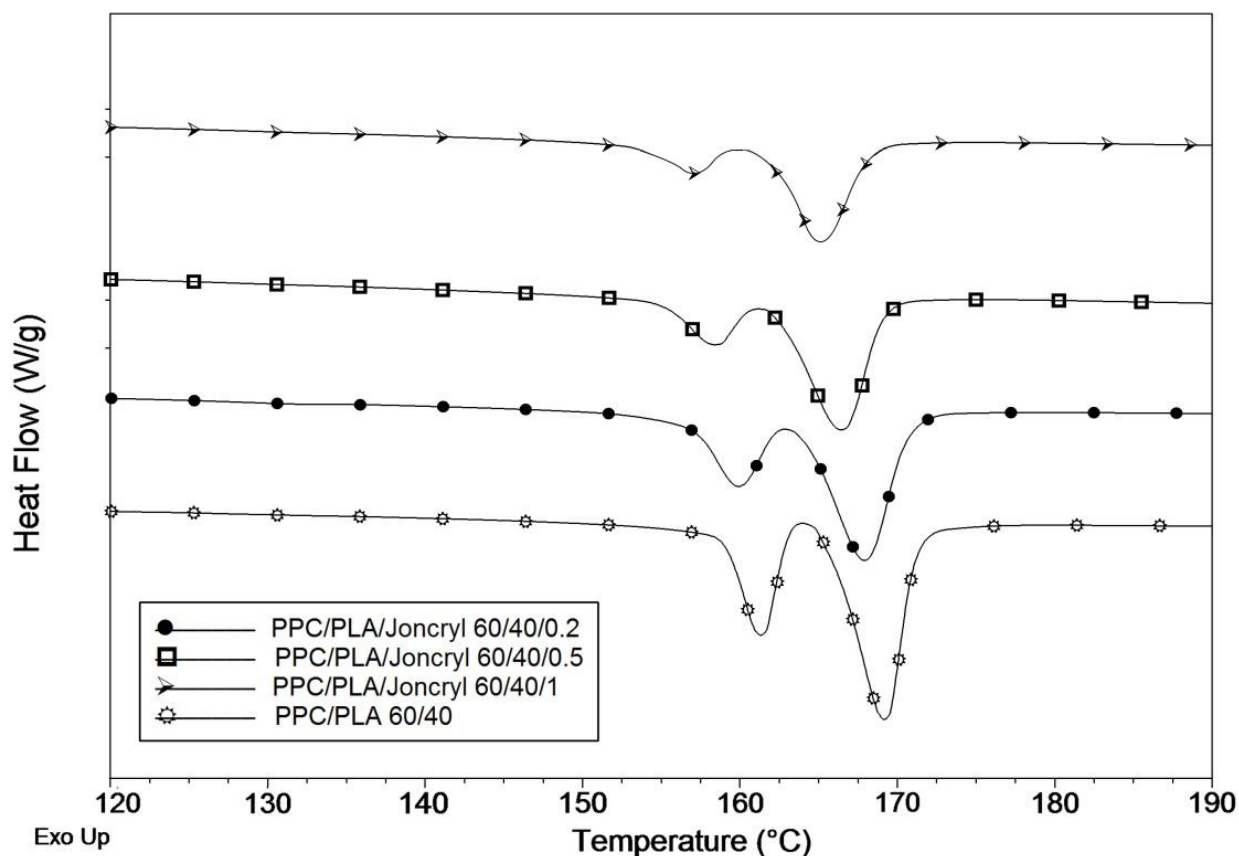
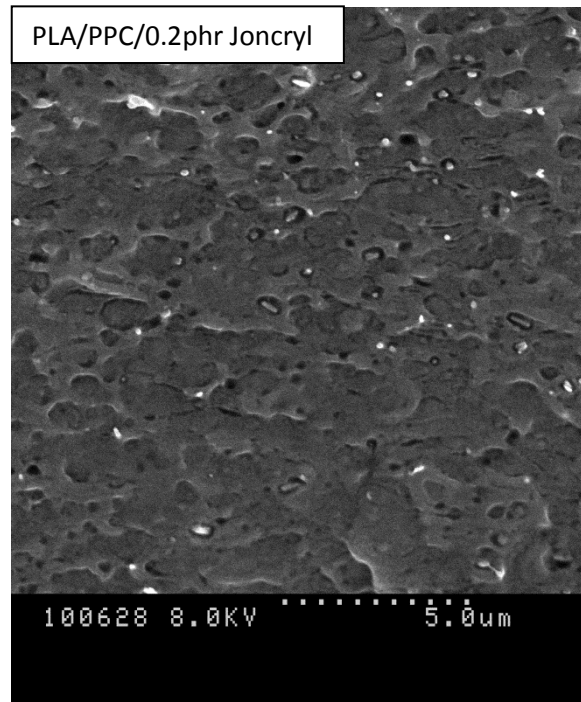
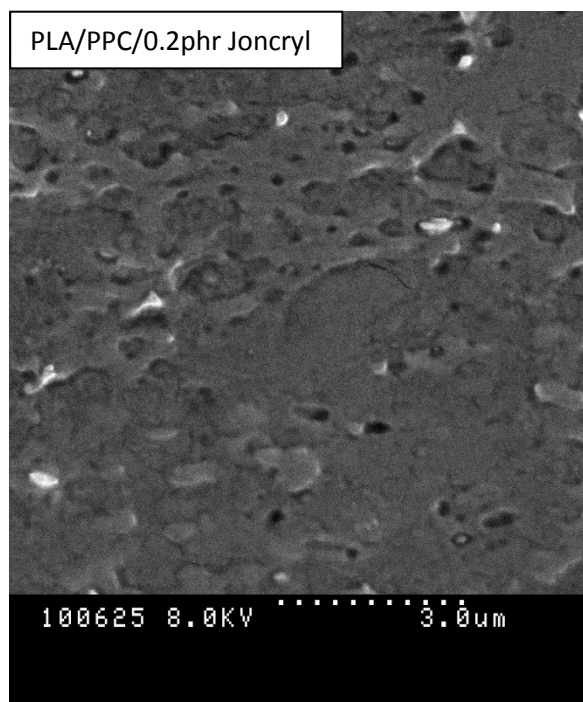
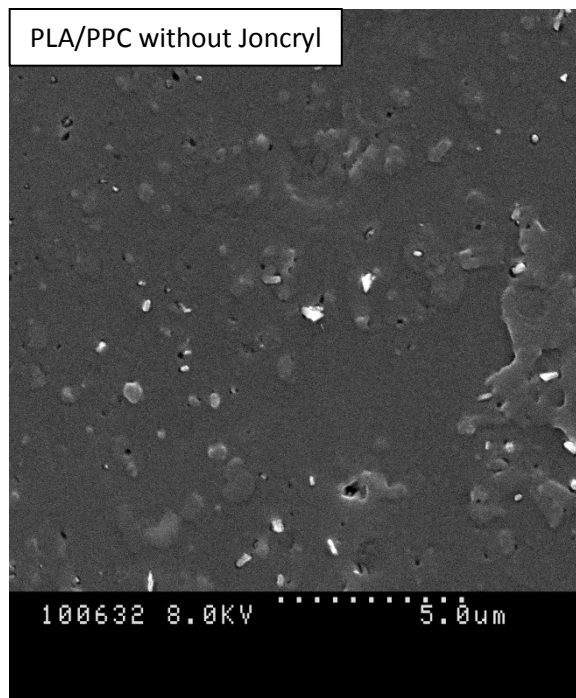
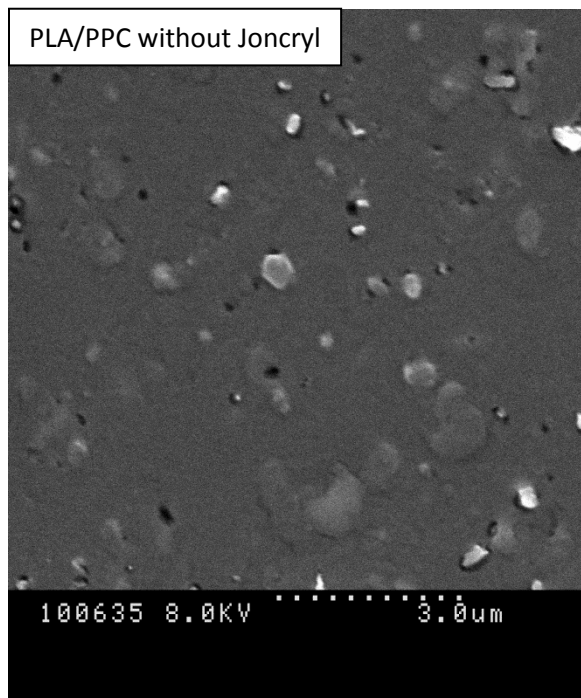


Figure 5.16 DSC second heating curves (heating rate of 10 °C/min) of PPC/PLA blend films and PPC/PLA blend films with 0.2%, 0.5% and 1% Joncryl from 120 °C and higher

5.5 Fracture Surface Morphology Analysis (SEM)

The morphological structure of the polymer blend is an important characteristic since it correlates with the mechanical properties, thermal behaviors, oxygen and water vapor permeability of the developed blend films¹²⁶. The morphological structure of PLA/PPC 40/60 blend films without and with the incorporation of Joncryl, were examined via Scanning Electron Microscopy (SEM) , and results are shown in Figure 5.17.

The SEM images of PLA/PPC blend film without Joncryl shows smooth fracture surface, indicating its relatively brittle fracture behavior. Elongated phase can be seen in the images but only in a few amounts. As the concentration of Joncryl continues increase from 0 to 0.5phr, it is observed that the fracture surface becomes tougher and tougher, illustrating more occurrences of ductile fracture behaviors. In addition, increasing amount of elongated phase is observed. This transformation from brittle fracture to ductile fracture demonstrates better interfacial adhesion and less tension between the two polymer phases, indicating better compatibility. The improved compatibility was caused by the formation of PLA-Joncryl-PPC copolymer through several reactions between PLA, Joncryl and PPC component in the blend, which was also seen in the FTIR study. However, when the concentration of Joncryl is increased to 1phr, the fracture surface becomes less tough along with fewer occurrences of elongated phases, signifying that less ductile fracture but more brittle fracture takes place. This can be correlated to the increasing density of long chain branching and cross-linking structures which restrained the elongation behavior of the blend. The observation from SEM can be supported with observations from the mechanical properties, where films with 0.5phr Joncryl exhibited enormous increase in elongation at break, whereas, drastic decrease in elongation at break was obtained for the films of 1phr Joncryl.



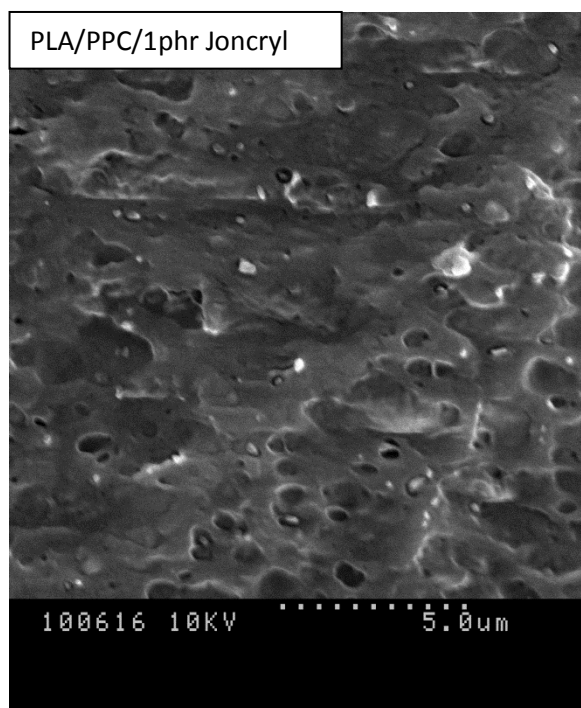
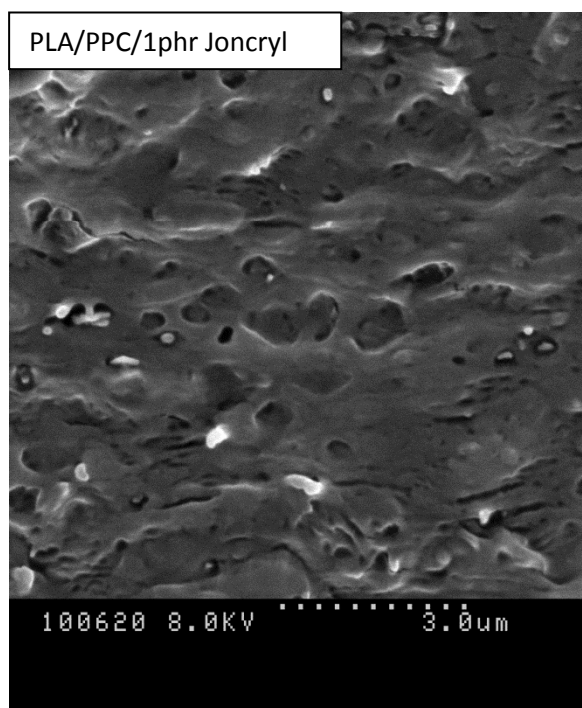
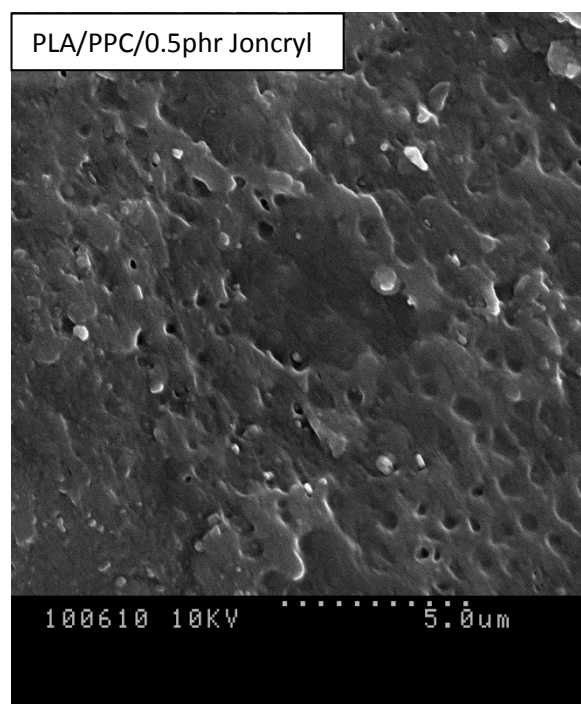
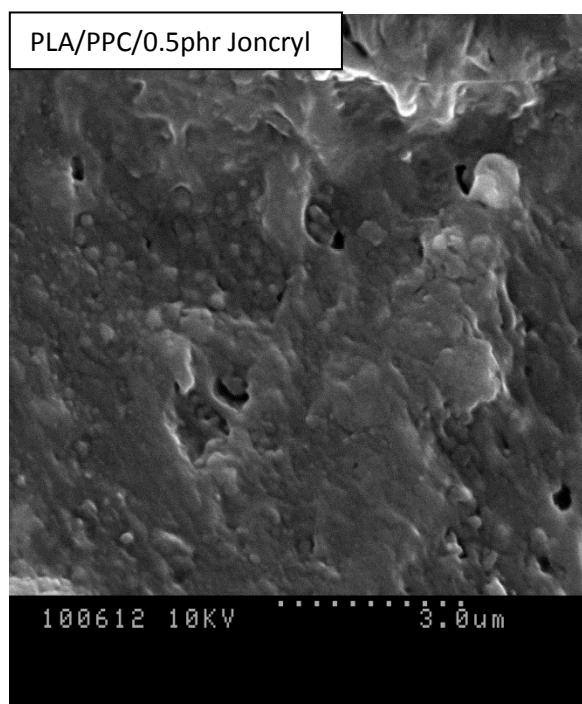


Figure 5.17 SEM images of cyro-fracutre surface of the PLA/PPC blend films with different concentration of Joncry

5.5 Water Vapor Permeability (WVP)

It was noted that optimal water vapor barrier properties of films are critical in light of maintaining the products' quality in addition to extending the shelf-life of the products^{127,128}. Hence, it is imperative to identify the water vapor barrier properties of the films we studied in this paper. The WVP values of neat PLA films, neat PPC films, PLA/PPC blend films and PLA/PPC blend films with different amounts of Joncryl were measured to evaluate the barrier performance of these films with regarding water vapor transmission. It was suggested that the WVP values of have large dependence on the relative humidity (RH) and partial pressure (ΔP) because higher RH and ΔP can reduce the capacity of the films to prevent the water vapor from diffusing through the materials to a large extent^{129,130}. Hence, it is necessary to control these variables when conducting the water vapor permeability tests⁸⁶. According to the ASTM F1249-06, all the experiments were conducted at 37.82 ± 0.1 °C and 100% relative humidity. The WVTR (water vapor transmission rate) values of the films were firstly obtained from the PERMATRAN-W® Model 3/33. After that, WVP with a unit of g*mil/ 100in² day mmHg was calculated for every film samples following the equation:

$$\text{WVP} = \text{WVTR} \times L / \Delta P$$

where the WVTR is the transmission rate of water vapor diffusion through the films with a unit of g/ m² • day, L is the thickness of films with a unit of (mil). The ΔP here is the saturated water vapor pressure at 37.82 °C with 100% RH, which is 49.17 mmHg. Figure 5.18 and Table 5-4 illustrates the WVP values of all six types of films. It can be noted that the neat PPC films exhibited the highest WVP value of 0.7202 g*mil/ 100in² day mmHg, indicating its poor barrier function to water vapor in comparison with the neat PLA and blends . It has been reported that

with respect to water vapor permeating behavior, a permeable amorphous structure facilitates the permeation of the water vapor molecules whereas the impermeable crystallites can prevent the molecules from permeating or creating more tortuosity in the transport path of the molecules¹³¹. In light of this, it can be explained that the high WVP values (poor water barrier performance) of neat PPC films are attributed to its amorphous structure which provides easy access for water vapor molecules to diffuse through. Another reason for the high WVP values of PPC could be correlated to the temperature (37.8°C) at which the test was performed. As the glass transition temperature of PPC is around 32°C which is lower than the testing temperature, the molecule chains in PPC were in a very mobile state, leaving more fraction free volume for the water molecules to diffuse through the film^{131,132}. It was observed that neat PLA films exhibited the lowest WVP value of 0.3688 g*mil/ 100in² day mmHg. After blending PLA with PPC, the WVP of the PPC/PLA blend films showed a balanced value of 0.4358 g*mil/ 100in² day mmHg which falls in between the WVP value of neat PLA films and Neat PPC films. Although the crystallinity was increased in the PLA/PPC blend mentioned in DSC analysis, the increased crystallinity did not help much with increasing water barrier performance. As for our further study on the films with addition of Joncryl, it can be observed that with 0.2phr addition of Joncryl into the blend, the WVP value of the films increased but not in a large extent from 0.4358 to 0.5428 g*mil/ 100in² day mmHg. This can be caused by the prevention effect on the crystallization of the blend induced by adding Joncryl. As aforementioned in the DSC analysis, the addition of Joncryl hinders the crystallization of the PLA in the blend, leading to lower crystallinity and less perfect crystal structure. Hence, Joncryl induced the reduction of the impermeable crystal structure while increasing the permeable amorphous fraction in the blend films, resulting in increased WVP value as Joncryl. When

increasing the Joncryl content to 0.5phr, WVP value only shows increase from 0.54 to 0.6292 g*mil/100in² day mmHg, which can be attributed to further decrease in the crystallinity while increasing the Joncryl content in the blend system. However, interestingly, a reduction of WVP values from 0.6292 (film with 0.5phr Joncryl) to 0.4854 g*mil/ 100in² day mmHg was observed for the PLA/PPC blend with 1phr Joncryl. This improvement of water barrier performance was considered to be caused by the formation of cross-linkings and branching structure among the polymer chains. As discussed before, for the blend with 1wt% Joncryl, Joncryl acted as a strong chain extender and induced cross-linkings among the polymer chains as well as branching polymer chains together^{133,134}. As such, the more intense distribution of the polymer chains and less fraction free volume restrains the diffusion of the water vapor molecules¹³⁸. Based on the statistical analysis, there is no significant difference between the water vapor permeability of PLA/PPC blend and blend with 1phr Joncryl.

Table 5-4 Means, Standard Deviations and Tukey Pairwise Comparisons of WVP of PLA/PPC/Chain extender blend films with vaious concentration of Chain extender (Joncryl)

Joncryl concentration in the PLA/PPC blend films	Water Vapor Permeability (g*mil/100in ² day mmHg)	Standard Deviation
0phr	0.4358 (C)	0.028
0.2phr	0.5428 (B)	0.009
0.5phr	0.6292 (A)	0.035
1phr	0.4854 (C)	0.047

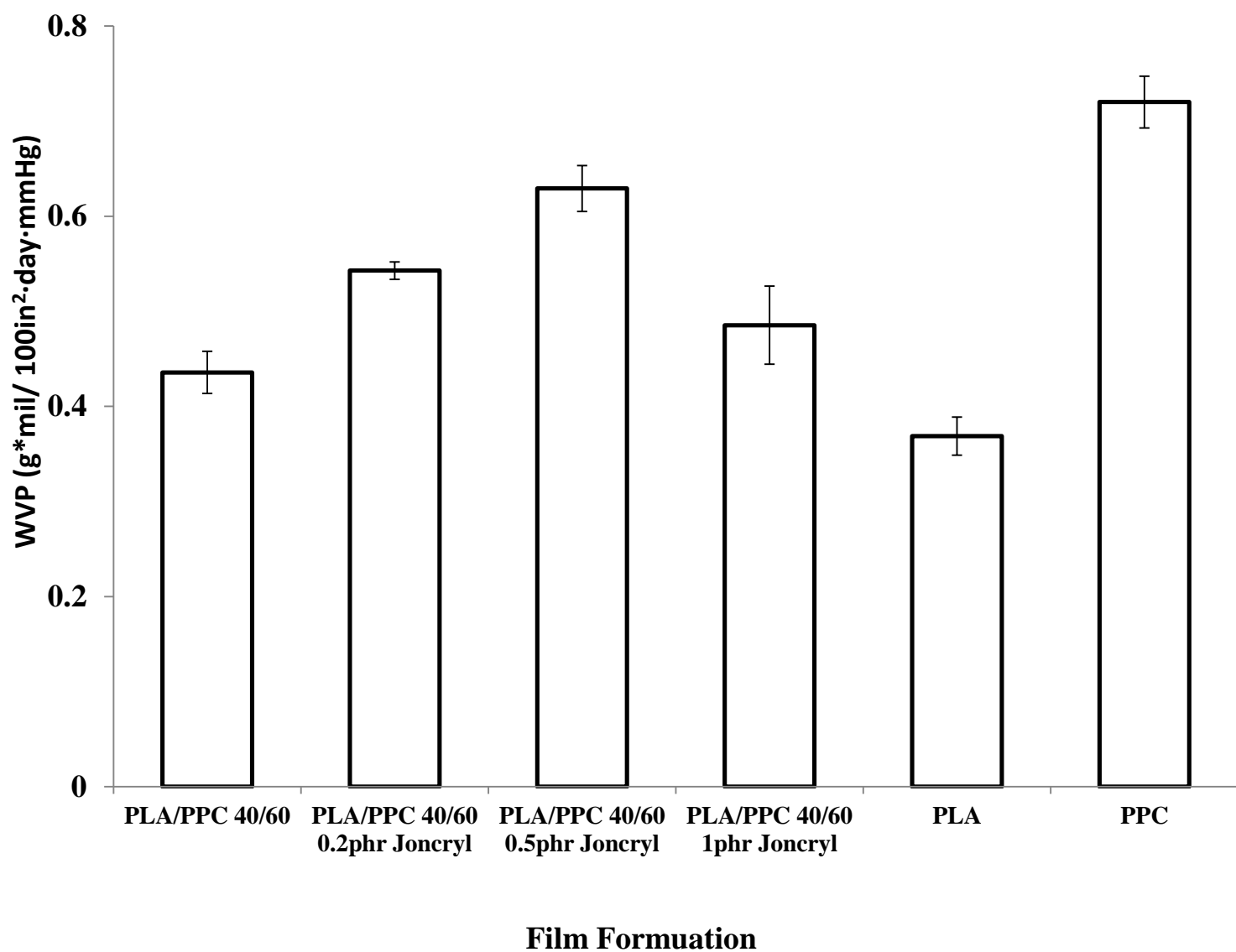


Figure 5.18 WVP of PPC films, PLA films and PPC/PLA blend films with and without Joncryl

5.6 Water Vapor Permeability (WVP) From Dish Method

The PLA/PPC blend film with 0.5phr Joncryl has been chosen to be investigated the water vapor permeability using dish method. Two film samples were measured. The intention of conducting this experiment is to confirm the WVP values obtained from previous method. The weight gain of the two samples was recorded every hour until it kept in a stable state, which took 18 hours. As shown in the Table 5-5, the weight gain for sample1 and sample 2 is 8.354mg/hr and 8.869mg/hr. The WVP for these two samples was calculated with the equation:

$$WVP = \frac{\frac{Wg}{S} \times L}{\Delta P}$$

where the Wg is the weight gain converted to a unit of g/day, the S is the test area which in our case is 19.625cm², L is the thickness of the film (mil) and ΔP is the the saturated water vapor pressure at 37.82 °C with 100% RH, which is 49.17 mmHg. The calculated WVP for the two samples tested by dish method were 0.5997 and 0.6049 g*mil/100in² day mmHg, while the mean and standard deviation of WVP from previous method was 0.6292 and 0.035 g*mil/100in² day mmHg. It is seen that both WVP values from this dish method experiment fall in the range of the WVP values from previous method. As such, it can be conclude that the WVP values tested with the previous method are valid.

Table 5-5 WVP from Dish Method

PLA/PPC blend films with 0.5phr Joncryl	Test Period (hr)	Weight Gain (mg/hr)	Calculated WVP coefficients (g*mil/100in ² day mmHg)
Sample 1	18	8.365	0.5997
Sample 2	18	8.869	0.6049

5.7 Oxygen Permeability (OP)

The oxygen barrier property of packaging materials is critically important in terms of providing long-term protection to the packaged products. Packaging materials with superior oxygen barrier present very low oxygen transmission rate. The unwanted damage of the products brought by contacting with excessive amount of oxygen can be suppressed via reducing the oxygen transmission rate of the packaging material^{129,135}. Maintaining long-term performance as well as extending the shelf-life of packaged products also requires the oxygen transmission rate to be very low⁷⁷⁻⁸⁰, especially for those oxygen-sensitive products such as fruits, salads and delicatessens. Therefore, it is critical for the packaging material to limit or prevent the oxygen from diffusing through either from outside environment to products or the other way. As great potential alternatives of the petroleum-based plastics, bioplastics can be restricted to be applied in the packaging application due to their moderate oxygen barrier properties⁸¹⁻⁸³. Thus, it is essential to investigate the oxygen barrier properties of the films that were studied in this paper. Oxygen permeability (OP) coefficients can be used to quantify the oxygen barrier properties. The oxygen permeability (OP) coefficients of the PLA/PPC blend film and films with various concentrations of Joncryl were determined to evaluate their oxygen barrier performance. Since partial pressure (ΔP) and relative humidity (RH) have great impact on the oxygen barrier performance of films, these two variables were set to be constant throughout all the experiments⁸⁴⁻⁸⁶. The oxygen transmission rate (OTR) values of blend films with a unit of $\text{cc}/\text{m}^2\text{-day}$ were originally measured from the OX-TRAN® Model 2/21 (USA, MOCON). OP coefficients with a unit of $\text{cc}\cdot\text{mil}/100\text{in}^2\text{-atm-day}$ was obtained afterwards for each film sample using this equation:

$$OP = \frac{OTR \times L}{\Delta P}$$

Where the OTR is the oxygen transmission rate of the sample, L is the thickness of films with a unit of (mil). The ΔP here is the partial pressure induced by the oxygen concentration gradient between the two sides of the sample. In our study, since 100% concentration of oxygen was applied in the experiment, ΔP should be 1atm (728mmHg) when doing the calculations. The OP coefficients of PLA/PPC blend films with different concentration of Joncryl and neat PLA film are depicted in Table 5-6 and Figure 5.19. Statistical analysis was completed on all the results by employing the Tukey Method of one-way ANOVA with a significance of 0.05 (Table 5-6). In regards to the OP coefficient of neat PPC film, no valid results could be obtained. The equipment has certain test range in terms of oxygen transmission rate. Once the value exceeds the test range, the sensor gives “over-range” alarm and equipment stops automatically without showing any valid results. The oxygen transmission rate (OTR) of the neat PPC film in this study is too high for the equipment to detect and give valid OTR value. This may be due to the total amorphous and structureless nature of PPC. There are mainly four steps that govern the permeation of a gas through the polymer films, which are the sorption of the gas on the surface of film, dissolution of gas molecules into the film material, diffusion of gas molecule throughout the film and final desorption of the gas from other side of the film surface^{132,136}. Among these four steps, the diffusion of the gas molecule takes up the major role during the permeation of gas through the film and it mainly proceeds in the amorphous structure in polymers. The crystal structure of polymers is considered to be the impermeable barrier to gases and water vapor whereas the amorphous structure is responsible for providing the path for the permeants to diffuse through^{31,137,138}. Higher OP coefficient represents lower oxygen barrier

property. As such, as aforementioned that the PPC is 100% amorphous, its oxygen barrier can be very poor and oxygen permeability coefficient can be a very high value.

Figure 5.19 shows that neat PLA film has the highest OP coefficient around 54.21 cc*mil/100in²-atm-day. After blending PLA with PPC, the PLA/PPC 40/60 blend film exhibits much lower OP coefficient than the neat PLA film. Considering that PPC also has a very high OP coefficient, the OP coefficient of the PLA/PPC blend does not follow the mixing rule of polymers. The combination of two relatively poor oxygen barrier polymers achieved a blend with much better oxygen barrier properties. This can be mainly ascribed to the higher crystallinity of PLA/PPC blend as compared to PLA, which was shown in the DSC study. It was observed that the incorporation of PPC can enhance the crystallization rate of PLA in the blend system, resulting in higher crystallinity than the crystallinity of neat PLA. Hence, the blend shows lower OP coefficient and better oxygen barrier property than that of both parent polymers.

As presented in Table 5-6 and Figure 5.19, with increasing concentration of Joncryl in the blend film, the OP coefficients of each formulation vary accordingly. The PLA/PPC blend film with 0.2phr concentration of Joncryl presents the highest OP coefficient, demonstrating the worst oxygen barrier. The lower crystallinity caused by the addition of Joncryl could be the cause, as the Joncryl hindered the crystallization of PLA in the blend. However, when increasing the Joncryl concentration in the blend, there are more formation of long chain branching and cross-linking structures, which diminish the fraction free volume in the structure of the blend^{133,134}.

Fraction free volume is another important factor that determines the diffusion of the gas molecules in the polymer. Higher fraction free volume promotes the diffusion, leading to higher permeability^{128,129}. In this case, when the concentration of Joncryl changes from 0.2phr to 0.5phr and 1phr the fraction free volume continually reduces. As a result, the OP coefficient

becomes lower and lower after the concentration of Joncryl is higher than 0.2phr. A similar observation was seen by other researchers when increasing the addition of Joncryl⁶⁵. As the concentration comes to 1phr, the OP coefficient presents no significant difference as compared to the blend without Joncryl. In conclusion, with small amount of Joncryl, the oxygen barrier of the PLA/PPC blend becomes poorer whereas the blend shows an upper trend in oxygen barrier property with concentration of Joncryl higher than 0.5phr.

Table 5-6 Means, Standard Deviations and Tukey Pairwise Comparisons of OP of PLA/PPC/Chain extender blend films with various concentration of Chain extender (Joncryl)

Joncryl concentration in the PLA/PPC blend films	Oxygen Permeability (cc*mil/100in ² -atm-day)	Standard Deviation
0phr	20.95 (C)	1.05
0.2phr	34.61 (A)	1.99
0.5phr	26.86 (B)	2.44
1phr	23.09 (B) (C)	1.95

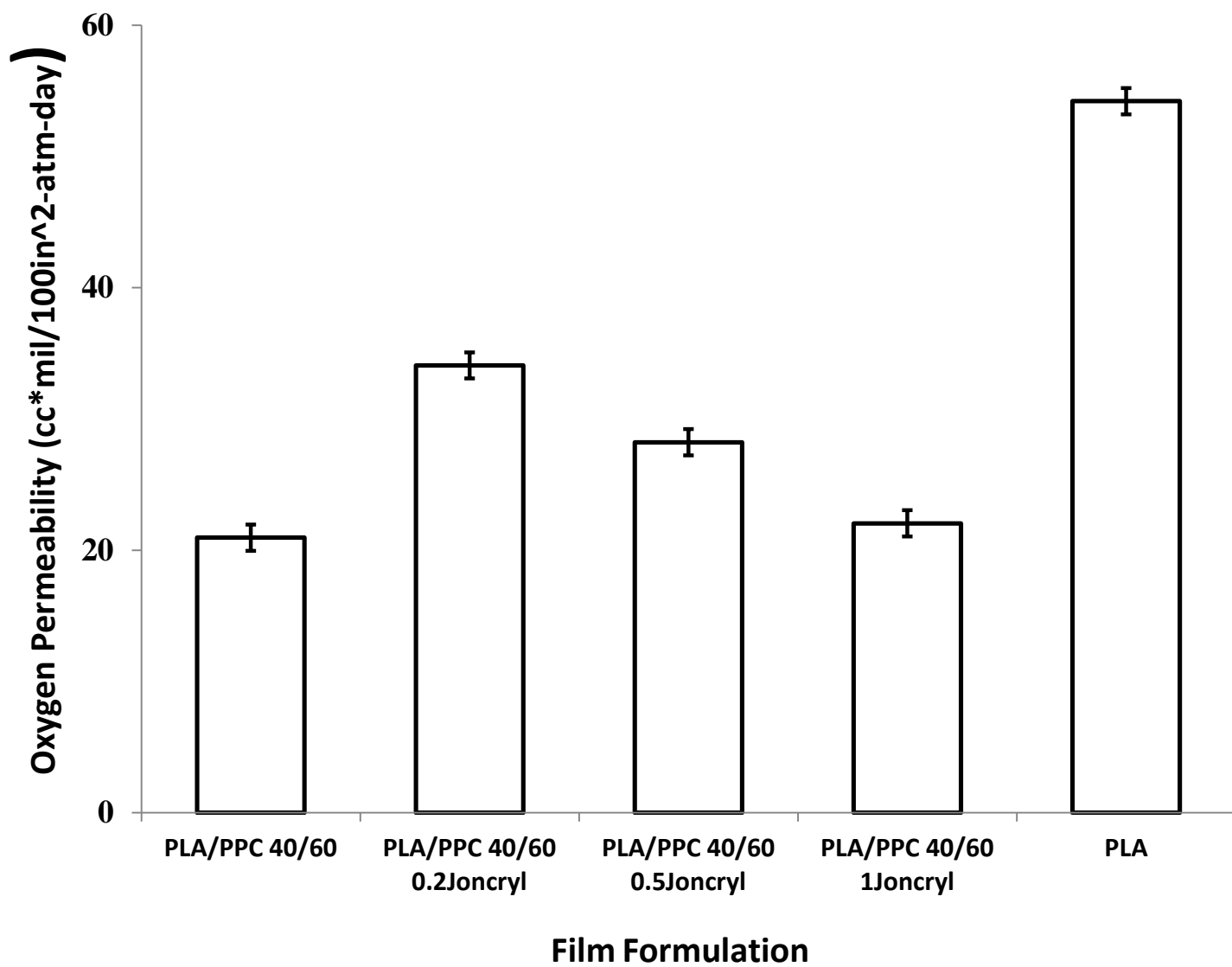


Figure 5.19 OP of PPC films, PLA films and PPC/PLA blend films with and without Joncryl

Chapter 6 Conclusion

PPC/PLA blend films with different content of Joncryl and without Joncryl were prepared; and their mechanical properties, thermal properties, morphology and possible chemical interactions between polymer matrix and Joncryl were investigated. With loading Joncryl into the blend system, the mechanical performance was largely enhanced with significant increment in elongation at break and slight increase in tensile strength. The films with 0.5% Joncryl loading exhibited the most optimal performance. The morphology and FTIR analysis revealed that the compatibility and interfacial adhesion between the polymers in the blend was significantly enhanced after loading Joncryl, which was caused by the formation of PLA-Joncryl-PPC copolymer through the reactions between Joncryl and PLA/PPC component. Joncryl was observed to have an adverse effect on the crystallization of PLA in the PLA/PPC/Joncryl film, resulting in lower crystallinity of the compatibilized films. Interestingly, PPC was found to be able to accelerate the crystallization rate of PLA. As for the water vapor barrier properties of these blend films, the incorporation of PLA into the PPC system has largely reduced the water vapor permeability, resulting in enhancing the water vapor barrier properties. When introducing the Joncryl into the blend system, the water vapor barrier properties showed a downward trend, which can be corresponded to the adverse effect of Joncryl on the crystallization. However, further increased Joncryl led to better water barrier properties as compared to films with lower Joncryl concentration. PLA/PPC blend film resulted in better oxygen barrier than both parent polymers due to the increased crystallinity of PLA. Lower Joncryl concentration compromised the oxygen barrier of the blend films as a result of hindering the crystallization, whereas, the films with higher Joncryl concentration showed increasingly better oxygen barrier than films with lower Joncryl concentration. It could be concluded that the incorporation of Joncryl into

the PLA/PPC blend films improved the overall performance of this PLA-PPC based films. This developed PLA-PPC based films compares well to the conventional flexible packaging plastics in terms of the mechanical and barrier properties. As for the cost competitiveness of this developed PLA-PPC film, the price of PLA keeps reducing recent years due to advancement of its research. Although PPC is still more costly than the conventional plastics owing to its immature synthesizing and manufacturing process, with the rapid advancing of technology, the price of PPC is expected to be reduced to the level that is close to the conventional plastics in the next few years. In conclusion, this developed PLA-PPC based film has great potential to be applied in the flexible packaging field for various applications.

Chapter 7 Reference

1. 1. Abdel-Bary, E. M. and Limited, R. T. Handbook of Plastic Films. (Rapra, 2003). at <<http://search.ebscohost.com.subzero.lib.uoguelph.ca/login.aspx?direct=true&db=nlebk&AN=234940&site=ehost-live&scope=site>>
2. Jung, B. and Theato, P. Chemical Strategies for the Synthesis of Protein – Polymer Conjugates. *Adv. Polym. Sci.* 1–34 (2012). doi:10.1007/12
3. Siracusa, V., Rocculi, P., Romani, S. and Rosa, M. D. Biodegradable polymers for food packaging: a review. *Trends Food Sci. Technol.* 19, 634–643 (2008).
4. Harding, K. G., Dennis, J. S., von Blottnitz, H. and Harrison, S. T. L. Environmental analysis of plastic production processes: Comparing petroleum-based polypropylene and polyethylene with biologically-based poly- β -hydroxybutyric acid using life cycle analysis. *J. Biotechnol.* 130, 57–66 (2007).
5. Criddle, C. S., Billington, S. L. and Frank, C. W. Renewable Bioplastics and Biocomposites From Biogas Methane and Waste-Derived Feedstock : Development of Enabling Technology , Life Cycle Assessment , and Analysis of Costs Contractor ' s Report Produced Under Contract By : (2014).
6. Pilla, S. Handbook of Bioplastics and Biocomposites Engineering Applications;(15 September 2011).
7. Soulestin, J., Prashantha, K., Lacrampe, M. F. and Krawczak, P. in *Handb. Bioplastics Biocomposites Eng. Appl.* 76–119 (2011). doi:10.1002/9781118203699.ch4
8. Mohanty, a. K., Misra, M. and Drzal, L. T. Sustainable Bio-Composites from renewable resources: Opportunities and challenges in the green materials world. *J. Polym. Environ.* 10, 19–26 (2002).
9. Ohji, T., Singh, M., Hoffman, E., Seabaugh, M. and Yang, Z. G. *Advances in Materials Science for Environmental and Energy Technologies II.* 89–95 (2013). doi:10.1002/9781118751176
10. Mohanty, A. K., Misra, M. and Drzal, L. T. Surface modifications of natural fibers and performance of the resulting biocomposites: An overview. *Compos. Interfaces* 8, 313–343 (2001).
11. Bhardwaj, R., Mohanty, A. K., Drzal, L. T., Pourboghra, F. and Misra, M. Renewable resource-based green composites from recycled cellulose fiber and poly(3-hydroxybutyrate-co-3-hydroxyvalerate) bioplastic. *Biomacromolecules* 7, 2044–2051 (2006).
12. Srikanth, P. Handbook of Bioplastics and Biocomposites Engineering Applications. (2011).
13. Imre, B. and Puk  nszky, B. Compatibilization in bio-based and biodegradable polymer blends. *Eur. Polym. J.* 49, 1215–1233 (2013).

14. Mishra, D. P. and Mahanwar, P. A. Advances in bioplastic materials. *Pop. Plast. Packag.* 45, 68–76 (2000).
15. Marjadi, D., Dharaiya, N. and Ngo, A. D. Bioplastic: a better alternative for sustainable future. *Everyman's Sci.* 90 (2010).
16. Gironi, F. and Piemonte, V. Bioplastics and petroleum-based plastics: strengths and weaknesses. *Energy Sources, Part A Recover. Util. Environ. Eff.* 33, 1949–1959 (2011).
17. Van der Wal, a., Verheul, a. J. J. and Gaymans, R. J. Polypropylene–rubber blends: 4. The effect of the rubber particle size on the fracture behaviour at low and high test speed. *Polymer (Guildf)*. 40, 6057–6065 (1999).
18. Jenkins, W. A. and Osborn, K. R. *Plastic Films: echnology and Packaging Applications*. (CRC Press, 1992).
19. Lepoutre, P. The manufacture of polyethylene. *New Zeal. Inst. Chem.* 1–5 (2013). at <<http://nzic.org.nz/ChemProcesses/polymers/10J.pdf>>
20. Wang, H., Ma, Z., Ke, Y. and Hu, Y. Synthesis of linear low density polyethylene (LLDPE) by in situ copolymerization with novel cobalt and zirconium catalysts. *Polym. Int.* 52, 1546–1552 (2003).
21. Micic, P. and Bhattacharya, S. N. Rheology of LLDPE, LDPE and LLDPE/LDPE blends and its relevance to the film blowing process. *Polym. Int.* 49, 1580–1589 (2000).
22. Ajji, a., Sammut, P. and Huneault, M. a. Elongational rheology of LLDPE/LDPE blends. *J. Appl. Polym. Sci.* 88, 3070–3077 (2003).
23. Natta, G. and Corradini, P. Structure and properties of isotactic polypropylene. *Nuovo Cim.* 15, 40–51 (1960).
24. Karger-Kocsis, J. *Polypropylene structure, blends and composites*. 2, (Springer Science and Business Media, 1995).
25. For, B. M. *Packaging Applications – a Review of Recent*. 7, 2506–2552 (2012).
26. Queiroz, A. U. B. and Collares-Queiroz, F. P. Innovation and industrial trends in bioplastics. *J. Macromol. Sci. Part C Polym. Rev.* 49, 65–78 (2009).
27. Crandall, L. Bioplastics: A burgeoning industry. *INFORM-CHAMPAIGN-* 13, 626–630 (2002).
28. Lim, L.-T., Auras, R. and Rubino, M. Processing technologies for poly(lactic acid). *Prog. Polym. Sci.* 33, 820–852 (2008).
29. Van Tuil, R., Fowler, P., Lawther, M. and Weber, C. J. Biobased Packaging Materials for the Food Industry. *J. Food Sci. Technol* (2000). at <<ftp://118.67.228.244/public/food/resource/se-food-update-62-res-05.pdf>>

30. Auras, R. a., Singh, S. P. and Singh, J. J. Evaluation of oriented poly(lactide) polymers vs. existing PET and oriented PS for fresh food service containers. *Packag. Technol. Sci.* 18, 207–216 (2005).
31. Auras, R. a., Harte, B., Selke, S. and Hernandez, R. Mechanical, Physical, and Barrier Properties of Poly(Lactide) Films. *J. Plast. Film Sheeting* 19, 123–135 (2003).
32. Li, B. H. and Yang, M. C. Improvement of thermal and mechanical properties of poly(L-lactic acid) with 4,4-methylene diphenyl diisocyanate. *Polym. Adv. Technol.* 17, 439–443 (2006).
33. Najafi, N., Heuzey, M. C. and Carreau, P. J. Crystallization behavior and morphology of polylactide and PLA/clay nanocomposites in the presence of chain extenders. *Polym. Eng. Sci.* 53, 1053–1064 (2013).
34. Vlachopoulos, J. and Strutt, D. Polymer processing. *Mater. Sci. Technol.* 19, 1161–1169 (2003).
35. Zhang, K., Mohanty, A. K. and Misra, M. A NEW BIODEGRADABLE BIOPLASTIC TERNARY BLEND AS NEW MATRIX SYSTEM FOR BIOCOMPOSITE USES.
36. Reddy, M. M., Misra, M. and Mohanty, A. K. Bio-based materials in the new bio-economy. *Chem. Eng. Prog.* 108, 37–42 (2012).
37. Mohanty, A. K., Misra, M. and Hinrichsen, G. Biofibres, biodegradable polymers and biocomposites: An overview. *Macromol. Mater. Eng.* 276-277, 1–24 (2000).
38. Zhai, L.; Li, G.; Xu, Y.; Xiao, M.; Wang, S.; Meng, Y. Poly (propylene carbonate)/ aluminum flake composite films with enhanced gas barrier properties. 41663, 1–6 (2015).
39. Matsui, Y. and Asahi, Y. Degradation and Stabilization of Poly (propylene oxide). *J. Soc. Chem. Ind. Japan* 70, 1212–1217 (1967).
40. Di Lorenzo, M. L., Ovynd, R., Malinconico, M., Rubino, P. and Grohens, Y. Peculiar crystallization kinetics of biodegradable poly(lactic acid)/poly(propylene carbonate) blends. *Polym. Eng. Sci.* 47, n/a–n/a (2015).
41. Li, X. H., Meng, Y. Z., Zhu, Q. and Tjong, S. C. Thermal decomposition characteristics of poly(propylene carbonate) using TG/IR and Py-GC/MS techniques. *Polym. Degrad. Stab.* 81, 157–165 (2003).
42. Ge, X. C., Li, X. H., Zhu, Q., Li, L. and Meng, Y. Z. Preparation and properties of biodegradable poly(propylene carbonate)/starch composites. *Polym. Eng. Sci.* 44, 2134–2140 (2004).
43. Li, X. H., Tjong, S. C., Meng, Y. Z. and Zhu, Q. Fabrication and Properties of Poly (propylene carbonate)/. *J. Polym. Sci. Part B Polym. Phys.* 41, 1806–1813 (2003).
44. Seo, J., Jeon, G., Jang, E. S., Khan, S. B. and Han, H. Preparation and properties of poly (propylene carbonate) and nanosized ZnO composite films for packaging applications. *J. Appl. Polym. Sci.* 122, 449–456 (2011).

45. Peng, S., Wang, X. and Dong, L. Special interaction between poly (propylene carbonate) and corn starch. *Polym. Compos.* 26, 37–41 (2005).
46. Ree, M., Bae, J. Y., Jung, J. H. and Shin, T. J. New copolymerization process leading to poly(propylene carbonate) with a highly enhanced yield from carbon dioxide and propylene oxide. *J. Polym. Sci. Part A Polym. Chem.* 37, 1863–1876 (1999).
47. Yang, D. Z. and Hu, P. Miscibility, crystallization, and mechanical properties of poly(3-hydroxybutyrate) and poly(propylene carbonate) biodegradable blends. *J. Appl. Polym. Sci.* 109, 1635–1642 (2008).
48. Luinstra, G. Poly(Propylene Carbonate), Old Copolymers of Propylene Oxide and Carbon Dioxide with New Interests: Catalysis and Material Properties. *Polym. Rev.* 48, 192–219 (2008).
49. Corre, Y.-M., Bruzard, S. and Grohens, Y. Poly (3-hydroxybutyrate-co-3-hydroxyvalerate) and Poly (propylene carbonate) Blends: an Efficient Method to Finely Adjust Properties of Functional Materials. *Macromol. Mater. Eng.* 298, 1176–1183 (2013).
50. Ma, X., Jiugao, Y. and Wang, N. Compatibility characterization of poly(lactic acid)/poly(propylene carbonate) blends. *J. Polym. Sci. Part B Polym. Phys.* 44, 94–101 (2006).
51. Lehermeier, H. J. and Dorgan, J. R. Melt rheology of poly(lactic acid): Consequences of blending chain architectures. *Polym. Eng. Sci.* 41, 2172–2184 (2001).
52. Liu, B. and Xu, Q. Effects of Bifunctional Chain Extender on the Crystallinity and Thermal Stability of PET. 2013, 9–15 (2013).
53. Eslami, H. and Kamal, M. R. Effect of a chain extender on the rheological and mechanical properties of biodegradable poly(lactic acid)/poly[(butylene succinate)-co-adipate] blends. *J. Appl. Polym. Sci.* 129, 2418–2428 (2013).
54. Loontjens, T. The action of chain extenders in nylon-6, PET, and model compounds. *J. Appl. Polym. Sci.* 65, 1813–1819 (1997).
55. Al-Itry, R., Lamnawar, K. and Maazouz, A. Improvement of thermal stability, rheological and mechanical properties of PLA, PBAT and their blends by reactive extrusion with functionalized epoxy. *Polym. Degrad. Stab.* 97, 1898–1914 (2012).
56. Pesetskii, S. S., Jurkowski, B., Filimonov, O. V., Koval, V. N. and Golubovich, V. V. PET/PC blends: Effect of chain extender and impact strength modifier on their structure and properties. *J. Appl. Polym. Sci.* 119, 225–234 (2011).
57. Guo, B. and Chan, C. Chain extension of poly (butylene terephthalate) by reactive extrusion. *J. Appl. Polym. Sci.* 71, 1827–1834 (1999).
58. Villalobos, M., Awojulu, a., Greeley, T., Turco, G. and Deeter, G. Oligomeric chain extenders for economic reprocessing and recycling of condensation plastics. *Energy* 31, 3227–3234 (2006).

59. Raffa, P., Coltelli, M.-B. and Castelvetro, V. Expanding the application field of post-consumer poly(ethylene terephthalate) through structural modification by reactive blending. *J. Appl. Polym. Sci.* 131, n/a–n/a (2014).
60. Duangphet, S., Szegda, D., Song, J. and Tarverdi, K. The Effect of Chain Extender on Poly(3-hydroxybutyrate-co-3-hydroxyvalerate): Thermal Degradation, Crystallization, and Rheological Behaviours. *J. Polym. Environ.* 22, 1–8 (2014).
61. Ea, E. V. *Polymeric Chain Extenders and Biopolymers.* (2008).
62. Dong, W., Zou, B., Yan, Y., Ma, P. and Chen, M. Effect of chain-extenders on the properties and hydrolytic degradation behavior of the poly(lactide)/ poly(butylene adipate-co-terephthalate) blends. *Int. J. Mol. Sci.* 14, 20189–20203 (2013).
63. Najafi, N., Heuzey, M. C., Carreau, P. J. and Wood-Adams, P. M. Control of thermal degradation of polylactide (PLA)-clay nanocomposites using chain extenders. *Polym. Degrad. Stab.* 97, 554–565 (2012).
64. Arruda, L. C., Magaton, M., Suman Bretas, R. E. and Ueki, M. M. Influence Of Chain Extender On Mechanical, Thermal And Morphological Properties Of Blown Films Of Pla/Pbat Blends. *Polym. Test.* 43, 27–37 (2015).
65. Najafi, N., Heuzey, M. C. and Carreau, P. J. Polylactide (PLA)-clay nanocomposites prepared by melt compounding in the presence of a chain extender. *Compos. Sci. Technol.* 72, 608–615 (2012).
66. Aniunoh, K. and Harrison, G. Effect of Material Properties and Processing Conditions on PP Film Casting.
67. Leephakpreeda, T. Dynamic control of crystallinity in polymer film casting process. Songklanakarin J. Sci. Technol. 26, 385 (2004).
68. Silagy, D., Demay, Y. and Agassant, J. F. Stationary and stability analysis of the film casting process. *J. Nonnewton. Fluid Mech.* 79, 563–583 (1998).
69. Lamberti, G., Titomanlio, G. and Brucato, V. Measurement and modelling of the film casting process 2 . Temperature distribution along draw direction. *Chem. Eng. Sci.* 57, 1993–1996 (2002).
70. Gohil, R. M. Morphology-permeability relationships in biaxially oriented PET films: A relationship between oxygen permeability and PROOF. *J. Appl. Polym. Sci.* 48, 1649–1664 (1993).
71. Chen, G. J., Wang, Y. Y., Wang, S. J., Xiao, M. and Meng, Y. Z. Orientation microstructure and properties of poly(propylene carbonate)/poly(butylene succinate) blend films. *J. Appl. Polym. Sci.* 128, 390–399 (2013).
72. Kovács, J.; Pataki, P.; Orbán-Mester, Á.; Nagy, G.; Staniek, P.; Földes, E.; Pukánszky, B. Melt stabilisation of Phillips type polyethylene, Part III: Correlation of film strength with the rheological characteristics of the polymer. *Polym. Degrad. Stab.* 96, 1771–1779 (2011).

73. Shiromoto, S. The Mechanism of Neck-in Phenomenon in Film Casting Process. (2014). doi:10.3139/217.2784
74. Hu, B.; Lei, C.; Xu, R.; Shi, W.; Cai, Q.; Mo, H.; Chen, C. Influence of melt-draw ratio on the structure and properties of poly(vinylidene fluoride) cast film. *J. Plast. Film Sheeting* 30, 300–313 (2013).
75. Lamberti, G., Titomanlio, G. and Brucato, V. Measurement and modelling of the film casting process 2. Temperature distribution along draw direction. *Chem. Eng. Sci.* 57, 1993–1996 (2002).
76. Lamberti, G. and Brucato, V. Real-time orientation and crystallinity measurements during the isotactic polypropylene film-casting process. *J. Polym. Sci. Part B Polym. Phys.* 41, 998–1008 (2003).
77. Aniunoh, K. and Harrison, G. M. The processing of polypropylene cast films. I. Impact of material properties and processing conditions on film formation. *Polym. Eng. Sci.* 50, 1151–1160 (2010).
78. Sakaki, K., Katsumoto, R. and Kajiawafw, T. Three-Dimensional Flow Simulation of a Film Casting Process. 1821–1831 (1821).
79. Alaie, S. M. and Papanastasiou, T. C. Film casting of viscoelastic liquid. *Polym. Eng. Sci.* 31, 67–75 (1991).
80. Acierno, D., Di Maio, L. and Ammirati, C. C. Film casting of polyethylene terephthalate: Experiments and model comparisons. *Polym. Eng. Sci.* 40, 108–117 (2000).
81. Y. Hong, S. . Coombs, J. . Cooper-White, M. . Mackay, C. . Hawker, E. Malmström, and N. Rehnberg. Film blowing of linear low-density polyethylene blended with a novel hyperbranched polymer processing aid. *Polymer (Guildf)*. 41, 7705–7713 (2000).
82. Beaulne, M. and Mitsoulis, E. Effect of viscoelasticity in the film-blowing process. *J. Appl. Polym. Sci.* 105, 2098–2112 (2007).
83. Leal, V., Lafuente, P., Alicante, R., Pérez, R. and Santamaría, A. New results on the correlation molecular architecture-melt elasticity-blowing process-film properties for conventional and metallocene-catalyzed polyethylenes. *Macromol. Mater. Eng.* 291, 670–676 (2006).
84. Choi, K.-J., Spruiell, J. E. and White, J. L. Orientation and morphology of high-density polyethylene film produced by the tubular blowing method and its relationship to process conditions. *J. Polym. Sci. Polym. Phys. Ed.* 20, 27–47 (1982).
85. Tsuji, H., Okino, R., Daimon, H. and Fujie, K. Water vapor permeability of poly(lactide)s: Effects of molecular characteristics and crystallinity. *J. Appl. Polym. Sci.* 99, 2245–2252 (2006).
86. Lee, Y., Kim, D., Seo, J., Han, H. and Khan, S. B. Preparation and characterization of poly(propylene carbonate)/exfoliated graphite nanocomposite films with improved thermal stability, mechanical properties and barrier properties. *Polym. Int.* 62, 1386–1394 (2013).

87. Luinstra, G. a. and Molnar, F. Poly(propylene carbonate), old CO₂ Copolymer with new attractiveness. *Macromol. Symp.* 259, 203–209 (2007).
88. Al-Itry, R., Lamnawar, K. and Maazouz, A. Rheological, morphological, and interfacial properties of compatibilized PLA/PBAT blends. *Rheol. Acta* 53, 501–517 (2014).
89. Astm. ASTM D882: Standard Test Method for Tensile Properties of Thin Plastic Sheeting. *ASTM Stand.* 12 (2012). doi:10.1520/D0882-12.2
90. Wang, Y.; Fu, C.; Luo, Y.; Ruan, C.; Zhang, Y.; Fu, Y. Melt synthesis and characterization of poly(L-lactic acid) chain linked by multifunctional epoxy compound. *J. Wuhan Univ. Technol. Mater. Sci. Ed.* 25, 774–779 (2010).
91. Zhang, Y., Yuan, X., Liu, Q. and Hrymak, A. The Effect of Polymeric Chain Extenders on Physical Properties of Thermoplastic Starch and Polylactic Acid Blends. *J. Polym. Environ.* 20, 315–325 (2012).
92. Maazouz, a, Mallet, B. and Lamnawar, K. Compounding and processing of biodegradable materials based on PLA for packaging applications: In greening the 21st century materials world. ... *Eng. (international J. ...* (2011). at <<http://www.ah2st.ma/fse/docpaper/M2003.pdf>>
93. Pilla, S. Kramschuster, A.; Yang, L.; Lee, J.; Gong, S.; Turng, L. S. Microcellular injection-molding of polylactide with chain-extender. *Mater. Sci. Eng. C* 29, 1258–1265 (2009).
94. Khonakdar, H. a., Morshednian, J., Wagenknecht, U. and Jafari, S. H. An investigation of chemical crosslinking effect on properties of high-density polyethylene. *Polymer (Guildf)*. 44, 4301–4309 (2003).
95. Jaszkievicz, a., Bledzki, a. K., van der Meer, R., Franciszczak, P. and Meljon, a. How does a chain-extended polylactide behave?: a comprehensive analysis of the material, structural and mechanical properties. *Polym. Bull.* 71, 1675–1690 (2014).
96. Alexy, P.; Bugaj, P.; Feranc, J.; Pavlačková, M.; Tomanová, K.; Benovič, F.; Plavec, R.; Mihalovič, M.; Botošová, M. Blends based on PLA and PHB with improved processing and mechanical properties. *Chem. List.* 105, (2011).
97. Zhu, Q., Meng, Y. Z., Tjong, S. C., Zhao, X. S. and Chen, Y. L. Thermally stable and high molecular weight poly (propylene carbonate) s from carbon dioxide and propylene oxide. *Polym. Int.* 51, 1079–1085 (2002).
98. Kuo, S. W., Huang, C. F. and Chang, F. C. Study of hydrogen - bonding strength in poly (ε - caprolactone) blends by DSC and FTIR. *J. Polym. Sci. Part B Polym. Phys.* 39, 1348–1359 (2001).
99. Fei, B.; Chen, C.; Peng, S.; Zhao, X.; Wang, X.; Dong, L. FTIR study of poly(propylene carbonate)/bisphenol A blends. *Polym. Int.* 53, 2092–2098 (2004).

100. Sengupta, R.; Chakraborty, S.; Bandyopadhyay, S.; Dasgupta, S.; Mukhopadhyay, R.; Auddy, K.; Deuri, a S. A Short Review on Rubber / Clay Nanocomposites With Emphasis on Mechanical Properties. *Engineering* 47, 21–25 (2007).
101. Qin, Y., Chen, L., Wang, X., Zhao, X. and Wang, F. Enhanced mechanical performance of poly(propylene carbonate) via hydrogen bonding interaction with o-lauroyl chitosan. *Carbohydr. Polym.* 84, 329–334 (2011).
102. Mekonnen, T., Mussone, P., El-Thaher, N., Choi, P. Y. K. and Bressler, D. C. Thermosetting proteinaceous plastics from hydrolyzed specified risk material. *Macromol. Mater. Eng.* 298, 1294–1303 (2013).
103. Lai, M. F., Li, J. and Liu, J. J. Thermal and dynamic mechanical properties of poly(propylene carbonate). *J. Therm. Anal. Calorim.* 82, 293–298 (2005).
104. Barreto, C., Altskjär, A., Fredriksen, S., Hansen, E. and Rychwalski, R. W. Multiwall carbon nanotube/PPC composites: Preparation, structural analysis and thermal stability. *Eur. Polym. J.* 49, 2149–2161 (2013).
105. Uzunlar, E. and Kohl, P. a. Thermal and photocatalytic stability enhancement mechanism of poly(propylene carbonate) due to Cu(I) impurities. *Polym. Degrad. Stab.* 97, 1829–1837 (2012).
106. Spencer, T. J. and Kohl, P. a. Decomposition of poly(propylene carbonate) with UV sensitive iodonium salts. *Polym. Degrad. Stab.* 96, 686–702 (2011).
107. Jiao, J., Wang, S. J., Xiao, M., Xu, Y. and Meng, Y. Z. Processability, property, and morphology of biodegradable blends of poly(propylene carbonate) and poly(ethylene-co-vinyl alcohol). *Polym. Eng. Sci.* 47, 174–180 (2007).
108. Barreto, C., Hansen, E. and Fredriksen, S. Advantages of polycarboxylic over dicarboxylic anhydrides in the melt modification of PPC. *Express Polym. Lett.* 7, 895–899 (2013).
109. Lu, X. L., Zhu, Q. and Meng, Y. Z. Kinetic analysis of thermal decomposition of poly(propylene carbonate). *Polym. Degrad. Stab.* 89, 282–288 (2005).
110. Beyler, C. L. and Hirschler, M. M. *Beyler_Hirschler_SFPE_Handbook_3*. 110–131
111. Peng, S.; An, Y.; Chen, C.; Fei, B.; Zhuang, Y.; Dong, L. Thermal degradation kinetics of uncapped and end-capped poly(propylene carbonate). *Polym. Degrad. Stab.* 80, 141–147 (2003).
112. Guo, C., Zhou, L. and Lv, J. Effects of expandable graphite and modified ammonium polyphosphate on the flame-retardant and mechanical properties of wood flour-polypropylene composites. *Polym. Polym. Compos.* 21, 449–456 (2013).
113. Shi, X. and Gan, Z. Preparation and characterization of poly(propylene carbonate)/montmorillonite nanocomposites by solution intercalation. *Eur. Polym. J.* 43, 4852–4858 (2007).

114. Varghese, J. K.; Na, S. J.; Park, J. H.; Woo, D.; Yang, I.; Lee, B. Y. Thermal and weathering degradation of poly(propylene carbonate). *Polym. Degrad. Stab.* 95, 1039–1044 (2010).
115. Papageorgiou, G. Z., Achilias, D. S., Nanaki, S., Beslikas, T. and Bikiaris, D. PLA nanocomposites: Effect of filler type on non-isothermal crystallization. *Thermochim. Acta* 511, 129–139 (2010).
116. Rahman, M. H. and Nandi, A. K. On the crystallization mechanism of poly (ethylene terephthalate) in its blends with poly (vinylidene fluoride). 43, 6863–6870 (2002).
117. Shibata, M., Inoue, Y. and Miyoshi, M. Mechanical properties, morphology, and crystallization behavior of blends of poly(l-lactide) with poly(butylene succinate-co-l-lactate) and poly(butylene succinate). *Polymer (Guildf)*. 47, 3557–3564 (2006).
118. Zhai, W., Ko, Y., Zhu, W., Wong, A. and Park, C. B. A study of the crystallization, melting, and foaming behaviors of polylactic acid in compressed CO₂. *Int. J. Mol. Sci.* 10, 5381–5397 (2009).
119. Kai, W., He, Y. and Inoue, Y. Fast crystallization of poly(3-hydroxybutyrate) and poly(3-hydroxybutyrate-co-3-hydroxyvalerate) with talc and boron nitride as nucleating agents. *Polym. Int.* 54, 780–789 (2005).
120. Al-Itry, R., Lamnawar, K. and Maazouz, A. Reactive extrusion of PLA, PBAT with a multi-functional epoxide: Physico-chemical and rheological properties. *Eur. Polym. J.* 58, 90–102 (2014).
121. Yao, M.; Deng, H.; Mai, F.; Wang, K.; Zhang, Q.; Chen, F.; Fu, Q. Modification of poly(lactic acid)/poly(propylene carbonate) blends through melt compounding with maleic anhydride. *Express Polym. Lett.* 5, 937–949 (2011).
122. Corre, Y. M., Duchet, J., Reignier, J. and Maazouz, A. Melt strengthening of poly (lactic acid) through reactive extrusion with epoxy-functionalized chains. *Rheol. Acta* 50, 613–629 (2011).
123. Yu, T., Chen, J. S., Wu, F. M. and Rocks, J. Crosslinking of Polyamide 6 by Reactive Processing. *Mater. Sci. Forum* 815, 576–582 (2015).
124. Yasuniwa, M., Tsubakihara, S., Sugimoto, Y. and Nakafuku, C. Thermal analysis of the double-melting behavior of poly(L-lactic acid). *J. Polym. Sci. Part B Polym. Phys.* 42, 25–32 (2004).
125. Zhang, G., Zhang, J., Wang, S. and Shen, D. Miscibility and Phase Structure of Binary Blends of Polylactide and Poly (methyl methacrylate). *Polymer (Guildf)*. 23–30 (2003).
126. Jaszkievicz, A., Bledzki, A. K., Duda, A., Galeski, A. and Franciszczak, P. Investigation of processability of chain-extended polylactides during melt processing - Compounding conditions and polymer molecular structure. *Macromol. Mater. Eng.* 299, 307–318 (2014).
127. Seo, J., Jeon, G., Jang, Eu. S., Bahadar Khan, S. and Han, H. Preparation and properties of poly (propylene carbonate) and nanosized ZnO composite films for packaging applications. *J. Appl. Polym. Sci.* 122, 1101–1108 (2011).

128. Suyatma, N. E., Copinet, A., Tighzert, L. and Coma, V. Mechanical and barrier properties of biodegradable films made from chitosan and poly (lactic acid) blends. *J. Polym. Environ.* 12, 1–6 (2004).
129. Hu, Y. S.; Liu, R. Y. F.; Zhang, L. Q.; Rogunova, M.; Schiraldi, D. a.; Nazarenko, S.; Hiltner, a.; Baer, E. Oxygen transport and free volume in cold-crystallized and melt-crystallized poly(ethylene naphthalate). *Macromolecules* 35, 7326–7337 (2002).
130. Olivas, G. I. and Barbosa-Cánovas, G. V. Alginate-calcium films: Water vapor permeability and mechanical properties as affected by plasticizer and relative humidity. *LWT - Food Sci. Technol.* 41, 359–366 (2008).
131. Shogren, R. Water vapor permeability of biodegradable polymers. *J. Environ. Polym. Degrad.* 5, 91–95 (1997).
132. Salame, M. Prediction of gas barrier properties of high polymers. *Polym. Eng. Sci.* 26, 1543–1546 (1986).
133. Yampolskii, Y. P.; Korikov, a. P.; Shantarovich, V. P.; Nagai, K.; Freeman, B. D.; Masuda, T.; Teraguchi, M.; Kwak, G. Gas permeability and free volume of highly branched substituted acetylene polymers. *Macromolecules* 34, 1788–1796 (2001).
134. Lee, W. M. Selection of barrier materials from molecular structure. *Polym. Eng. Sci.* 20, 65–69 (1980).
135. Dong, T.; Yun, X.; Li, M.; Sun, W.; Duan, Y.; Jin, Y. Biodegradable high oxygen barrier membrane for chilled meat packaging. *J. Appl. Polym. Sci.* 132, n/a–n/a (2015).
136. Miller, K. S. and Krochta, J. M. Oxygen and aroma barrier properties of edible films: A review. *Trends Food Sci. Technol.* 8, 228–237 (1997).
137. Cava, D., Gimenez, E., Gavara, R. and Lagaron, J. M. Comparative Performance and Barrier Properties of Biodegradable Thermoplastics and Nanobiocomposites versus PET for Food Packaging Applications. *J. Plast. Film Sheeting* 22, 265–274 (2006).
138. Lange, J. and Wyser, Y. Recent Innovations in Barrier Technologies for Plastic Packaging - A Review. *Packag. Technol. Sci.* 16, 149–158 (2003).